Molecular Studies on Dengue Virus-Host Interaction

Dissertation

Submitted to the

Combined Faculties for the natural sciences and for Mathematics

Of the Ruperto-Carola University of Heidelberg, Germany

For the degree of

Doctor of Natural Sciences

Presented by

Anil Kumar Victoria Ansalem

Born in Trivandrum, India

Oral Examination:

Declaration

The applicant, Anil Kumar Victoria Ansalem declares that I am the sole author of the submitted dissertation and no other sources or help from those specifically referred to have been used. Additionally, the applicant declares that he has not applied for permission to enter examination procedure at another institution and this dissertation has not been presented to other faculty and not used in its current or in any other form in another examination

_____   _____

Date   Signature

Table of Contents

1. List of Figures

2. List of Tables

3. List of Abbreviations

ADE   Antibody Dependent Enhancement
APS   Ammonium Persulfate
ATCC   American Type Culture Collection
ATP   Adenosine triphosphate
BHK-21   Baby Hamster Kidney 21
BSA   Bovine Serum Albumin
CHAPS   3-[(3-Cholamidopropyl)dimethylammonio]-1-propanesulfonate
CIAP   Calf Intestine Alkaline Phosphatase
CLSM   Confocal Laser Scanning Microscope
CPE   Cytopathic Effect
CTP   Cytidine triphosphate
DAPI   4',6-diamidino-2-phenylindole
DC-SIGN   Dendritic Cell-Specific Intercellular adhesion molecule-3-Grabbing Non-integrin
DENV   DENV
DF   Dengue Fever
DHF/DSS   Dengue Hemorrhagic Fever /Dengue Shock Syndrome
DMEM   Dulbecco modified Eagle's minimal essential medium
DMSO   Dimethyl sulfoxide
DNA   Deoxyribonucleic acid
DTT   Dithiothreitol
EDTA   Ethylene diamine tetraacetic acid
EGTA   Ethylene glycol tetraacetic acid
EM   Electron Microscopy
EMCV   Encephalomyocarditis virus
ER   Endoplasmic Reticulum
ERAD   Endoplasmic Reticulum Associated Degradation
FCS   Fetal Calf Serum
FLIP   Fluorescence Loss in Photobleaching
FRAP   Fluorescence Recovery After Photobleaching
GAPDH   Glyceraldehyde 3-phosphate dehydrogenase
GFP   Green Fluorescent Protein
GPI   Glycosylphosphatidylinositol
GTase   Guanyl Transferase
GTP   Guanosine triphosphate
h   Hour
HA   Hemagglutinin (of Influenza virus)
HCV   Hepatitis C Virus
HEK293T   Human Embryonic Kidney 293T
HEPES   4-(2-hydroxyethyl)-1-piperazineethanesulfonic acid
HIV-1   Human Immunodeficiency Virus type 1
HRP   Horseradish Peroxidase
IFN   IFN
IL-8   Interleukin-8
IPTG   Isopropyl β-D-1-thiogalactopyranoside

IRES	Internal Ribosome Entry Site
JEV	Japanese Encephalitis Virus
kb	Kilo Bases
kDa	Kilo Dalton
KUNV	Kunjin Virus
LB	Luria Broth
MCS	Multiple Cloning Site
MEM	Minimal Essential Medium
min	Minute
MOI	Multiplicity Of Infection
MTase	Methyl Transferase
NF-κB	Nuclear Factor κ-B
NGC	New Guinea C-Strain
NS	Non-structur
NTP	Nucleoside Triphosphate
ORF	Open Reading Frame
PAGE	Polyacrylamide Gel Electrophoresis
PFA	Paraformaldehyde
PFU	Plaque Forming Units
PNS	Post Nuclear Supernatant
qRT-PCR	Quantitative Real Time Polymerase Chain Reaction
RC	Replication complex
RdRP	RNA dependent RNA polymerase
RIPA	Radio immunoprecipitation Assay
RLU	Relative Luminescence Unit
RNA	Ribonucleic Acid
RRL	Rabbit Reticulocyte Lysate
RT-PCR	Real Time Polymerase Chain Reaction
SAM	S-Adenosylmethionine
SDS	Sodium Dodecyl Sulfate
STAT	Signal Transducers and Activators of Transcription
TCA	Trichloro Acetic acid
$TCID_{50}$	Tissue Culture Infectious Dose $_{50}$
TEMED	Tetramethylethylenediamine
Tris	Tris(hydroxymethyl)aminomethane
UAR	Upstream AUG Region
UTR	Untranslated Region
WHO	World Health Organization
WNV	West Nile Virus
WT	Wild Type
YFV	Yellow Fever Virus
ZO-1	Zona Occludens-1

4. Acknowledgement

5. Summary

Dengue is the most prevalent mosquito-borne viral disease world-wide. The causative agent Dengue Virus (DENV) is a positive strand RNA virus replicating predominantly in monocyte-derived macrophages and dendritic cells. The severity of the disease is strongly linked to the level of viral replication, which is determined, amongst others by pre-existing DENV-specific antibodies and genetic determinants of the virus and the host.

The aim of my thesis was to characterize the role of nonstructural protein 5 (NS5) for the DENV replication cycle. NS5 is a multifunctional protein involved in viral RNA replication, 5' end capping and blocking of interferon (IFN)-mediated signaling by degrading STAT2. Although DENV replicates in the cytoplasm, NS5 mostly accumulates in the nucleus of infected cells. This study investigated the determinants of NS5 nuclear transport and the effects of nuclear NS5 on viral replication and innate immunity. Nuclear accumulation of NS5 occurred independent from other viral proteins and was found in infected mammalian and mosquito cells arguing for an evolutionarily conserved property. A mutation analysis was used to identify amino acid residues in NS5 essential for nuclear accumulation. Replication analyses of these nuclear localization signal (NLS) mutants showed that even though a high level of nuclear NS5 is not required for efficient DENV replication, complete abrogation of nuclear transport significantly reduced viral replication. Interestingly, the poorly replicating NLS mutants could not be rescued by providing wild type protein *in trans* indicating that factors other than nuclear NS5 are responsible for their poor replication. To check whether these NLS mutations affect enzymatic activities of NS5, recombinant full length proteins were bacterially expressed and purified. Enzymatic assays showed that save for one, none of the NLS mutations impaired RNA-dependent RNA polymerase or methyl transferase activity. Moreover, IFN sensitivity of the NLS mutants was similar to wild type indicating that nuclear NS5 is not required to counteract IFN induced genes. Contrary to earlier observations no significant

difference was observed in induction of interleukin-8 by wild type and mutant NS5.

In the second part of my PhD study, I performed a genome-wide RNAi-based kinase screen to identify cellular kinases promoting or restricting DENV replication. An imaging based RNAi screening platform for DENV was developed, which included optimization of siRNA-mediated silencing in human hepatoma cells, viral infection, immunostaining, image acquisition and statistical data analysis. The primary screen was carried out with a kinase library targeting all known and putative cellular kinases with three siRNAs per gene. Approximately 100 kinases selected from the primary screen were validated in an infection based screen with a new siRNA library containing a different set of siRNAs against each gene. The screen identified 18 kinases essential for DENV replication and 15 kinases suppressing viral replication. The kinase siRNAs were later tested in a DENV subgenomic reporter replicon based screen to differentiate their role in viral entry or replication. The effect of selected kinases on DENV infection was further validated using chemical inhibitors. The kinases identified by this study can serve as targets for developing novel antiviral compounds against dengue infection.

6. Zusammenfassung

Das Denguefieber ist die am häufigsten von Stechmücken übertragene Viruskrankheit weltweit. Ursache für die Infektionskrankheit ist das Dengue Virus (DENV), ein einzelsträngiges RNA Virus, welches vorwiegend in von Monocyten abstammenden Makrophagen und dendritischen Zellen repliziert. Die Schwere des Krankheitsverlaufs ist abhängig von der Stärke der viralen Replikation, welche u. a. von bereits vorhandenen DENV-spezifischen Antikörpern und genetischen Determinanten des Virus und des Wirts abhängt.

Das Ziel meiner Arbeit ist die Charakterisierung der Funktion des Nicht-Struktur Proteins 5 (NS5) im Replikationszyklus des DENV. NS5 ist ein multifunktionelles Protein, welches in die Replikation der viralen RNA, der Erstellung der 5'-Cap-Struktur sowie der Blockierung Interferon (IFN)-induzierter Signalwege durch Degradation von STAT2 involviert ist. Obwohl DENV im Zytoplasma repliziert, akkumuliert das Protein hauptsächlich in den Nuklei infizierter Zellen. Im Laufe dieser Arbeit wurden die Determinanten für den Transport von NS5 in den Nukleus sowie den Einfluss des nukleären NS5 auf virale Replikation und die angeborene Immunabwehr untersucht. Die Akkumulierung von NS5 im Nukleus erfolgte unabhängig von den anderen DENV Proteinen und konnte sowohl in infizierten Säuger- als auch Stechmückenzellen gezeigt werden, was für eine evolutionär konservierte Eigenschaft des viralen Proteins spricht. Um Aminosäuren zu identifizieren, die für die nukleäre Akkumulation von NS5 essentiell sind, wurden Mutationsanalysen durchgeführt. Analysen der Replikation von Viren mit Mutationen im nukleären Lokalisationssignal (NLS) von NS5 zeigten, dass ein hoher Grad an NS5-Akkumulation im Kern für effiziente Replikation nicht nötig ist. Ist jedoch der nukleäre Transport des Proteins komplett blockiert, führt dies zu einer signifikanten Reduktion der viralen Replikation. Interessanterweise konnte die reduzierte Replikation der NLS-Mutanten nicht durch *in trans*-Komplementierung von Wildtyp-NS5 wiederhergestellt werden. Dies spricht dafür, dass zusätzlich zur Kernlokalisation weitere Eigenschaften des Proteins für die geringe Replikation verantwortlich

sind. Um zu überprüfen, ob Mutationen im NLS von NS5 Auswirkungen auf dessen enzymatische Aktivität haben, wurden rekombinante Volllänge-Proteine mittels eines bakteriellen Expressionssystems hergestellt und aufgereinigt. Enzymatische Analysen zeigten, dass - mit Ausnahme einer Mutante - keine der Mutationen die RNA-abhängige RNA-Polymerase- oder die Methyl-Transferase Aktivität beeinflusst. Außerdem war die IFN-Sensitivität der NLS-Mutanten vergleichbar mit der des Wildtyps, was dafür spricht, dass NS5 nicht notwendig ist, um IFN-indizierten Genen entgegenzuwirken. Im Gegensatz zu früheren Beobachtungen konnte kein signifikanter Unterschied in der Induktion von Interleukin-8 durch das Wildtyp- oder das mutierte NS5 festgestellt werden.

Im zweiten Teil meiner Arbeit führte ich einen genomweiten, RNAi-basierten Hochdruchsatz-Suchtest durch, um zelluläre Kinasen zu identifizieren, die die DENV Replikation unterstützen oder einschränken. Die Etablierungsphase beinhaltete das Erstellen von Versuchsprotokollen für einen bildbasierten Suchtest, was die Optimierung der Genexpressionshemmung in humanen Hepatomzellen, virale Infektion, Immunmarkierung infizierter Zellen, Bildaufnahme sowie die statistische Auswertung der Ergebnisse beinhaltete. Der primäre Suchtest adressierte alle bekannten und mutmaßlichen zellulären Kinasen mit je drei siRNAs pro Gen. Ungefähr 100 Kinasen wurden aufgrund des primären Suchtests in einem infektions-basierten Validierungs-Suchtest mit je drei weiteren unabhängigen siRNAs pro Gen untersucht. Der Suchtest identifizierte 18 Kinasen, die die DENV Replikation unterstützen und 15 Kinasen, die die virale Replikation einschränken. In einer weiteren Analyse mit einem subgenomischen Reporter Replikon wurde anschließend getestet, ob die Kinasen eine Rolle im Zelleintritt oder der RNA Replikation des Virus spielen. Der Effekt einzelner ausgewählter Kinasen auf das Virus wurde außerdem durch den Einsatz von chemischen Inhibitoren validiert. Die Kinasen, die in dieser Arbeit identifiziert wurden, können zur Entwicklung neuer antiviraler Wirkstoffe gegen das Denguefieber führen.

I. Introduction

I.1 Dengue

Dengue is the most prevalent mosquito-borne viral disease affecting humans. The disease is endemic to tropical and subtropical parts of the world causing an estimated 50-100million infections annually worldwide leading to approximately 20,000 deaths (9). In most cases the disease is self-limiting with either mild flu-like symptoms or acute febrile illness called dengue fever (DF). However 2- 5% of patients may develop more lethal form of the disease termed dengue hemorrhagic fever and dengue shock syndrome (DHF/DSS) characterized by hemorrhagic manifestations, capillary leakage, thrombocytopenia and hypovolemic shock (42). The last few decades witnessed rapid expansion in the geographical reach of the disease with outbreaks being presently reported from more than 100 countries (67). The frequent urban epidemics of DF/DHF have emerged as a major public health problem in many of the endemic countries with significant economic, political and social impact. Rapid urbanization, increased air travel, increased spread of vector population due to climatic changes and a inadequate sanitation and vector control efforts are some of the important factors contributed to global reemergence of this disease (42). Despite considerable research efforts over the past decades efforts of develop effective vaccines or drugs are not yet successful mainly due to higher genetic variability among dengue strains (114).

I.1.1 History and Epidemiology

The earliest reports of illness clinically compatible with dengue fever was found in a Chinese encyclopedia of disease symptoms and remedies first published during the Chin Dynasty [Common Era (CE) 265 to 420] and in similar reports later during the 7th and 10th centaury [Tang Dynasty (CE 610) and Northern Sung Dynasty (CE 992)]. The next reported incidence of illness with symptoms similar to dengue was from French West Indies and Panama during 1635 and 1639 respectively. One century later (1779-1788) cases with similar symptoms were reported from Batavia (present day Jakarta), Cairo,

Philadelphia, and Cadiz and Seville, Spain suggesting a possible pandemic. The higher incidence of the disease notably coincided with the increase in merchant shipping and human migration (42). By late 19th century dengue had established throughout the old world and the new world causing occasional pandemics. The increased global prevalence of DENV was also facilitated by the invasion of the African *Aedes aegypti* (*Ae. aegypti*) mosquito vector throughout the tropics, rapid urbanization, reduction in vector control efforts, rapid increase commercial air travel and climatic changes. By the beginning of 21st century all four serotypes became endemic in most tropical and subtropical countries. The circulation of various dengue strains in the same geographical area has dramatically increased the probability of occurrence of more severe forms of disease viz. DHF and DSS.The past few decades have seen dramatic increase in the number of DENV infections and the geographical spread of disease (Fig. 3).
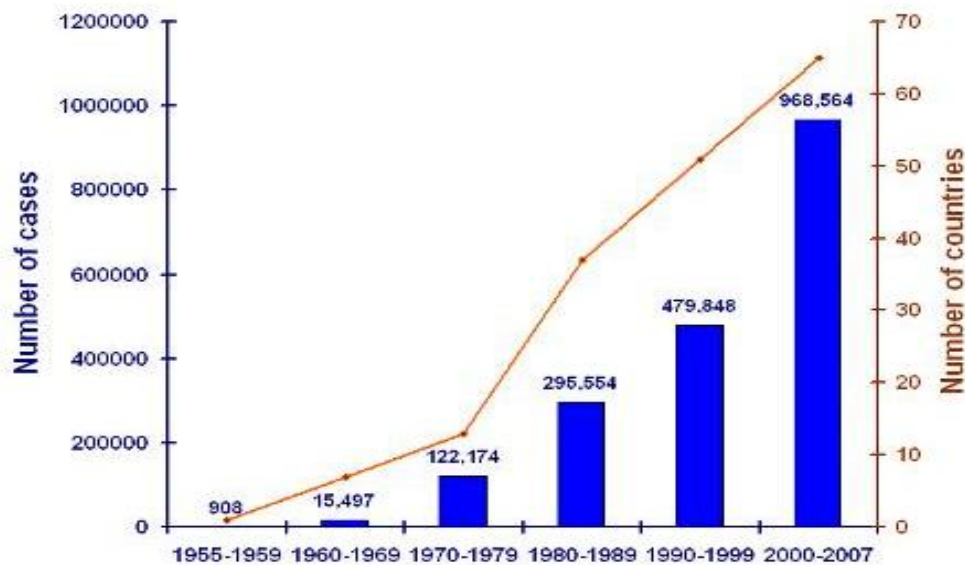
Fig.I.1 The global incidence of dengue over past six decades. The average number of dengue cases reported to World Health Organization (WHO) over various decades is depicted by blue bars and the number of countries reporting dengue indicated by brown line. Modified from WHO statistics on dengue (http://www.who.int/csr/disease/dengue/impact/en/index.html)

Presently an estimated 2.5 billion people live in dengue endemic areas spanning five continents (49). With nearly 500,000 patients developing the more severe DHF/DSS leading to more than 20,000 deaths, dengue has emerged as a major public health problem in many endemic countries (67).

I.1.2 Transmission, Symptoms and Pathogenesis

The virus is maintained in the wild by a transmission cycle between canopy-dwelling *Aedes* mosquitoes and lower primates in the rain forests of Asia and Africa (42). However these strains rarely cause wide-spread human infection. The most important transmission cycle from the public health standpoint is the urban transmission cycle in large urban centers in the tropics where the virus is maintained in an *A. aegypti* – human – *A. aegypti* cycle with periodic epidemics. Humans contract the disease when bitten by infectious mosquitoes belonging to species *A. aegypti* or *A. albopictus*. *A. aegypti*, the principal vector, is a small, black and white, highly domesticated tropical mosquito which prefers to breed in water collected in artificial containers including flower vases, old automobile tires, water storage containers, seasonal ponds and even septic tanks, producing large population of adult mosquitoes in immediate vicinity to human dwellings. The female mosquitoes alone bite humans and prefer to feed during day time with the peak feeding during few hours after dawn and few hours before dusk. The female mosquitoes are very nervous feeders, disrupting the feeding process at the slightest movement, hence end up probing multiple humans during a single blood meal. If the mosquito is infective, this behavior will result in infecting several persons in a short time. The virus is believed to be maintained by vertical transmission within the mosquito population during the inter-epidemic periods (44).

Once introduced into humans by an infective mosquito, the virus undergoes an incubation period averaging 4-7 days, after which the person may experience acute onset of fever accompanied by a variety of nonspecific signs and symptoms. During this acute febrile period, lasting 2-10 days, high titers of the virus are found in the peripheral blood. The virus can be acquired by mosquitoes feeding on infected persons during this period and can pass on to other uninfected persons after 8 to 12 days of incubation within the mosquitoes (42).

The clinical manifestations of DENV infection in humans includes a wide spectrum of illness ranging from inapparent to mild febrile illness to severe hemorrhagic fever and shock syndrome. The factors like the age, immune status and genetic background of the host and the strain and serotype of the

virus play an important role in determining the disease outcome. The most commonly reported outcome of DENV infection is Dengue fever (DF) characterized by a sudden onset of fever and a variety of nonspecific symptoms including headache, nausea, vomiting, body aches, retro-orbital pain, rashes and joint pains. The disease is generally self-limiting with the acute phase lasting up to a week followed by a convalescent phase extending to several weeks associated with weakness. In up to 2% of the cases (mostly in children under the age of 15) the disease may progress to a more sever DHF characterized by increased vascular permeability, thrombocytopenia and hemorrhagic manifestations from skin, nose, gum and gastro-intestinal tract (67). Some patient may exhibit DSS and succumb to circulatory failure due to hypovolemic shock induced by fluid leakage into interstitial spaces.

It is generally observed that the chances of developing DHF/DSS are higher during second time infection compared to first time infection. One of the prevalent theories extended to explain DHF/DSS pathogenesis is the phenomenon of antibody-dependent enhancement (ADE). This stems from the observation of higher incidence of DHF/DSS among patients contracting dengue for the second time with a different DENV serotype. The ADE theory suggests that antibodies generated against one serotype of DENV during the primary infection fails to cross –neutralize a different serotype during the second infection. These non-neutralizing antibodies facilitate an enhanced infection of monocytes and macrophages during second infection by forming virus-antibody complexes that are internalized by these cells by Fc receptor mediated endocytosis, resulting in their infection. This facilitates higher viral replication and immune activation accompanied by cytokine release (49).

The 'original antigenic sin' phenomenon is also attributed to the delayed virus clearance during secondary DENV infection where reactivation of cross-reactive T cells specific for the primary infection rather than the current infection results in ineffective virus clearance accompanied with increased cytokine release and apoptosis of both infected and uninfected bystander cells (77).

I.1.3 Vaccines and Treatment

Despite huge efforts made during the past few decades, there are no effective vaccines yet available against DENV (46, 47). Since all four dengue serotypes co-circulate in dengue endemic areas and ADE plays a crucial role in disease outcome, it is considered crucial that the vaccine must be able to protect against all strains of DENV. The leading vaccine candidates in clinical trial are the ChimeriVax (a yellow fever 17D vaccine strain expressing pre-membrane and envelope proteins of DENV) and various live attenuated strains developed by different companies (114). Since there are no effective drugs specifically targeting DENV, the current treatment regime is mostly symptom-based with close monitoring of vital signs during the critical infection periods. Platelet transfusion is given to patients suffering severe thrombocytopenia and intravenous infusions are administered to DHF/DSS patients to stabilize their blood volume level.

I.2 The Dengue Virus

I.2.1 Taxonomy and Evolution

DF and DHF/DSS, the most common arthropod-borne viral disease affecting humans is caused by four distinct but antigenically related serotypes (DENV-1, -2, -3 and -4) of DENV (67). DENV taxonomically belongs to the genus flavivirus in the family *Flaviviridae*. The genus flavivirus contains more than 55 species, including several important human pathogens like West Nile virus, Japanese encephalitis virus, Tick borne encephalitis virus and Yellow fever virus (YFV) which are mostly dependent on hematophagous arthropod vectors to complete their horizontal transmission cycle (50). The name flaviviruses originated from the latin word '*flavus*' meaning yellow that signifies jaundice, a common sign of infection with the prototypic Yellow fever virus. Viruses in the flavivirus genus are grouped taxonomically into three groups with regard to their vector association and antigenic relationships: (1) tick-borne, (2) mosquito-borne, and (3) viruses with no known arthropod vector (112) (Fig. I.1). DENV serogroup forms a distinct cluster within the group of mosquito-borne flaviviruses with an amino acid conservation of
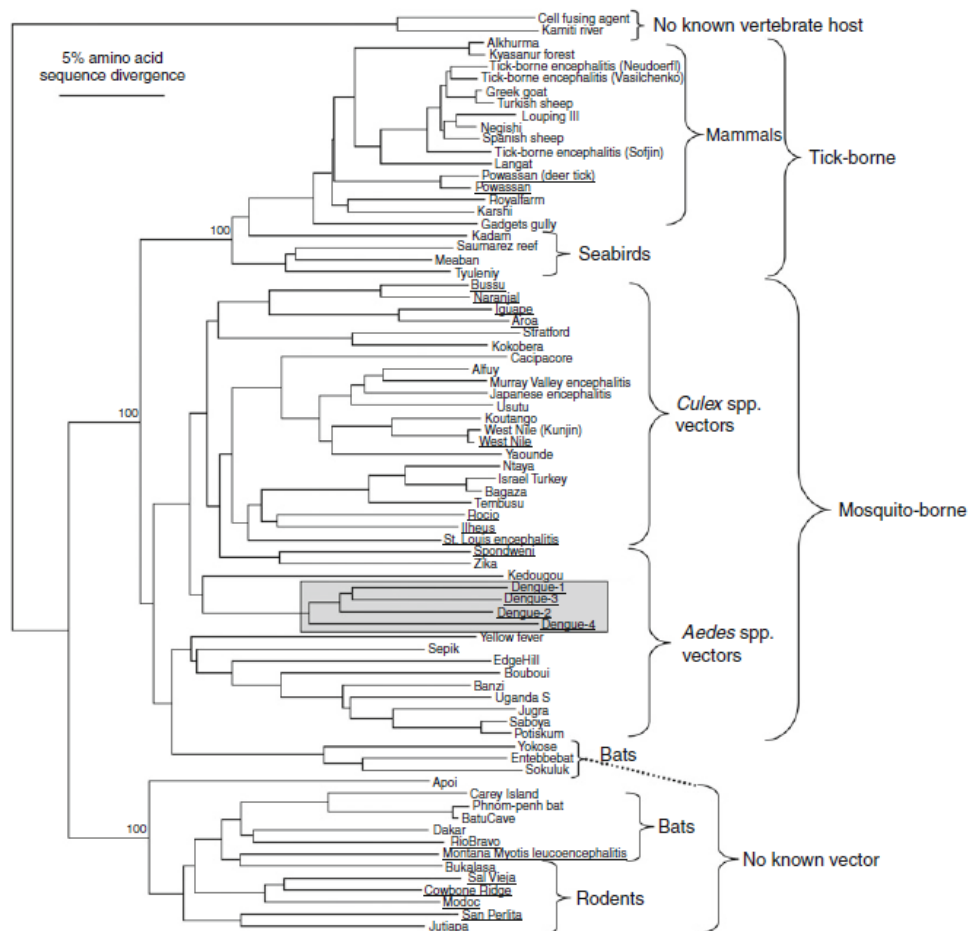
Fig.I.2 Phylogenetic tree of the Flaviviruses as deduced from partial NS5 sequences available in the GenBank library. Subtypes are written in parentheses after virus names. New World viruses are printed in bold and underlined. The tree was drawn using neighbor joining, and similar topologies were produced using Bayesian methods and maximum parsimony. Numbers indicate bootstrap values for major clades to the right. Reproduced from Weaver and Vasilakis, 2009 (113).

62-67% among the four serotypes (67). Among the four serotypes DENV-1 and DENV-3 are most closely related while DENV4 is the most divergent serotype and all the present serotypes evolved from their sylvatic ancestors within the last three centuries (109) (Fig.I.3). Each serotype is further classified into various 'genotypes' clustering DENV strains having nucleotide sequence divergence not greater than 6% within a given genomic region (96).

DENV is believed to have evolved from sylvatic strains in Africa or Asia that utilize nonhuman primate hosts and gallery forest-dwelling *Aedes* vectors. The sylvatic cycle is presumed to be ancestral because efficient inter-human transmission is thought to require a minimum human population size of 10,000 to 1 million, which did not exist until about 4000 years ago when ur-

ban civilizations arose (43). Extensive phylogenetic studies of endemic and sylvatic strains have supported the zoonotic origin of DENV serotypes progenitors within the last millennium (113) (Fig. I. 2) with South East Asia being the probable region of origin of all four serotypes of DENV. All the four serotype of DENV are thought to have evolved independently from ancestral sylvatic strains with concomitant changes in host range from arboreal *Aedes* mosquitoes to *Ae. albopictus* and later to *Ae. aegypti* and new vertebrate hosts.
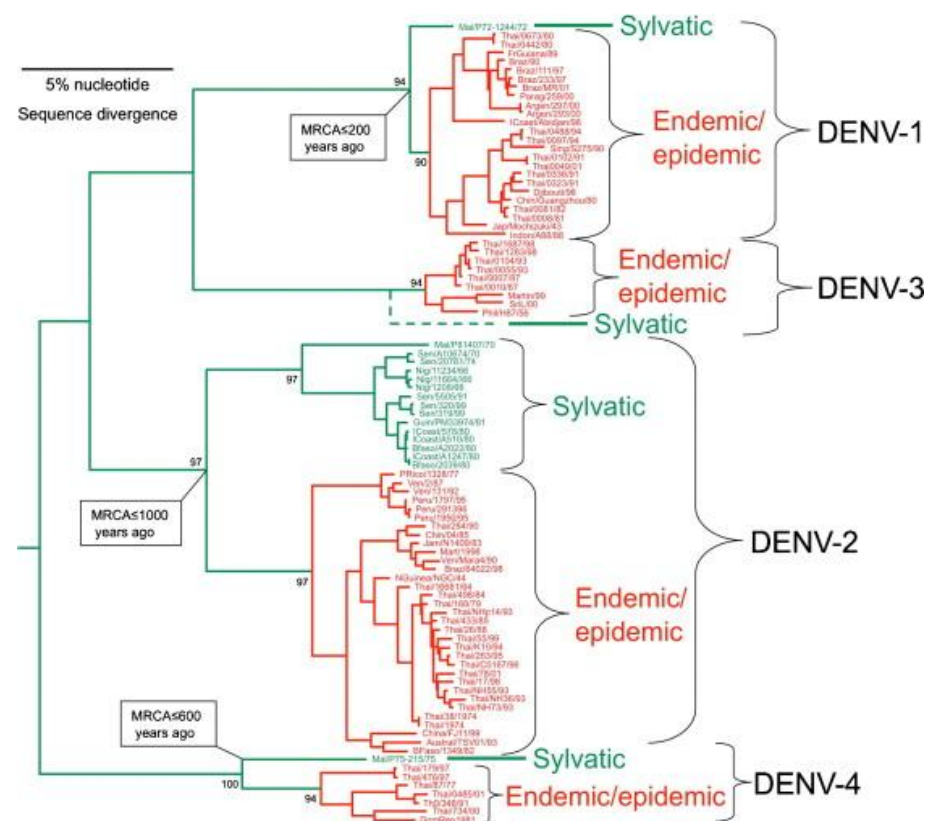
Fig.I.3 The sylvatic origin of DENV strains. Phylogenetic tree of DENV strains from four serotypes derived from complete open reading frames available in the GenBank library. The phylogeny was inferred using Bayesian analysis and all horizontal branches are scaled according to the number of substitutions per site. Bayesian probability values are shown for key nodes. Virus strains are coded by abbreviated country of collection/strain name/year of collection. Reproduced from Weaver and Vasilakis, 2009 (113).

I.3 Molecular biology of DENV

I.3.1 Genome organization

DENV genome is a single-stranded RNA molecule of 10.7 kb length with a positive polarity (Fig.I.4) and is readily translatable like cellular mRNA. The

genome contains a type I cap at the 5' end but is not polyadenylated at the 3'end. The first ~100 nucleotides at the genomic 5' end termed 5' untranslated region (UTR) are non-coding, highly structured and harbors regulatory elements involved in viral replication and translation. The predicted structure of 5'UTR consists of two stem-loops: a large stem-loop A (SLA) and a second short stem-loop B (SLB) which ends in the translation initiation AUG codon. SLB harbors a sequence known as 5'UAR (Upstream AUG region) that is complementary to sequence located at the 3' UTR (4). The 3' UTR is 384-466 nucleotides long and like 5'UTR is highly structured and contains important regulatory regions. The 3' end of 3'UTR folds into a highly conserved stem-loop (3'SL) which was found essential for viral replication. Upstream to 3'SL is the conserved sequence 1 (CS1) (74) which harbors the cyclization sequence (CS) that is complementary to sequence present at the 5' end of the genome. The 5'-3' long range interaction between CS and UAR elements at the 3'end with their complementary sequence at the 5' end cyclizes the genome and was found essential for virus replication (2, 3). Numerous viral and cellular proteins interact with the 5' and 3'UTRs and play a crucial role for viral replication (28, 30, 39, 91, 118).
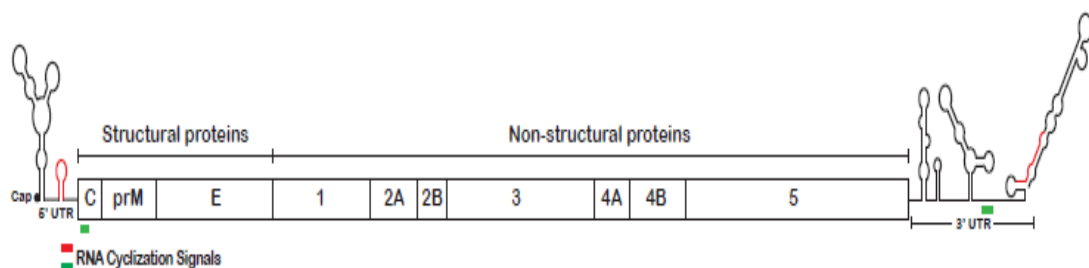
Fig.I.4 Genome organization of DENV.
The 5' URT (~100 nucleotides) and 3'UTR (~450 nucleotides) contains regulatory elements for translation and replication. The cyclization of genome by the CS (green) and UAR (red) elements is essential for replication. The genome encodes a single polyprotein (~3400 amino acids) which is co- and post translationally cleaved into 3 structural and 7 non-structural proteins.

I.3.2 Translation and polyprotein processing

The viral genome is a single stranded, capped RNA with positive polarity that can be directly translated as it is released into the cytoplasm. The genome contains a single open reading frame (ORF) encoding a polyprotein (~3400 amino acids) which is co- and post translationally processed by cellular and viral proteases.

The N-terminal part of the polyprotein is processed into three structural proteins (C-prM-E) which eventually form part of virions while the rest is cleaved into seven non-structural proteins (NS1-NS2A-NS2B-NS3-NS4A-NS4B-NS5) which organize the replication machinery of the virus (Fig.I.5) (9). The NS3 along with NS2B as co-factor forms the viral protease that cleaves the protein junctions between C/prM, NS2A/NS2B, NS2B/NS3, NS3/NS4A, NS4A/NS4B and NS4B/NS5. The endoplasmic reticulum (ER) luminal junctions between C/prM, prM/E, E/NS1 and NS4A/NS4B are processed by signalse, an ER resident host protease. The virion maturation is assisted by Golgi-resident furin endoprotease by processing prM to mature M protein. The identity of the protease cleaving NS1/2A junction is not known yet.
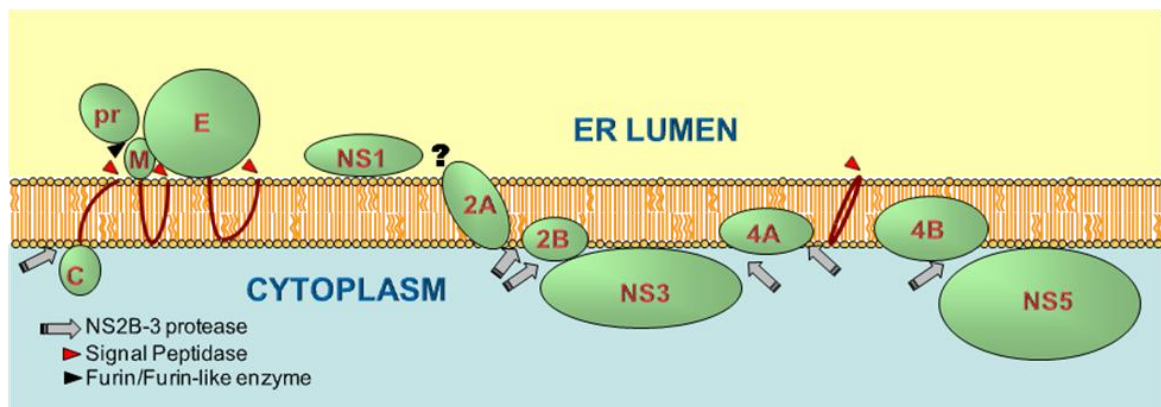
Fig.I.5 Processing of the DENV polyprotein. The viral NS3/2B protease processes the protein junctions on the cytoplasmic side whereas host-derived signalase process the ER luminal protein junctions. The protease cleaving NS1/2A is presently unknown.

I.3.3 Structure and Assembly of DENV particles

Infectious virus particles are approximately 50nm in diameter containing an electron-dense central nucleocapsid ($\sim$ 30nm diameter) enveloped by a lipid bilayer (65). The nucleocapsid is composed of multiple copies of highly basic C (capsid) protein complexed with a single copy of DENV genomic RNA. During virion assembly the nucleocapsid buds into ER lumen thereby getting enveloped in a membrane bilayer carrying the viral prM and E proteins (115). These immature particles are transported through the cellular secretory pathway, where the furin protease cleaves prM, resulting in formation of mature virus particles. Extensive structural rearrangements of E protein takes place during the virion maturation and fusion with host membrane in the en-

dosomal compartment (68). The E protein in immature virions is prevented from premature-fusion by formation a heterodimer with prM protein. The furin-mediated processing of prM results in formation of mature virions carrying E homodimers. The virions are internalized by receptor-mediated endocytosis. The reduction in pH in late endosomes induces formation of E-homotrimers triggering membrane fusion and release of nucleocapsid into cytoplasm starting a new round of infection.
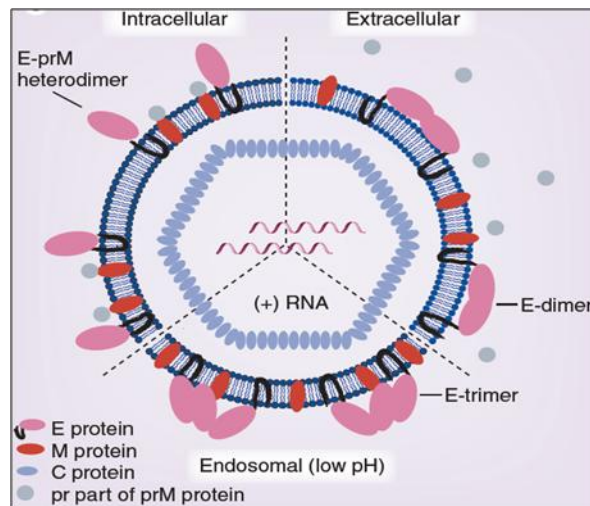
Fig.I.6 The structure of DENV virions. The nucleocapsid comprising multiple copies of C protein and single copy of genomic RNA is enveloped by a lipid bilayer carrying the E and M proteins. The membrane-bound E protein undergoes several structural rearrangements during virion maturation and during fusion in late endosomal compartment. Modified from Bartenschlager & Miller, 2008 (9).

I.3.4 DENV proteins and functions

The exact functions of all viral proteins are presently not known. All three structural proteins (C, prM and E) and genomic RNA are essential for assembly of infectious virions and all nonstructural proteins are indispensible for the organization of replication complexes in the cytoplasm (115) and are implicated in counteracting cellular antiviral defense (7, 57). The known functions of viral proteins are summarized in Table I.1.

Table I.1 Structural and functional properties of DENV proteins.

Pro-tein	M.W . (KDa.)	Localization	Known Modifi-cations	Known Functions	Protein inte-ractions
Capsid	12	Lipid droplets, Cytoplasm, Nucleus	None	RNA binding, nucleo-capsid precursor	Daxx (84), Sec3(13)
Mem-brane	11	ER membrane	gylcosylation	Virion morphogene-sis/transport	Envelope, v-ATPase (31), Claudin-1 (38)
Enve-lope	54	ER membrane	glycosylation	Virion assembly, re-ceptor binding, mem-brane fusion	prM, NKp44 (51), BiP, Cal-nexin, Calreti-culin (69)
NS1	46	ER lumen, plasma mem-brane, se-creted	glycosylation, GPI anchor (55)	Replication, virus ma-turation	NS4A (70),hnRNP C1/C2 (86), Clusterin (66), STAT3β (24)
NS2A	22	ER membrane	None	Replication	
NS2B	14	ER membrane	None	Replication, co-factor of NS3 protease	NS3
NS3	69	Cytoplasm	None	Protease, Helicase, NTPase, RTPase	NS2B, NS5, NS4B (110), NRBP (25), La (39)
NS4A	16	ER membrane	None	Replication, anti-STAT1	
NS4B	27	ER membrane	None	Replication, anti-STAT1	NS3
NS5	104	Cytoplasm, nucleus	phopshoryla-tion	Methyl transferase, guanyl transferase, RdRP, anti-STAT2	NS3, STAT2, Importin, ZO-1(33)

I.3.5 DENV infection cycle

DENV can replicate in both human and mosquitoe hosts. The female mosqui-toes of the genus *Aedes* become infected by feeding on DENV infected person or transovarially from its infected mother. After a blood meal from an infec-tious person the virus infects midgut epithelium and spreads possibly through tracheal system to other parts of the body including the neuronal system and salivary glands. The mosquitoes turn infectious by 4-14 days post-feeding

and remain so for rest of their life (99). The infectious mosquitoes inject the virus from salivary glands to blood stream of humans during feeding. Though a wide range of cells including B-cells, T-cells, endothelial cells, neuronal cells and hepatocytes can support DENV replication monocytes and macrophages and dendritic cells derived from them are considered the major sites of dengue replication in patients (6). Several cellular proteins and glycosaminoglycans are reported as cellular receptors for DENV. These include heparin sulfate, heat shock protein 70 (Hsp70), Hsp90, GRP78/BiP, CD14, and 37-kDa/67-kDa high affinity laminin receptor, as well as DC-specific intercellular adhesion molecule 3 (ICAM-3)-grabbing nonintegrin (DC-SIGN) and liver/lymph node-specific ICAM-3-grabbing nonintegrin (see (27) and references therein). The receptor-bound virus is internalized by endocytosis and the low pH in late endosome triggers structural rearrangement of E protein on virions resulting in fusion of viral envelope with endosomal membrane releasing the nucleocapsid into cytoplasm. The nucleocapsid disassembles and viral genomic RNA (vRNA) is translated by ER-associated ribosomes producing multiple copies of viral proteins. NS5 along with other viral non-structural proteins and presumably various host proteins organize replication complexes in virus-induced intracellular membrane structures (115). Within the replication complex the viral polymerase transcribes the vRNA to produce the complementary strand which serves as template for synthesis of subsequent vRNA copies. The replication is semi-conservative and asymmetric with a ten-fold excess of positive strands produced compared to negative strand. The newly synthesized vRNA is used for translation, assembly of new replication complexes or is assembled into virus particles. The virions bud into ER lumen and is released through the classic secretory pathway. The prM on the virions is cleaved to generate membrane (M) protein by cellular furins during its transit through trans-golgi network generating the infectious particles.
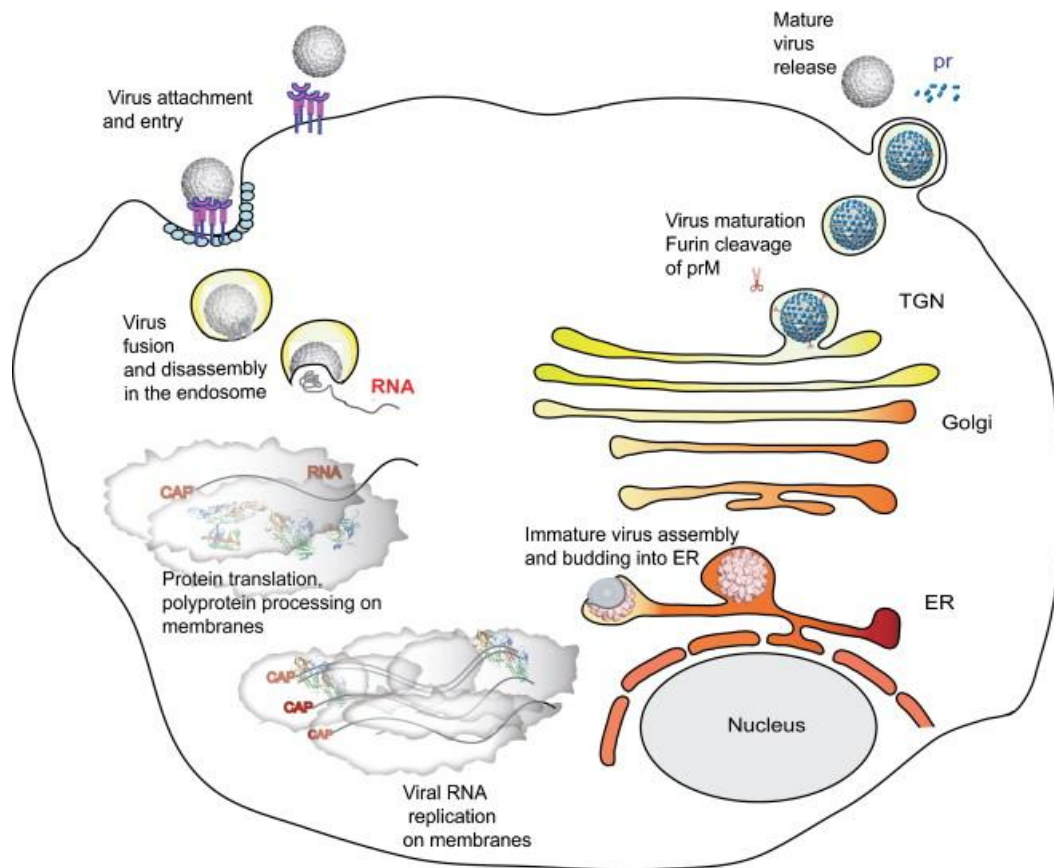
Fig.I.7 DENV replication cycle. Virions bind to cell-surface attachment molecules /receptors like heparan sulfate, DC-SIGN and are internalized through endocytosis. The low pH of late endosomes, triggers fusion of virions with endosomal membrane releasing viral RNA into cytoplasm. The viral RNA is translated by cellular machinery and viral non-structural proteins form the replication complexes where the viral RNA is amplified. Virions bud into the lumen of ER. The virion maturation occurs during their transport through the secretory pathway. New round of infection can be initiated by the mature virions released. Adapted from Sampath & Padmanabhan, 2009 (101)

I.4 Dengue NS5

NS5 is the largest (105kDa.) and most conserved protein encoded by flaviviruses. The protein is indispensible for viral replication and is essential for vRNA amplification and capping. Structural and biochemical studies had demonstrated that the N-terminal domain of NS5 harbors methyl transferase (MTase) and guanylyl transferase (GTase) activities whereas the C-terminal domain carries RNA-dependent RNA polymerase (RdRP) activity. (29). NS5 was also reported to interact with several viral and cellular proteins and in modulating the cellular immune response including blocking IFN signaling by degrading STAT2 protein (7, 54, 108, 117). NS5 associates with NS3 to form membrane-associated replication complexes and is also found in free form in

cytoplasm and nucleus (36, 56, 93, 94). The protein is believed to be partially phosphorylated and shuttle between the cytoplasm and nucleus and this process is considered essential for viral life cycle (29).

I.4.1 NS5 phosphorylation

The polymerase proteins of many flaviviruses are reported to be phosphorylated (11, 59, 79). In DENV infected cells the nuclear localized fraction of NS5 is reported to be phosphorylated (59). This phosphorylation is serine specific and modulates NS5 interaction with NS3 and probably its integration into replication complexes. A CKII phosphorylation site was identified in NS5 and this phosphorylation was found to inhibit nuclear import of NS5 (36). Recent mass spectrometric studies have identified threonine 449 as one of the phosphorylation sites which could be phosphorylated by protein kinase G (PKG) (12). The mutation of this threonine to a nonphosphoacceptor amino acid reduced viral replication indicating the importance of this phosphorylation to viral replication. Similarly viral replication was also reduced when PKG was silenced using RNA interference (RNAi). However the exact function of this phosphorylation in viral life cycle is still not clear.

I.4.2 Immune response modulation by NS5

The IFN (IFN) response is a key host defense against many viruses including flaviviruses. Cells treated with IFN-β prior to DENV infection was able to elicit a strong antiviral response and strongly reduce virus infection whereas addition of IFN-β to cells already infected with DENV had no effect on viral replication. Various studies have identified the involvement of different dengue nonstructural proteins in blocking various steps of IFN-induced antiviral defense. Signal transducers and activators of transcription (STAT) proteins play a key role in transmitting the signal from plasma membrane bound IFN receptors to the cell nucleus and initiating IFN induced gene expression. Previous studies have demonstrated that DENV NS4B and to a lesser extend NS2A and NS4A down regulate IFN-β mediated gene expression (82). The regions of NS4B responsible for this phenotype were mapped and NS4B was shown to reduce STAT1 phosphorylation and hence its activation (81, 82). Further studies reported the role of NS5 in preventing STAT2 phosphorylation

and accelerating its proteasome-mediated degradation (7, 72). The NS5 polymerase domain alone was necessary to inhibit STAT2 phosphorylation whereas viral polyprotein processing was shown to be essential for inducing STAT2 degradation.

I.4.3 Nuclear Localization of NS5

Despite all known functions of NS5 occurring in the cytoplasm, a significant amount of the protein localizes into the nucleus during infection (58, 76). Similar observations were also made for YFV NS5 (20) but not for other flaviviruses like WNV and KUNV. Previous studies have identified two functional nuclear localization signals (NLS) in NS5 namely β-NLS and $\alpha\beta$-NLS due to their interaction with either β-importin or both α- and β-importins (19, 36, 56). Mutational analyses indicated that $\alpha\beta$-NLS plays an essential role in nuclear localization of the protein (93). Viruses bearing mutation in $\alpha\beta$-NLS exhibited reduced NS5 nuclear accumulation, reduced viral replication and induced a transient increase in interleukin-8 (IL-8) secretion compared to wild type (93). Recent studies have shown that a portion of NS5 is transported out from the nucleus by CRM1 mediated nuclear export and this process is depended on a nuclear export sequence (NES) located in β-NLS (94). Mutations in the NES that reduced nuclear export of NS5 were found to moderately suppress IL-8 induction and enhance virus release. The crystal structure of DENV NS5 polymerase domain and methyl transferase domain (32, 117) revealed that contrary to earlier assumptions NLS sequence forms an integral part of NS5 polymerase domain. This indicates nuclear localization and enzymatic activity of NS5 could be strongly interrelated as evidenced from the observation that enzymatically less active form of NS5 is hyperphosphorylated and is mostly nuclear localized(59).

I.5 Cellular proteins involved in DENV replication cycle

Viruses are intracellular parasites depending entirely on its host for survival. They encode only a limited number of genes hence extensively exploit different cellular machineries at various steps in their life cycle. The viruses during their long association with hosts have evolved sophisticated methods to ex-

ploit host resources for their propagation and subvert the antiviral defense mounted by the host cell. The high error rate of viral polymerases ensures that RNA viruses exist as a population of quasi-species which enable them to quickly adapt and survive the selection pressure within the host. The viral and host proteins and nucleic acids exist in close proximity within the cell and depending on the nature of virus-host interaction the cellular protein can assist or oppose viral replication. The role of most of the viral proteins in infection process is presently known however only limited investigations were carried out to elucidate the role played by cellular proteins in infection outcome. More information in this field can help to develop a better understanding of virus biology and device novel therapeutic interventions.

In past large-scale studies investigating the role of cellular proteins on viral life cycle were restrained by technical difficulties. Conventionally such studies were limited to cellular proteins that were identified to have direct interaction with viral proteins or nucleic acids by techniques like yeast two hybrid studies or co-immunoprecipitation studies. These techniques were low throughput and often identified interactions which could not be assigned a functional role. The functional studies were also hampered by the absence of efficient techniques to regulate the expression cellular genes.

I.5.1 RNAi Screens

The double-stranded RNA mediated gene silencing initially demonstrated in *C. elegans* (35) developed into a powerful tool for reducing the mRNA levels of targeted genes resulting in downregulation of their gene products. The introduction of 21-27 nucleotide double stranded siRNAs extended this technique to mammalian cells which were prone to apoptosis in presence of longer double strand RNAs. The specificity of siRNAs combined with its amenability to high throughput screening methods turned RNAi to a powerful tool to study several cellular pathways. Several new genes involved in basic cellular pathways like endocytosis (90), cell division (60) and lipid droplet biogenesis (45) were identified in the past few years using this tool.

I.5.2 RNAi screens for identification of cellular genes influencing the viral life cycle

Genome-wide RNAi screens were also employed to identify cellular factors modulating the entry and replication of several human pathogen like Human Immunodeficiency virus (HIV) (17, 62, 119), Hepatitis C virus (HCV) (85, 106, 107), Influenza virus (61) ,WNV (63) and DENV (103).

The WNV RNAi screen was carried out in HeLa cells and genes showing variation in replication by more than two standard deviations compared to control siRNAs with two or more independent siRNAs were considered as hit. The candidates identified from WNV screen were later tested for their effect on DENV entry and replication to identify genes commonly affecting both viruses. Of the 283 genes identified essential for WNV replication, 36% had a significant effect on DENV replication as well. The pathways involving vATPase, ER associated degradation (ERAD) genes and Histone deacetylases (HDACS) were found conserved among both the viruses. Interestingly all the host resistance factors (HRFs) identified had similar effect for both WNV and DENV indicating similar antiviral mechanisms employed by the host against both pathogens. The RNAi study on the drosophila genes required for DENV replication identified 116 genes and among their 82 identifiable human homologues 42 had a significant effect of viral replication in Huh-7 cells. The gene candidate selection criteria was a expected sum rank (E[SR]) score below 0.065 with more than one siRNA against same gene (103). A comparative analysis of candidates generated by both screen indicate limited overlap between both screens except for genes vATPase and Sec61 probably due to the use of different cell lines and screening approaches. Moreover both studies did not primarily screen for mammalian cellular factors required for DENV replication rather tested host factors obtained as candidates in WNV and DENV arthropod screens for their effect on DENV infection in mammalian cells.

Another approach employed to identify host factors was use of know inhibitors of cellular genes. On this line a recent study screened a library of kinase inhibitors to identify potential kinase inhibitors involved in the entry, replication or release of DENV in Vero cells (23). The primary screen was imaging

based with a candidate selection criterion of reduction in number of virus infected cells by 50% compared to control treatment. The study identified and validated c-Src kinase as a cellular factor essential for efficient virus release and its inhibitor dasatinib as a potential therapeutic agent.

I.6 Objectives of this work

This thesis aimed at the investigation of the molecular aspects of virus- host interaction during DENV infection with the following two objectives

I.6.1 Studying the role of nuclear NS5 in viral replication and modulation of innate immune response

The NS5 protein of DENV is known to translocate to the nucleus upon viral infection even though viral replication takes place in the cytoplasm. The aim of this subproject was to systematically analyze nuclear NS5 transport by investigating the following aspects: first, a mutation analysis to identify residues in NS5 responsible for nuclear localization and to determine the effect of these mutations on DENV replication in cell culture; second, a biochemical analysis of full length NS5 proteins containing NLS mutations to determine their impact on RdRp and 5' end capping activities; third, trans-complementation studies to rescue NLS mutations; and fourth, an investigation of the response of NLS mutations on IFN response and IL-8 induction.

1.6.2 Identification of cellular kinases involved DENV infection and replication by using genome-wide RNAi screen.

RNAi screens have emerged as powerful tools to rapidly screen and identify genes significantly affecting various cellular processes and viral infections. In this subproject I wanted to identify cellular kinases promoting or inhibiting DENV infection and replication in human liver cells (Huh-7). For this purpose I had to establish an imaging-based screening system based on infection of Huh-7 cells and automated image analyses. Validated kinase genes should be studied in detail for their contribution of DENV replication, most notably nuclear localization of NS5.

II. Materials and Methods

II.1 Materials

II.1.1 Antibodies

Table II.1 The primary antibodies used in this study

Antibody	From (Organism)	Type	Source
Anti-DV2 E	Mouse	Monoclonal	ATCC, USA
Anti-DV2 NS5	Rabbit	Polyclonal	Miller et al, (75)
Anti-HA	Mouse	Monoclonal	Zymed, USA

Table II.2 The secondary antibodies used in this study

Antibody	From (Organism)	Specificity	Source
GαM, Alexa Fluor®546	Goat	Mouse IgG	Molecular Probes, Invitrogen USA
GαR, Alexa Fluor®546	Goat	Rabbit IgG	Molecular Probes, Invitrogen USA
GαM, Alexa Fluor®488	Goat	Mouse IgG	Molecular Probes, Invitrogen USA
GαR, Alexa Fluor®488	Goat	Rabbit IgG	Molecular Probes, Invitrogen USA
GαR HRP	Goat	Rabbit IgG	Sigma-Aldrich, Germany
GαM HRP	Goat	Mouse IgG	Sigma-Aldrich, Germany

II.1.2 Bacterial Strains

The following bacterial strains were used for the present study (table II.3). The strain DH5α was used for all regular cloning experiments whereas Rosetta (DE3) was used for protein expression in bacterial cells.

Table II.3 The bacterial strains

E. coli strain	Genotype
DH5α	F′ /endA1 hsdR17A($r_k^-m_k^+$) supE44 thi-1 recA1 gyrA (Nal^r) relA1 Δ(lacZYA-argF)U169 deoR (ϕ80dlac Δ(lacZ) M15)
Rosetta (DE3)	F$^-$ ompT hsdS$_B$(R$_B^-$ m$_B^-$) gal dcm λ(DE3 [lacI lacUV5-T7 gene 1 ind1 sam7 nin5]) pLysSRARE (Cam^R)

II.1.3 DNA and RNA oligonucleotides

The DNA oligos and siRNAs used in this work were procured from Eurofin MWG Operon AG (Ebersberg, Germany), Invitrogen (Karlsruhe, Germany), Qiagen (Hilden, Germany) or Ambion, Applied Biosystems (Darmstadt, Germany). The oligonucloetides were supplied as lyophilized powder which is resuspended in double distilled water or in appropriate buffer as suggested by the manufacture. The list of all DNA oligos and siRNAs used in this study are listed in later sections.

II.1.4 Instruments

Table II.4 Instruments used in this study

Instrument	Manufacturer
ABI Prism™ 310 Genetic Analyzer	Perkin-Elmer Cetus, USA
Bacterial Shaker TR-225	INFORS, Switzerland
BioChem-VaccuCenter BVC21 Cell culture	Vacuubrand GmbH & Co, Wertheim
Branson Sonifier 450	G. Heinemann, Schwäbisch Gmünd
Centrifuge 5417 C	Eppendorf, Hamburg
Centrifuge 5417 R	Eppendorf, Hamburg

Centrifuge Multifuge 3 S-R	Heraeus Instruments, Hanau
Centrifuge Sorvall RC-5C plus	Sorvall, Langenselbold
Cold Trap	H. Saur, Reutlingen
Cold Trap Pump	KNF Neuberger Laboport, Freiburg
Curix 60 Developer Machine	AGFA, Cologne
Digital Weighing Balance	Sartorius, Göttingen
DNA gel chamber and apparatus	EMBL workshop, Heidelberg
Electric Power Supply EPI 500/400	Amersham Pharmacia Biotech, Frei-
Gel documentation Instrument	Intas, Göttingen
Geldryer 1125B Dual Temperature	BioRad, Munich
HeraFreeze Deep freeze Refrigerator	Heraeus Instruments, Hanau
HeraSafe Laminar flow cabinet	Heraeus Instruments, Hanau
Immunofluorescence Microscope Leica	Leica, Mannheim
Incubator Stericult 200	Forma Scientific, USA
Inversion mixer REAX 2	Heidolph, Darmstadt
Lab pH-Meter CG-842	Schott AG, Mainz
Luminometer Lumat LB 9507	Berthold Technologies, Bad Wildbad
Magnetic Stirrer RTC basic	IBS, Switzerland
Microfuge B	Beckmann, Krefeld
Microwave Oven	CIAtronic
Minishaker MS2	IKA®, Staufen
PipetteBoy*acu*	IBS, Switzerland
Protein-Gel chamber and apparatus	Biorad, Munich
Rocking platform Biometra WT 16	Biometra, Göttingen
Semidry-Blot apparatus	H. Hölzel, Wörth
Thermomixer compact	Eppendorf, Hamburg
Ultrasound Sonicator pump and Cup horn	G. Heinemann, Schwäbisch Gmünd
UV Spectrophotometer Ultospec 2100 pro	Amersham Pharmacia Biotech, Frei-
UV Transilluminator	Vilber Lourmat, Eberhardzell

| Waterbath GFL 1083 | GFL, Hannover |

II.1.5 Enzymes, Kits and other reagents used

Table II.5 The list of Kits, Enzymes and other reagents used in this study

Product	Manufacturer
ABI Prism™ Big Dye	ABI, Darmstadt
Amicon® Ultra-15 Centrifugal Filters	Millipore, USA
Anti-HA Agarose conjugate	Sigma-Aldrich, Germany
Biomax MR, MS and ML Films	Kodak, Stuttgart
Calf Intestinal Phosphatase (CIP)	New England Biolabs, Frankfurt/Main
Casein Kinase 1 inhibitor, CKI-7	USBiological, USA
Casein Kinase 1 inhibitor, D4476	Calbiochem, USA
Casein Kinase 1 inhibitor, D4476	Calbiochem, USA
Casein Kinase 1 inhibitor, IC-261	Calbiochem, USA
Casein Kinase 2 inhibitor, DMAT	Calbiochem, USA
Casein Kinase 2 inhibitor, TBB	Sigma-Aldrich, Germany
Casein Kinase inhibitor, D4476	Calbiochem, USA
Casein Kinase inhibitor, SP600125	Sigma-Aldrich, Germany
Centricon Plus-20 Ultracel PL Filter	Millipore, USA
Dioctanoylglycol	Santa Cruz Biotechnology, USA
DNAse	Promega, Mannheim
dNTPs	Roche, Mannheim
ECL$_{plus}$ Western Blot Detection System	Amersham Pharmacia Biotech, Frei-
FideliTaq™	USB, USA
Hygromycin B	Invitrogen, Karlsruhe
Interferon-α	Sigma-Aldrich, Germany
Interferon-γ	Sigma-Aldrich, Germany
IPTG	Applichem, Darmstadt

Klenow	New England Biolabs, Frankfurt/Main
Leptomycin B	Sigma-Aldrich, Germany
Lipofectamine ™2000	Invitrogen, Karlsruhe
Nitrocellulose Western Blot Membrane	Schleicher & Schuell, Dassel
n-Octyl-β-D-glucopyranoside	Calbiochem, USA
NP-009245	AnalytiCon Discovery, Germany
NucleoSpin® Extract II kit, Plasmid kit	Macherey & Nagel, Düren
Polynucleotidekinase (PNK)	Amersham Pharmacia Biotech, Frei-
ProFection® Mammalian Transfection	Promega, Mannheim
Protease Inhibitor Cocktail (Complete)	Roche, Mannheim
Protein G-Sepharose® 4B	Sigma-Aldrich, Steinheim
QIAgen™ Plasmid Maxi Kit	Qiagen, Hilden
QIAshredder	Qiagen, Hilden
R59-022	Santa Cruz Biotechnology, USA
RNA cap structure Analogues	New England Biolabs, Frankfurt/Main
RNasin	Promega, Mannheim
rNTPs	Roche, Mannheim
RRL-Nuclease treated	Promega, Mannheim
SeaPlaque GTG Agarose	Biozym, Oldendorf
Sinefungin (Insolution)	Calbiochem, USA
T4 DNA-Ligase	MBI-Fermentas, St. Leon-Rot
T7 RNA-Polymerase	Promega, Mannheim
TNF-α (Human recombinant)	PeproTech GmbH, Hamburg

II.1.6 Buffers and Solutions

Table II.6 The Buffers and Solutions used in the course of this work

For DNA and RNA	
3M Sodium Acetate (pH 4.5)	3M Sodium Acetate, pH adjusted to 4.5 with Glacial Acetic acid
2M Sodium Acetate (pH 6.8)	2M Sodium Acetate, pH adjusted to 6.8 with Glacial Acetic acid
DNA loading dye	1mg/ml Bromophenol blue, 2mg/ml Xylene cyanol, 1mM EDTA, 50% (w/v) Saccharose
NEB buffer 1	10 mM Bis Tris Propane-HCl, 10 mM MgCl2, 1 mM DTT (pH 7.0 at 25°C)
NEB buffer 2	10 mM Tris-HCl, 10 mM MgCl2, 50 mM NaCl, 1 mM DTT (pH 7.9 at 25°C).
NEB buffer 3	50 mM Tris-HCl, 10 mM MgCl2, 100 mM NaCl, 1 mM DTT (pH 7.9 at 25°C).
NEB buffer 4	20 mM Tris-acetate, 10 mM magnesium acetate, 50 mM potassium acetate, 1 mM DTT (pH 7.9 at 25°C).
FideliTaq PCR-buffer (10x)	100mM Tris-HCl (pH 8.3), 500mM KCl, 15mM $MgCl_2$, 0.01% (w/v) Gelatine
RNA loading buffer	0.25mg/ml Bromophenol blue, 0.25mg/ml Xylene cyanol, 1mM EDTA (pH 8.0), 50% (v/v) Glycerol
RRL buffer (5x)	400mM HEPES (pH 7.5), 60mM $MgCl_2$, 10mM Spermidin, 200mM DTT
T4-DNA Ligase Buffer	400mM Tris-HCl (pH 7.8), 100mM $MgCl_2$, 100mM DTT, 5mM ATP
TAE (50x)	2M Tris, 2M Acetic Acid, and 50mM EDTA, pH 8.3
TE	10mM Tris-HCl (pH 8.0), 1mM EDTA

SDS PAGE and Western Blot

Acrylamide solution	A filtered and degassed solution of 29:1 Acrylamide and Bisacrylamide
Wester blot Blocking buffer	1x PBS, 0.5% (w/v) of Tween20, 3% Protease free Milk Powder
Coomassie Staining solution	0.25% (w/v) Coomassie Brilliant Blue R-250, 50% (v/v) Methanol, 10% Glacial Acetic acid
Destaining solution	5% (v/v) Methanol, 5% (v/v) Glacial acetic acid
Protein Loading (Laemmli) buffer (2x)	200mM Tris-HCl (pH8.8), 5mM EDTA, 0.1% (w/v) Bromophenol Blue, 10% (w/v) Sucrose, 3% (w/v) SDS, 2% (v/v) β-Mercaptoethanol
Stacking gel buffer	1M Tris-HCl (pH 6.8), 0.8% (w/v) SDS
Antibody Binding Buffer	1x PBS, 0.5% (w/v) of Tween20, 3% Protease free Milk Powder
Semi-dry Blotting Buffer	48mM Tris, 39mM Glycine, 0.00375 (w/v) SDS, 20% (v/v) Methanol
Nitrocellulose membrane Stripping Solution	0.2M Glycine, 0.5M NaCl, pH 2.8
TGS-Buffer	150mM Tris, 1,92M Glycine, 1% (w/v) SDS
Resolving gel buffer	1.5M Tris-HCl, pH8.8, 0.4% (w/v) SDS
Western blot Wash Buffer	1x PBS, 0.5% (w/v) Tween20

Immunofluorscence

Paraformaldehyde (4%)	4g Paraformaldehyde is dissolved in 100ml 1x PBS by heating to 60°C
Blocking buffer	3% Normal Goat Serum in 1x PBS

Luciferase Assay

Luciferase Assay Buffer	25mM Glycine-Glycine (pH 7.8), 15mM Potassium phosphate buffer (pH 7.8), 15mM $MgSO_4$, 4mM EGTA, freshly add 1mM DTT and 2mM ATP just before use
Luciferase Lysis Buffer	1% (w/v) Triton X100, 25mM Glycine-Glycine (pH 7.8), 15mM $MgSO_4$, 4mM EGTA, keep at 4°C. freshly add 1mM DTT just before use
Luciferin substrate	Dilute 1:5 1mM Luciferin solution with 25mM Glycine-Glycine pH 7.8
Renilla Substrate	Luciferase assay buffer without DTT and ATP, 1.5µM coelenterazine

Antibiotics and Bacterial culture medium

Ampicillin (1000x stock)	100mg/ml in double distilled water, filter sterilized and stored at -20°C
Kanamycin (1000x stock)	30mg/ml in double distilled water, filter sterilized and stored at -20°C
Luria Broth (LB) medium	10g Bacto-Trypton, 5g Yeast extract, 2.5g NaCl in 1L deionized water and autoclaved
LB-Agar	10g Bacto-Trypton, 5g Yeast extract, 2.5g NaCl, 20g Agar in 1L deionized water and autoclaved

Medium for Cell culture

DMEM complete	Dulbecco's Modified Minimal Essential Medium (GIBCO, Invitrogen) containing 2mM L-Glutamin (GIBCO, Invitrogen), 1x Nonessential Aminoacids (GIBCO, Invitrogen), 100u/ml Pencillin (GIBCO, Invitrogen), 100u/ml Streptomycin (GIBCO, Invitrogen) and 10% Fetal Calf Serum (heat inactivated at 56°C for 30 minutes (GIBCO, Invitrogen)
DMEM$_{without antibiotics}$	DMEM$_{complete}$ without Pencillin and Streptomycin
DMEM$_{infection}$	DMEM$_{complete}$ with 2% fetal calf serum
DMEM$_{methionine labeling}$	DMEM without L-Methionine, L-Cysteine and Sodium Pyruvate (GIBCO, Invitrogen) and freshly added 2mM Glutamine, 10mM HEPES, 100μCi[^{35}S]/ml
DMEM $_{orthophosphate labeling}$	Phosphate free DMEM supplemented with 10% dialyzed FCS, 1mCi[^{32}P]/ml
MEM	Minimal Essential Medium (GIBCO, Invitrogen) supplemented with 10mM HEPES, 2 mM L-glutamine, nonessential amino acids, 100 U/ml of penicillin, 100 µg/ml of streptomycin, and 10% fetal calf serum
OptiMEM	Chemically defined medium with low serum requirement (Gibco, Invitrogen)

Other Solutions

Bradford Reagent	100mg Coomassie G250 is dissolved in 50ml 99% Ethanol and added to 100ml 85% Phosphoric acid and volume made up to 1L , Filtered and stored at 4°C
Cytomix	120mM KCl, 0.15mM CaCl$_2$, 10mM Potassium phosphate buffer (pH 7.6), 25mM HEPES (pH 7.6), 2mM EGTA, 5mM MgCl2, adjust the pH to 7.6 using KOH, freshly add 2mM ATP (pH 7.6, adjusted with KOH), 5mM Glutathion and 1.25% DMSO
PBS (10x)	80mM Di-Sodium Hydrogen phosphate, 20mM Sodium dihydrogen phosphate, 1.4M NaCl

II.1.7 Radioactive Reagents

The in vitro RNA polymerase assay was carried out in presence of [^{32}P] GTP (3000Ci/mMol), whereas S-[Methyl-^{3}H] Adenosyl-L-Methionine, (12-18 Ci/mmol) was used for methyl transferase assay . The orthophosphate labeling was done with [^{32}P] orthophosphoric acid (8500-9120Ci/mMol) while L-[^{35}S]-Methionine (1000Ci/mmol) was used for protein labeling. All radioactive chemicals were sourced from Perkin Elmer, Germany.

II.1.8 Cell lines

Table II.7 Cell lines used in this study

BHK-21	Baby Hamster Kidney cell line(37, 105)
Huh-7	Human Hepatoma cell line(83)
Huh-7/DENV replicon	Huh-7 cells stable expressing DV2(NGC) subgenomic replicon carrying hygromycin resistance (75)
Vero	African Green Monkey Kidney cell line(80)
A549	Carcinomic Human alveolar epithelial cells(40)
C6/36	*Aedes albopictus* fibroblast (53, 104)
HEK 293T	Human embryonic kidney cells expressing the SV40 large T-antigen(41)

II.1.9 Cloning Vectors and Plasmids

Table II.8 Cloning Vectors and plasmids used in this study

pcDNA3.1(+)	The high-copy plasmid carries a CMV promoter driving the expression of the gene of interest in eukaryotic cells and a T7 promoter for expression in cells expressing T7 polymerase. The selection in eukaryotic

	cells is mediated by a neomycin resistance gene driven by SV40 promoter whereas a β-lactamase gene provide ampicillin resistance for selection in *E. coli*. Commercially supplied by Invitrogen
pDVWSK601	The low copy plasmid pDVWS601 carries the full length genome of Dengue 2 (New Guinea C-strain) under T7 promoter (92)
pDVWSK601-LucUbi	pDVWSK601 carrying the first 32 amino acids of capsid fused to a firefly reporter and ubiquitin auto-protease followed by the full length polypeptide of DV2.
pET21b	A bacterial protein expression vector. The pET-21b (+) vectors carry an N-terminal T7 promoter sequence and C-terminal Histidine tag sequence and β-lactamase gene provide ampicillin resistance for selection in *E. coli*. Commercially supplied by Novagen
pSM	A pTM1 derived vector carrying an N-terminal T7 promoter sequence followed by an EMCV IRES and C-terminal T7 terminator sequence, and a low copy bacterial origin of replication from pBR322 and β-lactamase gene provide ampicillin resistance for selection in *E. coli*.

II.1.9 siRNAs

Table II.9 siRNAs used in this study

Gene	siRNA sequence (5'→3')	Manufacturer
DENV NS1	ACACCAGAAUUGAAUCACAtt	MWG-Biotech Germany
DENV NS3	GAAGGAACAUUCCAUACAAtt	MWG-Biotech Germany
RSF1-1	GGAAAGACAUCUCUACUAUtt	MWG-Biotech Germany
RSF1-2	UAAAUGAUCUGGACAGUGAtt	MWG-Biotech Germany
CAPN2-1	UGAAGAAAUCCUGGCUCGAtt	MWG-Biotech Germany
CAPN2-2	GACUUCACCGGAGGCAUUGtt	MWG-Biotech Germany

BHMT-1	AAGCCTGAAGATACAAGACTA	Qiagen, Germany
BHMT-2	CAAGAGTGAAACTGAAGTCAA	Qiagen, Germany
NPHP3-1	AAGGAAAGTTTCAAGGATTAA	Qiagen, Germany
NPHP3-2	AAGCTTTGCCATTATATGAAA	Qiagen, Germany
ASCC3L1-1	ACCCAGGTGTTTAACACTGTA	Qiagen, Germany
ASCC3L1-2	ATGAATGAAATCGTCTATGAA	Qiagen, Germany
HCV-321	AGGUCUCGUAGACCGUGCAtt	MWG-Biotech Germany
P53	GACUCCAGUGGUAAUCUACtt	MWG-Biotech Germany

II.1.10 Virus

DENV Type 2 New Guinea C-strain (a kind gift from Progen, Heidelberg). The virus was isolated in 1957 and passaged in mouse brain. The virus stocks used in the present study were generated in Vero cells.

II.2 Methods

Standard molecular biological techniques were followed in handling and manipulating nucleic acids and proteins as described in reference manuals like 'Molecular Cloning: A Laboratory Manual'(100) or 'Current Protocols: Molecular Biology'(8). Unless mentioned otherwise all routine practices like plasmid DNA purification, RNA purification, elution of DNA from gels, Restriction endonuclease digestions, ligations etc. were carried out according to the protocol provided by the reagent manufacturers.

All centrifugation steps mentioned in this section were done in a table top Eppendorf 5417 C (at room temperature) or in 5417R (at specified temperatures) unless otherwise specified.

II.2.1 Cell culture and Viruses

II.2.1.1 Cell culture

The mammalian cell lines Huh-7, BHK-21, HEK 293T, Vero E6 and A549 cells were grown as monolayer on cell culture dishes or in culture flasks (Falcon, Becton-Dickinson) in DMEM$_{complete}$ in 37°C incubator with 5% CO_2 and 90% relative humidity. The DENV replicon cell lines (monocistronic dengue replicon carrying DENV UTRs, NS proteins and Hygromycin phosphotransferase selection marker) were maintained similarly but in presence of 75μg/ml Hygromycin. The cells were sub cultured twice a week. The medium over the cells was removed and cells were washed twice with sterile 1xPBS and trypsinized with trypsin-EDTA solution (Gibco-BRL, Eggstein) for 5 minutes. The trypsinization was monitored under an inverted light microscope and the cells were detached by gently tapping the culture dishes. The cells were resuspended in DMEM and plated into culture flasks or dishes with a split ration of 1:5 to 1:10 depending on the cell type. C636 cells were maintained in Minimal Essential Medium (MEM) supplemented with 10% FCS at 28°C with 90% relative humidity.

II.2.1.2 Long term storage of Cell lines

The long term storage of cell lines was done at -196°C in liquid nitrogen containers. The cells were screened for mycoplasmal contamination and checked for proper growth before selecting for long term storage. The cells were harvested at 80-90% confluency by trypsinization and resuspended in DMEM. The cells were pelleted at 700g for 5 minutes at room temperature in a table top centrifuge (Multifuge 3 S-R, Rotor 75006441, M&S Lab equipments), and washed once with 1x PBS. The washed cell pellet was resuspended in ice-chilled Cryomedium (90% fetal calf serum and 10% DMSO (Carl Roth GmbH)) and aliquoted in Cryo vials (Nunc). The cryo vials were initially kept in -70°C freezer for two days and later moved into liquid nitrogen containers for long term storage.

II.2.1.3 Counting cells using Haemocytometer

The cells were counted using a haemocytometer (Neubauer-Cell counter). The haemocytometer and the cover glass were cleaned with 70% ethanol before use. 5-10µl of diluted cell suspension was applied on the haemocytometer and the number of cells within four large quadrants was counted under an inverted light microscope. Each large quadrant had a volume of 0.1µl and the cell density per millilitre was calculated by multiplying the average cell number per large quadrant with 10,000.

II.2.1.4 Transfection of Eukaryotic cells with plasmid DNA

The transient protein expression experiments were done by transfecting plasmids into appropriate cell lines using Lipofectamine™ 2000 (Invitrogen) according to manufacturer's protocol. Briefly, overnight grown 80-95% confluent cells were washed once with DMEM$_{without\ antibiotics}$ and grown in same medium one hour prior to transfection. Suggested amount of Lipofectamine™2000 (depending on well size) was mixed with OptiMEM and incubated for five minutes at RT. This complex was added to plasmid DNA diluted in OptiMEM, mixed well and incubated for 20 minutes. The DNA:liposome complex was later added drop-wise on cell monolayer and incubated for 4h. After 4h the medium is exchanged with DMEM$_{complete}$ and the protein expression was monitored after specific time points.

II.2.1.5 Infection with DENV2

All infection experiments with DENV2 were carried out in the Biosaftey level 3 (BSL3) laboratory. Depending on the experimental requirements a multiplicity of infection (MOI) of 0.5 to 5 was used. The cells were washed once with 1xPBS and supplied with appropriate volumes of virus stocks in $DMEM_{infection}$. The infection volume was kept to a minimum for maximizing infection efficiency. The plates were placed on a rocking platform when minimal volume was used. The infection was carried out for 4h at 37°C. The infection medium was later removed and replenished with fresh medium.

II.2.1.6 Passaging DENV2

For virus passage the supernatant from cells transfected or infected with DENV were collected at various time points and filtered through a filter (0.22μm pore size). Depending on the MOI required for subsequent use the virus supernatant was either used as such for infecting fresh cells or was concentrated by passing through an Amicon® concentrator. The long term storage of virus stocks was done in -80°C refrigerators.

II.2.1.7 Concentrating virus stock

The cell culture supernatant from cells transfected or infected with DENV2 or mutants thereof were harvested at particular time points (48h-96h post infection/transfection). The supernatant was filter purified (0.22μm pore size) to remove cell debris and loaded (15ml at a time) into Amicon® Ultra-15 centrifugal filter unit and centrifuged at 4000xg for 20 minutes in a swing-bucket rotor. The volume of supernatant was reduced to 200-500μl (~60x). The supernatant was harvested and stored at -80°C until use. The viral tire was determined by either plaque assay or $TCID_{50}$ method.

II.2.1.8 Virus Titer estimation: Plaque Assay

Plaque assays were carried out in Huh-7 cells grown in 6-well plates. Duplicate wells of semi-confluent Huh-7 cells were infected with virus stock serially diluted in $DMEM_{infection}$. The infection was carried out in 37°C incubators for 2h. Later the

infection medium was removed and the cells were overlaid with $DMEM_{complete}$ containing 0.5% SeaPlaque GTG-Agarose (Biozym, Oldendorf) to block the spread of the virus within the wells. The agarose is prepared as a 2.5% stock in water, melted by boiling and cooled down to 37°C before adding to $DMEM_{complete}$. The overlaid cells were briefly kept at 4°C for the agarose to solidify and moved into 37°C and incubated for 5-7 days. The plates were examined for cytopathic effects (CPE) routinely, and after 5-7 days the overlay was carefully removed and the monolayer was fixed and stained with Coomassie staining solution (0.25% (w/v) Coomassie Brilliant Blue R-250, 50% (v/v) Methanol and 10% (v/v) acetic acid) for 1h at room temperature. The staining solution was later removed, monolayer washed thrice with deionised water and the number of plaques were counted manually. The virus titer was estimated as 'plaque form-ing units' (PFU) using the formula PFU/ml = $X*10^{Y}$, where 'X' is the number of plaques per well and 'Y' is the positive exponent of the virus dilution which is applied to that particular well.

II.2.1.9 Virus Titer Estimation: $TCID_{50}$ method

$TCID_{50}$ (Tissue Culture Infectious Dose 50 or Median Tissue Culture Infectious Dose) is an end point dilution technique to estimate virus titer. A 10-fold dilution series of the virus stock wass used to infect a semi-confluent monolayer of Huh-7 cells seeded in 96-well plates. The plates were incubated for 5-10 days at 37°C and routinely examined under microscope for cytopathic effects (CPE) of the monolayer. The wells are scored either as infected or uninfected based on CPE. For virus constructs that does not show CPE, the cells were processed for indi-rect immunofluorescence assay using E-protein antibody and the wells are scored for infection based on immunofluorescence signal. The TCID50 was calcu-lated based for the formula TCID50/ml = 10*10x(-0.5+(1/Y-Z), where X is the positive exponent for virus dilution where the wells are positive for virus infec-tion, 'Y' is the number of wells infected with each dilution of virus stock and 'Z' is the number of wells positive for virus which are infected with a 10x or higher dilution.

II.2.1.10 Electroporation of DENV RNAs into mammalian cells

The BHK-21, Huh-7 or A549 cells were trypsinized and PBS washed single-cell suspension of cells were resuspended at a concentration of 1.5 x 10^7 cells per ml for BHK-21 and $1x10^7$ cells per ml for Huh-7 and A549 cells in Cytomix (111) containing 2 mM ATP and 5 mM glutathione. 10 µg of in vitro-transcribed RNA was mixed with 400 µl cell suspension is transferred to an electroporation cuvette (BioRad, 0.4cm gap width) and electroporated with a Gene Pulser system (Bio-Rad, Munich, Germany at 960 µF and 270 V. Cells were immediately resuspended in 12 ml DMEM$_{complete}$ and seeded into appropriate cell culture dishes. For a typical time course experiment $5x10^5$ cells are seeded into each well of a 6-well plate for harvest after 4h or 24h whereas $2.5x10^5$ cells were seeded for harvest after 48h, 72h or 96h.

II.2.1.11 Firefly Luciferase based Virus replication assays

The cells plated in duplicate wells in 6-well plates were lysed after appropriate time intervals in 350µl lysis buffer (1% Triton X-100, 25 mM glycylglycine, 15 mM MgSO4, 4 mM EGTA and 1 mM DTT, pH 7.8) frozen and thawed. For each well, two times 100 µl lysate was mixed with 360 µl assay buffer (25 mM glycylglycine, 15 mM MgSO$_4$, 4 mM EGTA, 1 mM DTT, 2 mM ATP and 15 mM K$_2$PO$_4$, pH 7.8) and, after addition of 200 µl of a luciferin solution (200 µM luciferin, 25 mM glycylglycine, pH 8.0), measured for 20 s in a luminometer (Lumat LB9507; Berthold, Freiburg, Germany). Kinetics of replication was determined by normalizing the relative luminescence units (RLU) of the different time points to the RLU at 4h post electroporation.

II.2.1.12 Visualization of protein localization by immunofluorescence

Huh-7 cells were seeded on glass cover slips in 24-well plates at a density of $1x10^5$ cells per well. Overnight grown cells were transfected with pcDNA constructs using Lipofectamine 2000 (Invitrogen) according to manufacturer's protocol. The overnight transfected cells were washed thrice with 1X PBS and fixed with 2% paraformaldehyde (Applichem GmBH, Darmstadt, Germany) and permeabilized with 0.5% Triton X100 in PBS. The primary staining was done with

anti-NS5 rabbit polyclonal antibody (115) in PBS-3% normal goat serum for 45 minutes and after extensive washes with PBS the secondary staining was done with Alexa Fluor 488 and Alexa Fluor 546 conjugated anti-rabbit or anti-mouse antibody (dilution 1:1000 in PBS- 3% normal goat serum) for 45 minutes. DAPI (Molecular Probes, Karlsruhe, Germany) diluted at 1:5000 was used to visualize cell nuclei. The samples were mounted on slides with FluormountG (Southern Biotechnology Associates, Birmingham, USA) and analyzed by confocal laser scanning microscope. The quantitation of immunofluorescence signal intensity was done using ImageJ software package (National Institute of Health, Bethesda, MD, USA).

II.2.2 Working with DNA and RNA

II.2.2.1 Transformation of competent bacteria

Competent Escherichia coli (*E.coli*) DH5α were generated by CaCl2-method (8, 100). The plasmid DNA (100ng-1μg) or ligation reactions was mixed with 100μl of competent bacteria and incubated on ice for 5min. Afterwards the cells were subjected to heat shock at 37$\circ$C for 2 minutes and incubated on ice for 15min. The bacteria is resuspended in 200μl plain LB and incubated at 37$\circ$C shaking for 20min, and plated on LB-agar plates containing appropriate antibiotics and grown overnight at 37$\circ$C for development of colonies.

The *E.coli* BL21(DE3) competent cells for electroporation was generated as described (102). 10ng of plasmid DNA is mixed with 30µl of competent bacteria, transferred into a electroporation cuvette (BioRad, 0.2cm gap width) and electroporated with a Gene Pulser system (Bio-Rad, Munich, Germany at 25µF and 2.5kV and pulse controller at 400 ohms). The bacteria is resuspended in 1ml plain LB after electroporation, grown at 37$\circ$C for 20 minutes and 10µl is plated on LB-agar plates containing appropriate antibiotics and grown overnight at 37$\circ$C for development of colonies.

II.2.2.2 Plasmid purification

The plasmids from bacterial cultures were prepared using silica membrane based spin column kits (Nucleospin Plasmid, Macherey & Nagel) following supplier's protocol. Mini preperations were done with either 4ml bacterial cultures for high copy plasmids or 25ml for low copy (genomic DENV plasmids) appropriately scaling up the amount of reagents. The midi preparations were done using 100ml bacterial cultures for low copy plasmids or 300ml cultures for high copy plasmids by scaling up the mini preparation protocol and using five spin columns for each preparation. The DNA from mini preparations was eluted in $100\mu l$ water while midi preparations were eluted in water to a total volume of $500\mu l$.

II.2.2.3 DNA purification or extraction from agarose gels

The plasmid DNA following restriction reactions or gel electrophoresis was purified by silica membrane affinity purification spin columns (Nucleospin ExtractII, Macherey & Nagel) following supplier's protocol

II.2.2.4 DNA sequencing

DNA sequencing PCR reaction was performed with 300-500ng template DNA, $5\mu M$ sequencing primer, 0.5x sequencing buffer and $2\mu l$ Big Dye (containing polymerase and dideoxy and deoxy nucleotides) version 1.1 (Applied Biosystems) in a $10\mu l$ final volume. PCR cycles were as following: $95°C/20sec-50°C/20sec-60°C/240sec$ (30 cycles). $1\mu l$ 20% SDS was added to the PCR products and volume adjusted to $100\mu l$ with water and heated to $95°C$ for 5min. DNA was precipitated by addition of $250\mu l$ ethanol and $10\mu l$ 3M sodium acetate pH6.8 to the reaction mix and centrifugation for 20 minutes at 14000g. The pellet was washed 70% ethanol, air dryed and resuspended in $20\mu l$ formamide. The sequencing was done by an ABI 320 sequencer (Applied Biosystems). The sequences generated were analyzed using Vector NTI software.

II.2.2.5 Polymerase Chain Reaction (PCR)

The PCR reactions for generating DNA fragments for cloning consisted of 300-$500\mu g$ template DNA, $2\mu M$ forward and reverse primer, 1xPCR buffer and $0.25\mu l$

FedeliTaq® DNA polymerase (USB Corporation) in a reaction volume of 50μl. 15 cycles of amplification was carried out with annealing at 48°C for 30 seconds and extension at 68°C. The extension time was calculated as 1minute for amplification of one kilobase. The PCR products were later purified using spin columns (Macherey&Nagel).

II.2.2.6 Site-directed Mutagenesis

The site directed mutagenesis was carried out using fusion PCR technique. The mutations were incorporated into two fusion PCR primers (with opposite 5'→3' orientation) designed to anneal to the mutation target and have at least 18 nucleotide overlap. The flanking primers (forward and reverse) are designed to carry restriction sites for cloning. The products generated from the two first round PCR involving each flanking primer along with matching fusion primer are purified and used as template in the subsequent PCR reaction where the priming is done with the flanking primers. The products generated are treated with restriction endonucleases and cloned into target plasmid.

II.2.2.7 In vitro Transcription

The full length genomic constructs were linearized by digestion with XbaI. 10μg of Phenol:Chloroform purified DNA template is used for *in vitro* transcription reaction mixture containing 80mM HEPES (pH7.5), 12mM $MgCl_2$, 2mM spermidine, 40mM dithiothreitol (DTT) and 3.125mM ATP, UTP and CTP , 1.56mM GTP, 1mM m_7GpppG cap analogue (New England Biolabs), 1 U of RNasin (Promega, Mannheim, Germany) per μl, 0.1 μg plasmid DNA/μl, and 0.6 U of T7 RNA polymerase (Promega) per μl. After incubation for 2.5 h at 37°C, 0.3 U of T7 RNA polymerase/μl reaction mixture was added, followed by another 2.5 h of incubation at 37°C. Transcription was terminated by addition of 1.2 U of RNase-free DNase (Promega) per μg of plasmid DNA and 60 min of incubation at 37°C. The RNA was extracted with acidic phenol and chloroform, precipitated with isopropanol, and dissolved in RNase-free water. Denaturing agarose gel electrophoresis was used to check RNA integrity, and the concentration was determined by spectrophotometer.

II.2.2.8 Isolation of total cellular RNA

Total cellular RNA was isolated using the Nucleo Spin RNAII kit (Macherey&Nagel) as recommended by the manufacturer. Approximately $1x10^6$ cells were harvested for purification with spin column. The purified RNA is eluted with 60μl of RNase free water and stored at -70°C until further use. The RNA concentration was measured by spectrophotometer.

II.2.2.9 RNA quantification by RT-PCR.

The RT-PCR reactions were carried out with One Step RT-PCR kit (Qiagen, Hilden, Germany) and 100nl of the total cellular RNA sample in a ABI PRISM 7000 sequence detector system (Applied Biosystems, Foster City, CA). RT-PCRs for each primer set was conducted in triplicates according to manufacturer's instruction using the following primers (MWG-Biotech, Martinsried, Germany): Dengue (forward:5'ttgagtaaactgtgcagcctgtagctc3', reverse5'gggtctcctctaacctctagtcct3'), GAPDH (forward5'gaaggtgaaggtcggagt3', reverse5'gggtctcctctaacctctagtcct3'), IL-8 (forward 5'atgacttccaagctggccgtg3', reverse 5'ttgataaatttggggtggaaa3'). The total volume of the reaction mix was 15 μl, and reactions were performed in three stages by using the following conditions: step 1, 30 min at 50°C (reverse transcription); step 2, 15 min at 95°C (heat inactivation of reverse transcriptase and activation of Taq polymerase); and step 3, 40 cycles of 15 s at 95°C and 60 s at 60°C (amplification). The amount of DENV RNA was calculated by standard curve method using serial dilutions of known amount of *in vitro* transcribed RNA template. For cellular genes the ΔΔCT method was used to calculate the relative expression levels.

II.2.3 Working with Proteins

II.2.3.1 Subcellular fractionation of infected cells

Huh-7 cells infected with DENV at an MOI of 2-5 were harvested 48h post infection washed twice with 1xPBS and resuspended in ice-cold swelling buffer (10 mM Tris, pH 8.0, 10 mM sodium acetate, 1.5 mM $MgCl_2$) at a density of 5×10^6 cells per ml and incubated on ice for 10 min. The cells were lysed by applying 20

strokes in a dounce homogenizer. Cell lysis was monitored by trypan blue stain-ing. The homogenate obtained was centrifuged at 800 x g for 10 min to obtain the crude nuclear (N) pellet fraction and a postnuclear supernatant (PNS). Nuc-lear fractions were resuspended in swelling buffer containing 10% sucrose and 1% Triton x100 incubated on ice for 30 minutes. Later the nuclei was pelleted by centrifugation in a refrigerated centrifuge at 1,800 x g for 10 min through two volumes of a 30% sucrose cushion, followed by two washes with swelling buffer to remove cellular debris and obtain purified nuclear fraction. The purity of the fractions was analyzed by western blot using various antibodies directed against cellular markers.

II.2.3.2 Immunoprecipitation

Cell grown on 6cm dish were washed twice with PBS and scrapped out and pel-leted. The pellets were resuspended in 50µl 1x SDS sample buffer, sonicated and incubated at 98°C for 10 min. The cell lysate was then diluted to a final vo-lume of 0.5ml with NPB (50mM Tris HCl pH7.5, 150mM NaCl, 1% NP40, pro-tease inhibitor cocktail (Roche) and phospatase inhibitors 5mM sodium orthova-nadate and 50mM sodium fluoride). The protein G-sepharose 4B (Sigma-Aldrich, Steinheim) was washed twice with NPB buffer and 30µl beads were incubated with 5µl of NS5 antibody in 500µl NPB buffer for 2h in an inversion mixer (REAX 2, Darmstadt) at 4°C. Later the beads were washed thrice with NPB buffer and the cell lysate was added to the beads and incubated for 2h in an inversion mix-er at 4°C. The beads were washed five times with NPB buffer, the bound pro-teins eluted by boiling with SDS sample buffer.

II.2.3.3 Standard SDS PAGE

The cells were resuspended in PBS and lysed by addition of equal volume of 2x SDS sample buffer. The viscosity of the samples was reduced by sonication in a cup-horn Sonifier (Brandson 450) which shears the genomic DNA. The sample was then heated to 98°C for 10 min and cooled to RT. The polyacrylamide gels were prepared according to standard protocols (8) and gel electrophoresis was

carried out at constant current of 200V for 3-4h (15x15cm gels). Pre-stained protein markers (New England Biolabs) was used as molecular size marker.

II.2.3.4 Western Blot Analysis

Following gel electrophoresis the proteins were transferred to nitrocellulose membranes (Schleicher& Schuell) using a semidry blotter (BioRad) for 90 min at a constant current of $1mA/cm^2$. The membrane was blocked with blocking buffer (5% milk powder in PBS-0.5% Tween20 (PBST)) for 2h at RT or overnight at 4°C. The membrane was incubated with the primary antibody diluted in blocking buffer for 2h followed by three washes for 10 min with PBST. Similarly the secondary antibody diluted in blocking buffer was incubated for 90 minutes and washed thrice with PBST. The chemiluminescence signal was revealed using ECLplus kit (Amersham) according to manufacturer's instructions and detected photographically by exposure to BioMax ML film (Kodak).

Table II.10 Antibodies used for western blot

Antibody	Generated in	Dilution	Manufacturer
α-NS5	Rabbit polyclonal	1:1000	In-house
α-Calnexin	Rabbit polyclonal	1:1000	Stressgen, Canada
α-p53	Mouse monoclonal	1:500	BD Pharmingen, USA
α-Lamin A/C	Mouse monoclonal	1:500	SantaCruz
α-Rabbit IgG Perox-	Goat polyclonal	1:20000	Sigma-Aldrich, Germany
α-Mouse IgG Perox-	Goat polyclonal	1:15000	Sigma-Aldrich, Germany

II.2.4.1 NS5 expression in Rosetta (DE3)

E. coli Rosetta (DE3) strain (Novagen, Merk) was transformed with pET21b NS5 and plated in LB-agar plates containing 100μg/ml ampicillin and 1% glucose. Starter cultures were prepared by inoculating single colonies into 5ml LB medium containing 100μg/ml ampicillin and 1% glucose and overnight incubation. The expression culture was inoculated with 1% starter culture and grown at 37°C until the optical density (OD) at 600nm was 0.8 to 1.0. The protein expres-

sion was induced by a cold shock at 4°C for 30 min followed by addition of 50μM isopropyl-β-D-thiogalactopyranoside (IPTG) and 2% ethanol. After overnight incubation at 18°C, cells were harvested by centrifugation at 6000 x *g* for 10 min at 4°C, and the cell pellet was stored at -80°C until further processing.

II.2.4.2 NS5 purification

The cells pellet was resuspended in lysis buffer (50mM Tris pH7.5, 500mM NaCl, 20% glycerol, 1% β-octylglucopyranoside, 50mM imidazol, 1mM DTT and Protease Inhibitor Mix (Roche)) containing 1 mg/ml Lysozyme (Fluka, Buchs, Switzerland) and 5u/ml Benzonase (Merk, Darmstadt, Germany) was incubated at 4°C for 30 min, lysed by sonication. The lysate was clarified by centrifugation at 12000 *g* for 15 min at 4°C. The supernatant was purified by metal affinity, using a Nickel NTI column (Qiagen, Hilden, Germany) equilibrated with lysis buffer. The unbound proteins were washed away with 5 column volumes of wash buffer (50mM Tris pH7.5, 500mM NaCl, 20% glycerol, 0.1% β-octylglucopyranoside, 50mM imidazol, 1mM DTT and Protease Inhibitor cocktail (Roche)) and the protein was eluted with elution buffer (50mM Tris pH7.5, 500mM NaCl, 20% Glycerol, 0.1% β-octylglucopyranoside, 400mM imidazol, 1mM DTT and Protease Inhibitor cocktail (Roche)). The fractions containing the protein of interest were identified and quantified by Bradford method and purity determined by SDS-PAGE. Similar fractions were pooled, aliquoted and stored at -80°C.

II.2.4.3 Polymerase assay

The RdRP assay was carried out using 400ng of DENV genomic RNA generated by *in vitro* transcription and 50-200 ng purified NS5. The 50μL assay was performed in presence of 50mM HEPES pH 8.0, 10mM KCl, 5mM $MgCl_2$, 3mM $MnCl_2$,1mM DTT, 1U/μl RNasein (Promega, Mannheim, Germany) and 0.5mM each of ATP, CTP and UTP and 10μM GTP and 10μCi ^{32}P GTP (3,000 Ci/mmol; Perkin Elmer) for 2h at 30°C. Assays using homopolymeric templates included 400ng poly(C) (GE Healthcare, Munich, Germany) or 400ng poly(C) with 5 pmol oligo(G_{12}) primer (MWG, Germany), respectively. The samples were precipitated with 10% trichloroacetic acid (TCA) and 0.5% tetrasodium pyrophosphate,

passed through GF-C microfilters (GE Healthcare), washed five times with 1% TCA and 0.1% tetrasodium pyrophosphate, and air dried. After the addition of 4 ml of Ultima Gold (Perkin-Elmer), samples were subjected to liquid scintillation counting. All measurements were done in duplicate.

II.2.4.4 Methyl transferase assay

The methyltransferase assay was carried out using 1μg of uncapped or M[7]capped DENV genomic RNA (1-175 nt) as template and 100ng purified NS5. The 50μl assay was performed in presence of 50mM Tris pH7.0, 10mM KCl, 2mM MgCl$_2$, 2mM MnCl$_2$, 0.05% CHAPS, 2mM DTT and 2μCi ^{3}H SAM (Perkin El-mer) for 2h at 22°C. Following the assay 10 μl of 3 M Na-acetate and 20μg gly-cogen were added to each reaction mixture and volume adjusted to 100μl. Sam-ples were extracted with phenol-chloroform, and nucleic acid was precipitated with 0.7 volume of isopropanol. The pellet was washed with 70% ethanol, air dried and resuspended in100μl water. After the addition of 4 ml of Ultima Gold (Perkin-Elmer), samples were subjected to liquid scintillation counting. All mea-surements were done at least in duplicate.

II.2.5 Plasmids and viral constructs

II.2.5.1 Plasmid construction

The plasmid containing full-length DENV2 NGC strain (pDVWSK601) and subge-nomic construct (pDVWSK601∆CprME) were a kind gift from Andrew Davidson, School of Medical Sciences, Bristol, UK. These constructs were modified in an earlier work (75) by insertion of firefly luciferase reporter or hygromycin phos-photransferase gene to develop the dengue luciferase reporter (pDVWSK601-FL-Luc-Ubi-DV) and and dengue subgenomic replicon respectively (pDVWSK601∆CprME-hpt-Ubi).

DENV genomic construct with *AgeI-SacI* restriction sites (pDVWSK601 -AgeI-SacI): For ease in introduction of NLS mutations into NS5 by fragment exchange restriction sites *AgeI* and *SacI* were introduced as silent mutations flanking NS5 NLS by fusion PCR using primers 5'accatggcagctatgaaacaaaacaaaccggttcagcatcat

ccatggtg3′ and 5′tgttgaagatagtaggttttgggagctcgttgacaaggaaagga3′ respectively and flanking primers (Forward 5′gaatgtaagagaagtcaaaggcctgacaaaagga3′ and 5′atcttcaacagcctcacgtgccgacttcca3′) and cloned into *StuI* and *PmlI* of full length genomic construct.

The αβNLS mutants were cloned by fusion PCR between *AgeI* and *SacI* of pDVWSK601 -AgeI-SacI using following primers (KK371-372 forward 5′ acccaa-gaaccgaaagaaggcacagcggcactaatgaaaatcacggca3′, KK371-372 reverse 5′ acc-caagaaccgaaagaaggcacagcggcactaatgaaaatcacggca3′, KK387-388 forward 5′ gagtggctttggaaagaactaggggccgcaaagacacctaggatgtgcac3′, KK387-388 reverse 5′ gtgcacatcctaggtgtctttgcggcccctagttctttccaaagccactc3′, KK388-389 forward 5′ gagtggctttggaaagaactagggaaggcagcgacacctaggatgtgcac3′, KK388-389 reverse 5′ gtgcacatcctaggtgtcgctgccttccctagttctttccaaagccactc3′, KKK387-389 reverse 5′ gagtggctttggaaagaactaggggccgcagcgacacctaggatgtgcac3′, KKK387-389 reverse 5′ gtgcacatcctaggtgtcgctgcggcccctagttctttccaa agccactc3′, RE396-397 reverse 5′ aagacacctaggatgtgcactgcagccgaattcacaagaaaggtgagaag3′, RE396-397 reverse 5′ cttctcacctttcttgtgaattcggctgcagtgcacatcctaggtgtctt3′, EE397-398 forward 5′ aa-gacacctaggatgtgcactagagccgcattcacaagaaaggtgagaag3′, EE397-398 reverse 5′ cttctcacctttcttgtgaatgcggctctagtgcacatcctaggtgtctt3′, REE396-398 forward 5′ aa-gacacctaggatgtgcactgcagccgcattcacaagaaaggtgagaag3′, REE396-398 reverse 5′ cttctcacctttcttgtgaatgcggctgcagtgcacatcctaggtgtctt3′, RK401-402 forward 5′ ag-gatgtgcactagagaagaattcacagcagccgtgagaagcaatgcagcc3′, RK401-402 reverse 5′ ggctgcattgcttctcacggc tgctgtgaattcttctctagtgcacatcct3′) and flanking primers (forward 5′ tatgaaacaaaacaaaccggttcagcatca3′ and reverse 5′ ttccttgtcaac-gagctcccaaaacctactatcttcaaca3′).

The pcDNA NS5 was constructed by PCR amplification of NS5 from full length genomic construct using following primers (forward- 5′taccgagctcggatccatggg aactggcaacata3′ and reverse 5′ataattctagactaccacaggactcc tgcctcttcctcttc3′) and inserted between *BamHI* and *XbaI* sites of pcDNA 3.1.

The deletion mutations of NS5 NLS were constructed using the following primers and inserted between AgeI and PmlI sites in pcDNA NS5 *AgeI-SacI*. Deletion of β-NLS (forward 5′caaaacaaaccggttcagcatcatccaagaaactaatgaaaatcacggcagagtgg

ctttgg3', reverse 5' ttcaacagcctcacgtgccgacttccactt3'), deletion of αβNLS (forward 5' tatgaaacaaaacaaaccggttcagca3', reverse 5' cagcctcacgtgccgacttccactt gttctcatcagtgaatatggcccccaaggctgcatttgtgccttctttcggttcttgggttctcgtgtccacttt3'), deletion of both NLS (forward 5'gctatgaaacaaaacaaaccggttcagcatcatccaatgcag ccttgggggccatattcactgatgagaacaagtggaagtcggcacgtgaggctgttgaa3' and reverse 5' ttcaacagcctcacgtgccgacttccacttgttctcatcagtgaatatggcccccaaggctgcattggatgatgctg aaccggtttgttttgtttcatag3')

The kunjin virus αβ-NLS was inserted into DENV genomic constructs using following primers (forward 5' gttgtgggcgttcctggcacgagaaaagcgtcccagaatgtgctcg cgagaggaatttataaggaaggtcaatagtaatgcagccttggggggccata3' and reverse 5' cgcttttctcgtgccaggaacgcccacaaccagttggtggtttcattgagcacatactttgtgccttctttc ggttcttg3') between restriction sites *AgeI* and *SacI*.

The NLS mutations were transferred from the full length constructs by fragment exchange between restriction sites *StuI* and *PmlI*.

Hexa Histidine tag was introduced at C-terminus of NS5 in DENV genomic construct between StuI and HpaI by fusion PCR using following primers (forward 5' tgtgtgaggcgttaaccttagcgacc3', reverse 5' Tggtcctcctttttgtcaggcctttgacttc3' fusion forward 5' Aacacgagaaggggaactggcaaccatcaccatcaccatcacataggagagacgcttggagagaaa3', fusion reverse 5' tttctctccaagcgtctctcctatgtgatggtgatggtgatggttgccagtt ccccttctcgtgtt3')

Mutations in putative CK2 phosphorylation site (T395→A) was inserted between *AgeI* and *PmlI* in pcDNA NS5 *AgeI-SacI* using primers (forward 5' gaaacaaaacaaaccggttcagcatcatccatggtgaacggagtggtcag3', reverse 5' cccaaaacctactatcttcaacagcctcacgtgccgacttccacttgttc3', fusion forward 5' gaagaaaaagacacctaggatgt gcgctagagaagaattcacaagaaagg3', fusion reverse 5' cctttcttgtgaattcttctctagcgcacatcctaggtgtcttttttcttc3').

The pET21b HA-NS5-His was generated by PCR amplification of NS5 (forward 5' ttcccctctagaaataattttgtttaactttaagaag gagatatacatatgtacccatacgacgtcccagactacgctggaactggcaacataggaga3' and reverse 5'agaggatccctactagtgatggtgatggtgatgcc acaggactcctgcctctt3') and cloning between XbaI and BamHI in pET21b. αβNLS

mutations were transferred into this construct by fragment exchange from full length constructs using restriction sites *StuI* and *PmeI*.

II.2.6 RNAi Screen

II.2.6.1 Preparation of siRNA spotted chambered slides

The siRNA-gelatin transfection solutuion was prepared in 384 well plates (Nalge-Nunc) as follows. 5μl of a 30μM siRNA stock solution was mixed with 3.5μl Lipofectamine 2000 (Invitrogen) and 3μl Opti-MEM (Invitrogen) containing 0.4M sucrose and incubated at room temperature for 20 minutes. After incubation 7.25μl of 0.2% gelatine (G-9391, Sigma-Aldrich), 3.5x10-4 % fibronectin (Sigma-Aldrich) was added. The solution were arrayed on to single well, chambered Lab-Tek cover glass tissue culture dishes (Nalge-Nunc) using a Chip Writer Compact Robot (Bio-Rad) with Solid pins (Point Technologies) resulting in a spot diameter of approximately 400μm. The spot volume was approximately 4nl. The Lab-Tek chamber glasses were dried in plastic boxes containing silica gel (Merk) at least over night.

II.2.6.2 Cell seeding and Infection

Low passage (10-20) Huh-7 were seeded on arrayed chamber slides at a density of $1.5x10^5$ cells per chamber in a total volume of 3ml DMEM$_{complete}$ and incubated at 37°C under 5% CO_2. After 48h incubation, the cell culture medium was removed and cells were infected with DENV-2 NGC strain at a MOI of 2-5 in 1ml DMEM$_{infection}$. Four hours later the medium was replaced with DMEM$_{complete}$ and incubated for 24h. The chambered slides were fixed after 24h and immunostained.

II.2.6.3 Immunostaining

The cell monolayer was washed twice with PBS and fixed with 2% paraformaldehyde (Sigma Aldrich). Permeabilization was carried out with 0.5% Triton X 100 (Merk) in PBS. The primary antibody (anti-E protein, mouse monoclonal, hybridoma-HB46, ATCC) was diluted 1:100 and secondary antibody anti-mouse Alexa Fluor 546 (Invitrogen, A11030) was diluted 1:500 in PBS-3% normal goat

serum. Both antibodies were incubated for 45min each with three washes in be-tween with PBS. The staining procedure was repeated twice to improve the sig-nal intensity. The cells were washed thrice with 1x PBS, nuclei stained with DAPI (1:5000) in PBS for 1 min. Finally the slides were stored with PBS containing 0.05% sodium azide for image acquisition.

I.2.6.4 Image acquisition

The images of each siRNA spot was captured using Olympus Scan^R wide-field microscope (Olympus Biosystems) with Scan^R image acquisition program at 10X magnification. The acquisition time was 5ms for DAPI signal and 50ms for E-protein signal.

II.2.6.5 Image processing and statistical analysis

The acquired images were analyzed with image analysis software described elsewhere (71). The primary screen was conducted in 12 repetitions (in dupli-cate over six independent days). All siRNA spots with less than 125 or more than 500 cells were excluded from the analysis. As additional quality control for staining artefacts all images were analyzed by eye (out of focus images, dirt/dust particles, staining variations, intensity oversaturation) resulting in an overall exclusion of 15% of the images and three repetitions. Statistical analysis of processed imaging data was carried out in R Version 2.8.0 (R Development Core Team, http://www.R-project.org), using the Bioconductor packages RNAither (97) and cellHTS (15). In brief, signal intensities were normalized for effects of differing cell counts using locally weighted scatterplot smoothing (LO-WESS) (26). B-score normalization was used to remove spatial effects within individual LabTeks (18). Variability between plates was addressed by subtracting the plate median from each measurement and dividing by the plate median ab-solute deviation. Replicates were summarized using the mean; furthermore, a t-test was carried out to determine whether siRNA effects differed significantly from zero. The mean score indicates the magnitude of an effect, whereas the p-value is a measure of the reproducibility. A knock-down was scored positive when its p-value was <0.05 and its score lower than -1 in case of dependency

factors or higher than +1 in case of restriction factors. This combination of p-value and score allows identification of genes with a relatively small, but consistent effect.

II.2.6.6 Validation siRNA screen in 96-well format

The method of reverse siRNA transfection was adapted to the 96-well plate format as described elsewhere (34). In brief, 3 µl OptiMEM (containing 0.4 M sucrose) were mixed with 3.5 µl Lipofectamine 2000 (Invitrogen) and 5 µl of the respective siRNA (30µM stock) in a 384 well plate by using an automated liquid handler. After incubation for 20 min at RT 7.25 µl of a 0.08 % (w/v) gelatin solution containing 3.5×10^{-4} % (v/v) fibronectin were added. Seventeen µl of the source siRNA transfection solution were added to 850 µl of MilliQ water in each well of a 96-deep-well plate. Fifty-one µl of the transfection mixture were transferred into 96-well plates (Greiner, cat. no. 655098) and plates were dried in a multiwell Speed Vac for 2.5 h at medium drying force.

For DENV infection based validation screen 5×10^{3} Huh-7 low passage cells were seeded per siRNA-coated well of a 96-well plate in a volume of 100 µl. After 24h cells were infected with DENV2 (16681 strain) renilla reporter virus (developed by Wolfgang Fischl; Unpublished) using an MOI of 0.5 and medium was exchanged 4h later. 48h post infection cells were washed once with PBS, lysed in 50 µl luciferase lysis buffer and stored at -70°C until measuring *Renilla*- and *Firefly*-Luciferase activity. The plates were measured using home-made substrates for both firefly and renilla luciferases using a luminometer (Mitras LB940). The validation screen was performed twice in duplicates and statistically analyzed as follows. The signal intensities were first normalized for cell count effects using locally weighted scatterplot smoothing, and then normalized to the negative controls by subtracting the median signal of the negative controls from each measurement and dividing by the median absolute deviation of the negative controls. Replicates were summarized using the mean. Hits were defined based on a score threshold of +/- 2.0 for at least one siRNA per gene.

The DENV luciferase reporter replicon based validation screen was carried out similar to infection based validation screen with the following modifications. Huh-7 cells bearing DENV sub-genomic replicon bearing a renilla luciferase reporter (developed by Wolfgang Fischl; Unpublished) was seeded into siRNA pre-spotted 96-well plates and 48h later the cells were washed once with PBS and lysed in 50µl luciferase lysis buffer. The luciferase measurement and statistical analysis were carried out similar to infection based validation screen. Hits were defined based on a score threshold of +2.0 or -1.5 for at least one siRNA per gene.

III. Results

III.1 NS5 nuclear accumulation and viral replication

III.1.1 Effect of extrinsic factors on NS5 nuclear accumulation

III.1.1.1 Localization of NS5 upon DENV infection in various cell types

NS5 protein of DENV and YFV are reported to localize to nucleus in infected cells (59). To check whether the nuclear localization of NS5 is cell type specific we analyzed the localization of DENV NS5 after infection in a diverse range of cell lines including Huh-7, A549, Vero, BHK-21, HepG2 and C636. Immunofluorescence-based studies have revealed that majority of detectable NS5 signal localize into nucleus of infected cells from earliest to very late time point of infection in all cell lines examined. Albeit the western blot analysis followed by cell fractionation of infected cells have shown that nearly 50% of the protein is localized in the cytoplasm on contrary to immunofluorescence staining where more than 90% of the signal is found to localize to the nucleus.   This discrepancy could possibly be due to the diffused distribution of NS5 in the cytoplasm and to the signal detection limits of immunofluorescence technique.
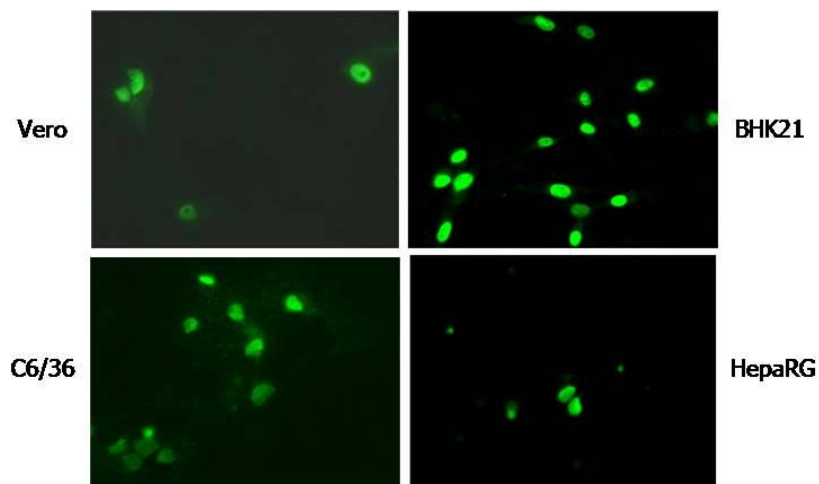
Fig.III.1 Localization of NS5 in different cell lines. The cells were infected with DENV2 NGC strain at an m.o.i. of 5 and harvested 72h post infection and analyzed by immunofluorescence assay using anti-NS5 antibody.

III.1.1.2 Study on phosphorylation of NS5

Previous biochemical studies indicated that at least a portion of DENV NS5 is phosphorylated and the hyperphosphorylated form is detected only in the nucleus implying a role for phosphorylation in nuclear transport of NS5 (5, 59). However it was also observed that this hyperphosphorylated form appears only upon serum starvation. To address the question of NS5 phosphorylation during viral replication, we labelled Huh-7 DENV replicon cells with [^{32}P] orthophosphate and NS5 was immunoprecipitated with anti-NS5 antibody and analyzed on a SDS-PAGE. Huh-7 HCV replicon cells lysate subjected to immunoprecipitation with anti-NS5A antibody were used as control. No phosphorylated form of DENV NS5 could be immunoprecipitated in our experiment while hypophosphorylated and hyperphosphorylated forms of HCV NS5A could be readily observed. The efficiency of immunoprecipitation was determined with [^{35}S] methionine labelled replicon cells lysate where a single prominent band corresponding in size of NS5 was observed indicating successful immunoprecipitation. These results have three possible explanations; first the proportion of NS5 that is phosphorylated may be below the detection limit of the assay; secondly the NS5-specific antibody used for immunoprecipitation may preferentially recognize the nonphosphorylated form of NS5; third phosphorylation is induced only during cellular stress such as serum starvation.
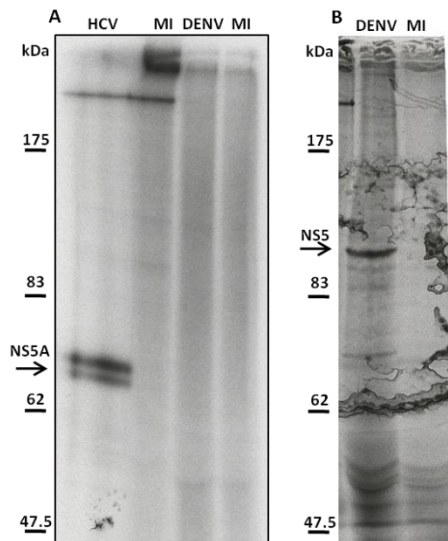
Fig.III.2 Orthophosphate labelling of DENV NS5. A. DENV replicon cells were labelled with 1.5mCi/ml of [^{32}P] Orthophosphate for 6h and harvested in SDS sample buffer, boiled, diluted in RIPA buffer, immunoprecipitated with anti-NS5 antibody and resolved in an 8% PAGE. HCV replicon cells similarly labelled and immunoprecipitated with anti-NS5A antibody was used as control. B. Immunoprecipitation control. DENV replicon cells were labelled with 100µCi/ml of [^{35}S] Methionine for 6h and harvested in SDS sample buffer, boiled, diluted in RIPA buffer, immunoprecipitated with anti-NS5 antibody and resolved in an 8% PAGE

III.1.1.3 Biochemical fractionation of NS5

A cell fractionation assay was carried out to biochemically analyze the NS5 localization in various cellular compartments. The nuclear and cytoplasmic fractions of Huh-7 cells infected with DENV were separated by osmolysis followed by douncing. The nuclear fraction was further purified by detergent treatment and pelleting through a sucrose cushion to remove the contaminating cellular membranes. The separated fractions were analyzed by SDS-PAGE. The purified nuclei were devoid of detectable amount of Calnexin whereas the nuclear marker Lamin was absent from post nuclear supernatant (PNS) fraction indicating absence of cross contamination. Interestingly higher amount of p53 was observed in the cytoplasmic fractions even though the signal is mostly located in the nucleus in immunofluorescence analysis. In all fractions NS5 migrated as a single band indicating absences of detectable amount of modified form of the protein. It was also noted that significant amount of the protein was observed in the cytoplasmic fractions which were not observed by immunofluorescence assay.
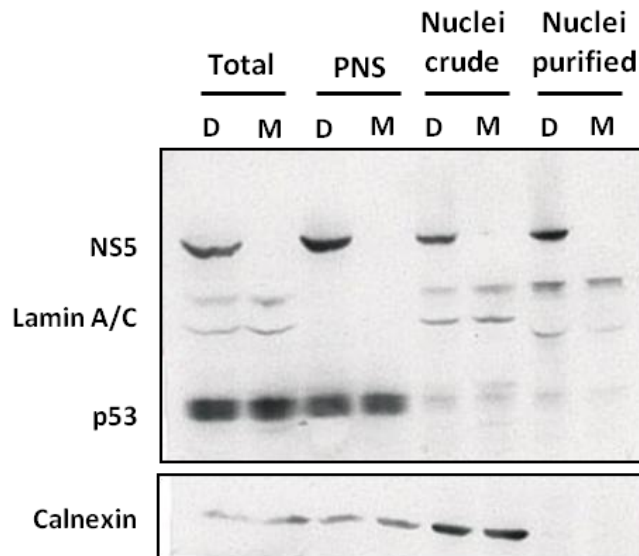
Fig.III.3 Biochemical characterization of NS5. Huh-7 cells infected with DENV and harvested 48h post infection were resuspended in swelling buffer and lysed with a dounce homogeniser. After separation of post nuclear supernatant (PNS) fraction, the crude nuclear fraction was purified by treatment with 1% triton and sedimenting through a 30% sucrose cushion to remove ER contamination. The fractions were analyzed by western blot using antibodies against NS5 and various cellular markers.

III.1.1.4 Role of DENV proteins in NS5 nuclear transport

NS5 accumulates in nucleus of DENV infected cells. To study the effect of other DENV proteins in NS5 nuclear transport we analyzed the protein localization using various deletion constructs. The NS5 localization in subgenomic replicon expressing NS1-NS5 was similar to full length virus indicating that structural proteins are not necessary for its efficient nuclear transport. However when expressed alone as a T7-promoter driven gene, most cells showed a cytoplasmic accumulation of NS5. To study the influence of other DENV non-structural (NS) proteins on NS5 nuclear transport, we designed a NS1-NS5 construct expressing all NS proteins. Surprisingly in the context of this construct also NS5 showed predominantly cytoplasmic accumulation of the protein suggesting that NS proteins did not influence this phenotype. In cells expressing NS5 fused to GFP similar localization was observed as well. However when NS5 construct was expressed under the control of CMV immediate early (IE) promoter, NS5 localized to nucleus as observed in the context of an infection. GFP-NS5 fusion protein also showed similar localization under CMV promoter. CMV IE promoter driven

constructs were used in the subsequent studies due to their more authentic protein localization. The exact reason from anomalous localization of NS5 expressed under T7-promoter is not presently know.
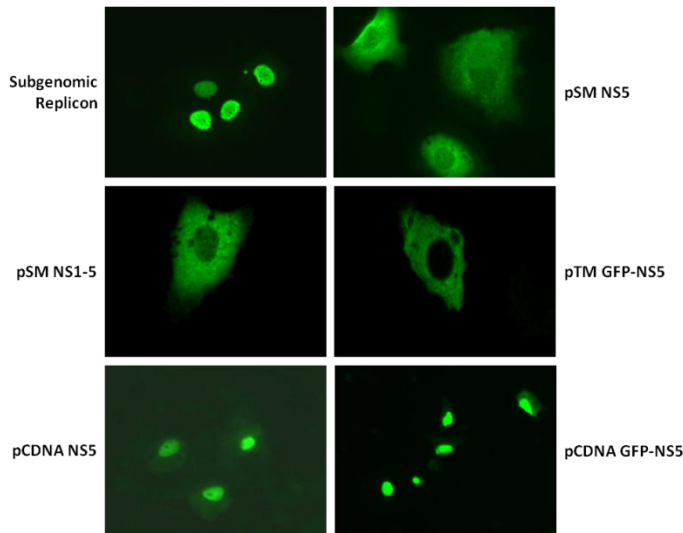
Fig.III.4 Localization of NS5 under various protein expression systems. The subgenomic replicon was transfected into Huh-7 cells and NS5 localization analyzed by immunofluorescence assay using anti-NS5 antibody. The T7 promoter driven constructs (pSM and pTM) were transfected into Huh-7-T7 cells and 8h later harvested and analyzed by immunofluorescence assay using anti-NS5 antibody. The pcDNA constructs were transfected into Huh-7 cells and harvested 16h later and NS5 localization analyzed as above mentioned.

III.1.1.5 Effect of Casein kinases on NS5 nuclear accumulation

Earlier investigations (36) have identified a consensus CKII phosphorylation site (T395REE) within the $\alpha\beta$-NLS which could be phosphorylated *in vitro* when β-galactosidase reporter fused to $\alpha\beta$-NLS was treated with CKII. This phosphorylation however inhibited the nuclear transport of the reporter. We used a panel of CKI and CKII inhibitors to study the effect of the phosphorylation mediated by these kinases on NS5 nuclear accumulation. However none of the CKI or CKII inhibitors tested had an effect on the nuclear transport of the protein (Fig.3.5.panels a and b). In addition the mutation of NS5 CKII phosphorylation site did not have any significant effect on the nuclear transport of the protein indicating that CKII phosphorylation may not have a major role in the nuclear transport of NS5.
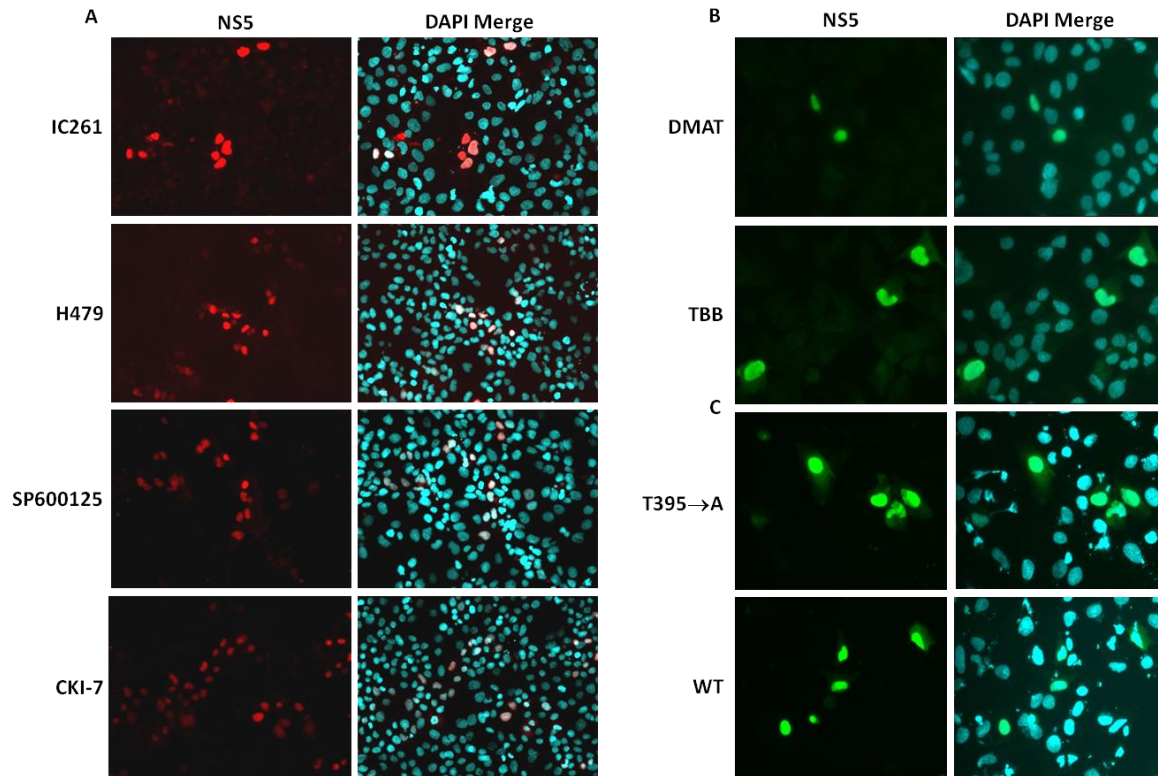
Fig.III.5 Role of Casein Kinases mediated phosphorylation in NS5 nuclear accumulation. A. Huh-7 cells electroporated with DENV sub genomic replicon were treated 48h post electroporation with casein kinase inhibitors IC261(100µM), H479 (20µM), SP600125 (50µM) and CKI-7 (200µM) for 24h and NS5 localization determined by immunofluorescence. B. Huh-7 cells electroporated with DENV genomic reporter viruses were treated 4h post electroporation with CK2 inhibitors DMAT (2µM) and TBB (50µM). Cells were harvested 72h post electroporation and NS5 localization analyzed by immunofluorescence. C. pcDNA-eGFP-NS5 constructs containing mutation at putative CK2 phosphorylation site (T395→A) was transfected into Huh-7 cells and NS5 accumulation 16h post electroporation determined by GFP fluorescence.

III.1.1.6 Study of mobility of NS5 between cellular compartments

NS5 is present in the cytoplasm and the nucleus of infected cells with the hyper-phosphorylated form accumulating mostly in the nucleus (59). Recent studies have also shown that blocking CRM1-mediated export by leptomycin B resulted in higher amounts of nuclear NS5 together with higher release of virus particles (94). These results suggested that NS5 is exported out of the nucleus. To study the mobility of NS5 within the nucleus and between nucleus and cytoplasm, we generated NS5 fusion constructs containing eGFP at their N-terminus. NS5 mobility was monitored in Huh-7 cells by FRAP or FLIP analysis. Similar to DENV infection NS5-eGFP localized mostly in nucleus of transfected cells. FRAP analy-

sis showed very high mobility of the protein ($T_{0.5}$=3.7sec) within the nucleus indicating free diffusion.   However the import of the protein from cytoplasm to nucleus was slower compared to mobility within the nucleus ($T_{0.5}$=138sec) indicating active transport of the protein into the nucleus rather than free diffusion between cytoplasm and nucleus (Fig. III.6B). FLIP experiment was carried out to study the rate of export of NS5 from nucleus to cytoplasm. The nuclear export of NS5 ($T_{0.5}$=20min) was much slower compared to import explaining the net accumulation of the protein in the nucleus. The export was CRM1-dependent as evident from the complete block of NS5 nuclear export in presence of leptomycin-B (Fig. III.6D).
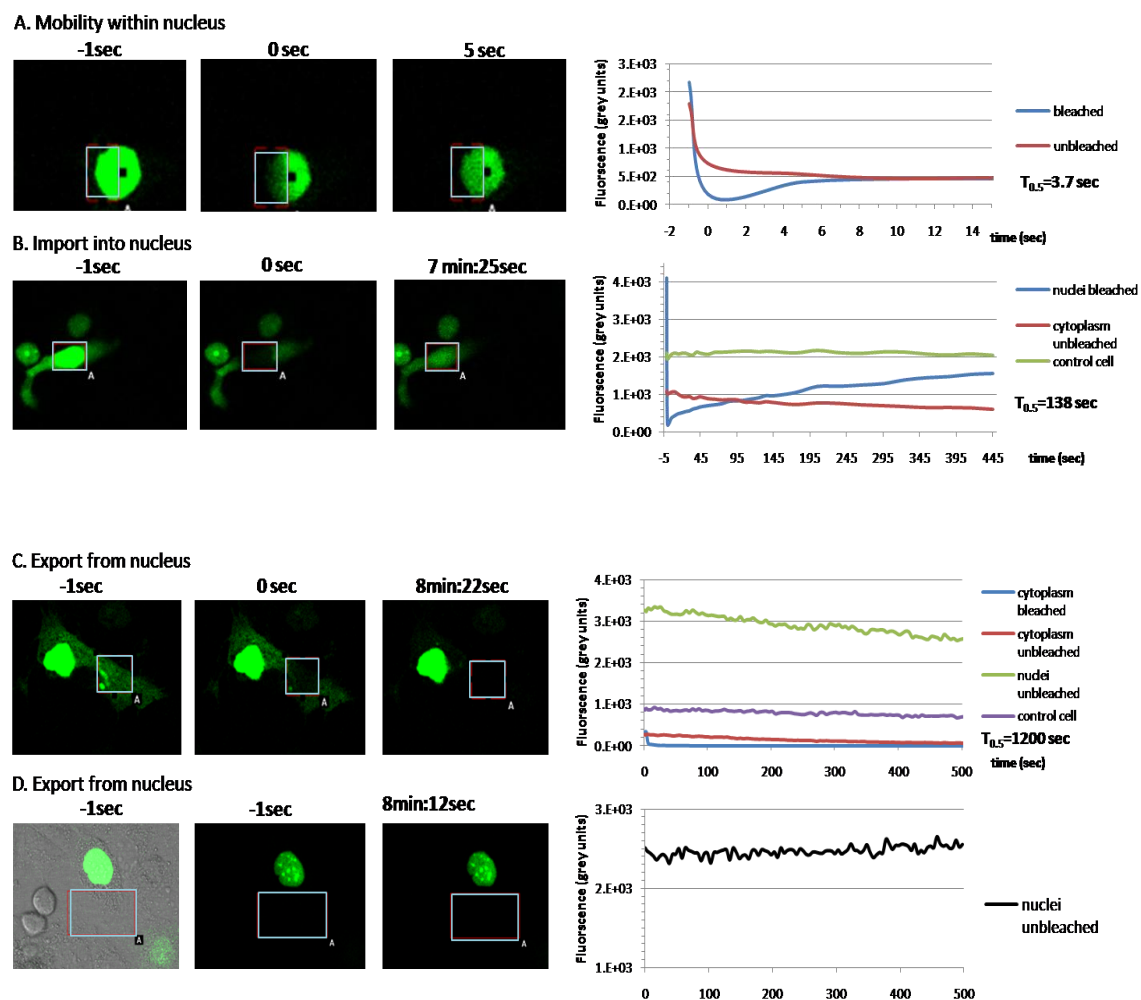
Fig.III.6 Mobility analysis of DENV NS5. CMV IE promoter driven NS5-eGFP construct was transfected into Huh-7 cells seeded in imaging plates and 16h later imaged under a CLSM. A. FRAP

analysis of NS5 mobility within the nucleus. B. FRAP analysis of NS5 import from cytoplasm into nuclei. C. FLIP analysis of NS5 export from nucleus to cytoplasm D. FLIP analysis two hours after addition of 5ng/ml of Leptomycin B.

III.1.2 Identification of determinants within NS5 affecting nuclear accumulation

III.1.2.1 Introduction of restriction sites for cloning NLS mutants

To study the NS5 nuclear accumulation in detail, NLS deletion and mutation constructs had to be generated. However restriction sites suitable for cloning were not present in region flanking the NLS. To circumvent this problem two restriction sites were inserted flanking NLS region by silent mutagenesis. An *AgeI* site and a *SacI* site were inserted at amino acids 312 and 436 respectively. The newly generated construct was compared with the wild type for its replication and infectivity titer production. The *AgeI-SacI* construct showed comparable levels of replication and supernatant infectivity compared to wild type (Fig.III.7A). The localization of NS5 was also found similar to wild type after electroporation into Huh-7 cells indicating that the construct was suitable for further studies. This construct was used for generation of all deletion and mutation constructs used in this study.
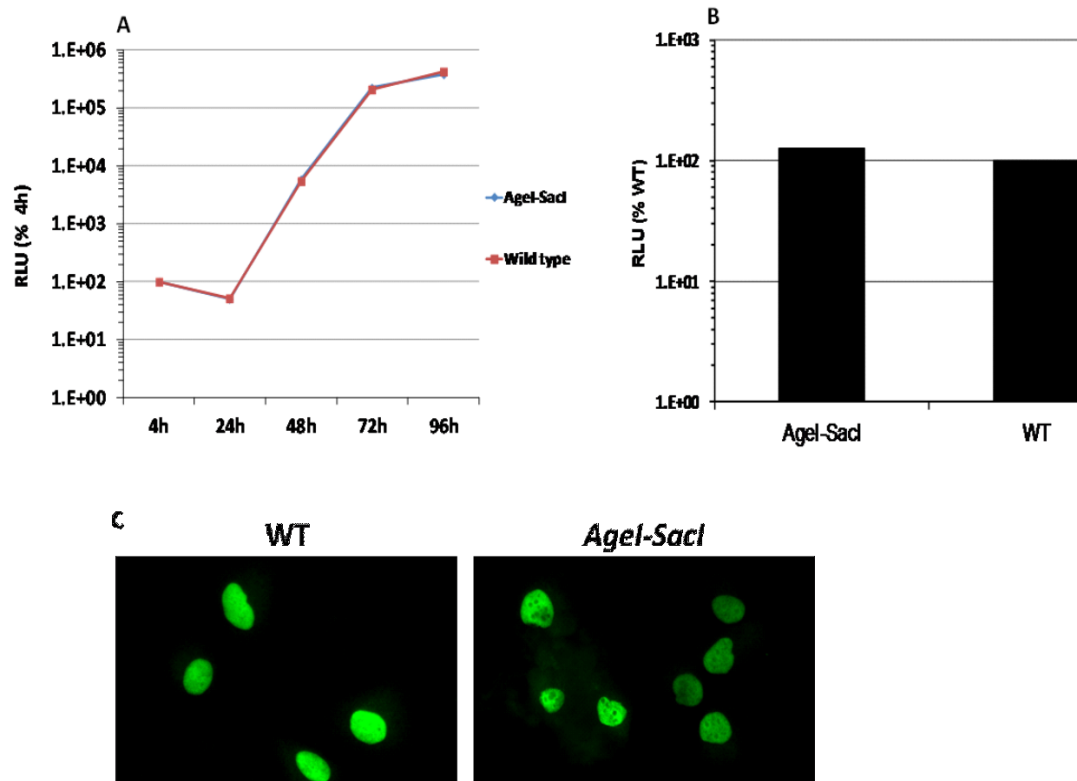
Fig.III.7 Characterization of DENV construct carrying *AgeI-SacI* cloning sites. A. Replication of *AgeI-SacI* bearing construct. *In vitro* transcribed RNA of DENV reporter virus bearing *AgeI-SacI* or wild type were electroporated into Huh-7 cells and virus replication analyzed by luciferase reporter assay. B. Cell culture supernatants were harvested 72h post electroporation and used to infect naive Huh-7 cells which were harvested 72h later and analyzed by luciferase assay. C. NS5 localization in cells 72h post electroporation was analyzed by immunofluorescence using anti-NS5 antibody.

III.1.2.2 Role of β-NLS and αβ-NLS on NS5 nuclear localization

DENV NS5 accumulates in nucleus of infected cells upon infection. We examined the role of viral components other than NS5 in nuclear transport by comparing the localization of NS5 during infection to expression of NS5 alone from a pcDNA expression vector. We observed that NS5 was able to accumulate in the nucleus to similar levels as during infection indicating that NS5 alone is sufficient for its nuclear transport. NS5 has two nuclear localization signal (NLS) sequences which were shown to be able to target proteins fused to them into nucleus (19) . To ascertain the contribution of both NLS to NS5 nuclear localization, deletion mutants lacking either β-NLS or αβ-NLS or both were generated. The NS5 dele-

tion mutants were expressed from a pcDNA expression vector in Huh-7 cells and the extent of nuclear accumulation was determined by immunofluorescence assay. We could observe that deletion of β-NLS reduced the nuclear accumulation of NS5 but did not completely block the nuclear transport whereas deletion of αβ-NLS totally abrogated the transport of NS5 into nucleus (Fig.III.8). NS5 was totally retained in the cytoplasm also when both NLS were deleted. This experiment demonstrated that αβ-NLS plays the most important role in nuclear transport of NS5 and was in line with the previous observations (93).
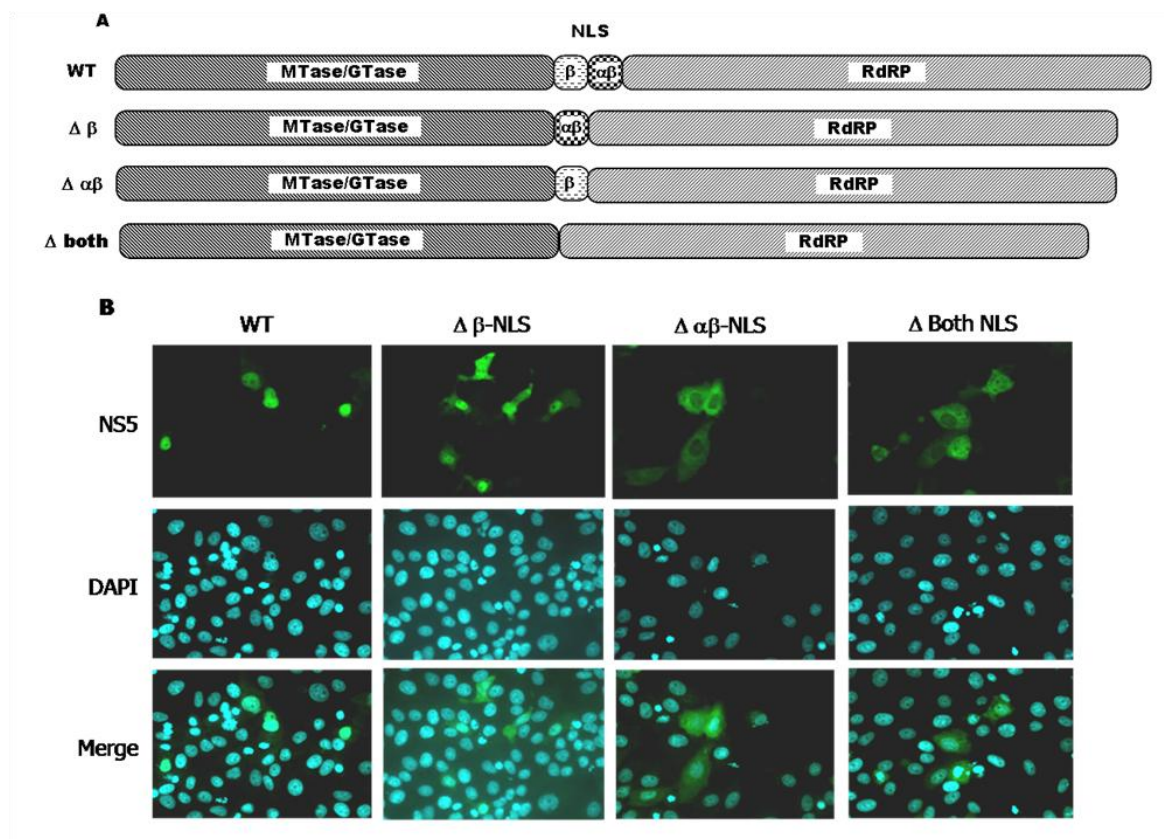
Fig.III.8 Localization of NS5 NLS deletion mutants. A. Schematic map of NLS deletion constructs generated. B. Immunolocalization of NS5. The Huh-7 cells were transfected with different NS5 constructs and harvested 16h post transfection, fixed, permiabilized and immunostained with anti-NS5 antibody. The nucleus was visualized by DAPI staining.

III.1.2.3 Construction and immunolocalization of NLS mutants

To systematically map the residues within αβ-NLS that are critical for nuclear accumulation we generated a panel of mutants where the charged amino acids

clusters were mutated to alanine (Fig.III.9). The localization of αβ-NLS mutants were analyzed by transient expression in Huh-7 cells. The mutations in the classical bipartite NLS residues (KKxxxxxxxxxxxxxxKKK) reduced the nuclear localization but did not abrogate nuclear accumulation of NS5 with residues 387-389 having a stronger impact compared to residues 371-372. Surprisingly mutations in residues downstream of bipartite NLS showed pronounced effect of nuclear accumulation with the mutations in residues 396-398 completely preventing the nuclear transport of NS5 (Fig.III.10). The mutant 397-398 also exhibited substantial retention of NS5 in the cytoplasm. In summary a panel of NLS mutants with varying levels of nuclear accumulation of NS5 could be generated by mutational analysis. The complete abrogation nuclear accumulation by mutations in residues 396-398 indicates that contrary to earlier data residues apart from classical bipartite within αβ-NLS also play a crucial role in NS5 nuclear transport.

Fig.III.9 Schematic diagrams of DENV NS5 & NLS mutations. NS5 is 900 amino acids long and possesses two domains, the N-terminal methyltransferase domain (MTase) and the C-terminal RNA-dependent RNA polymerase (RdRP) domains. The RdRP domain (aa 296-900; diagonal stripes) contains two adjacent NLSs designated β-NLS (aa 320-368; vertical stripes) and αβ-NLS (aa 369-405; horizontal stripes). The latter is bipartite (KKX$_{14}$KKK) and recognized by Importins α/β. Mutations introduced into the NLS are shown below with the alanine substitutions indicated by bold letters.

Fig.III.10 Subcellular localization of NS5 αβ-NLS mutants. (A) Huh-7 cells were transfected with plasmids directing expression of NLS mutants under control of the CMV promoter and cells were fixed 16h post transfection. Subcellular localization of NS5 was determined by immunofluorescence using a NS5-specific antibody. Images were captured with a confocal laser scanning microscope (CLSM). (B) Quantification of NS5-specific immunofluorescence by using ImageJ software. Extent of nuclear localization of NLS mutants was determined by quantifying the ratio of the NS5 signals inside the nucleus and the cytoplasm (Fn/c). Result represents the mean ± SD (n ≥50) of two independent experiments

III.1.3 Viral replication and NS5 nuclear accumulation

III.1.3.1 Effect of NS5 nuclear accumulation on viral replication

We tested the effect of NS5 nuclear accumulation on replication competence of the virus by inserting the αβ-NLS mutations exhibiting varying nuclear localization into genomic dengue luciferase reporter virus. The virus replication was measured by luciferase activity of reporter virus electroporated into BHK-21cells.

The replication assay showed that several mutations in $\alpha\beta$-NLS had a substantial effect on viral replication (371-372, 388-389, 387-389, 397-398, 396-398 and 401-402) (Fig.III.11). Higher replication was generally correlated with higher accumulation of NS5 in the nucleus except for mutant 397-398. Lower replication also showed correlation with reduced NS5 nuclear accumulation except for mutant 401-402. The supernatant infectivity of the mutants was directly correlated to their replication levels indicating no additional effect of NLS mutations on viral release or infectivity. To rule out any effect of the luciferase reporter gene on replication ability of the mutants, the mutations were also inserted into wild type DENV and the replication was ascertained by qRT- PCR following electroporation in BHK-21 cells. The replication of mutants in wild type virus context was more robust compared to the luciferase however the relative rate of replication of mutants was similar to reporter construct.
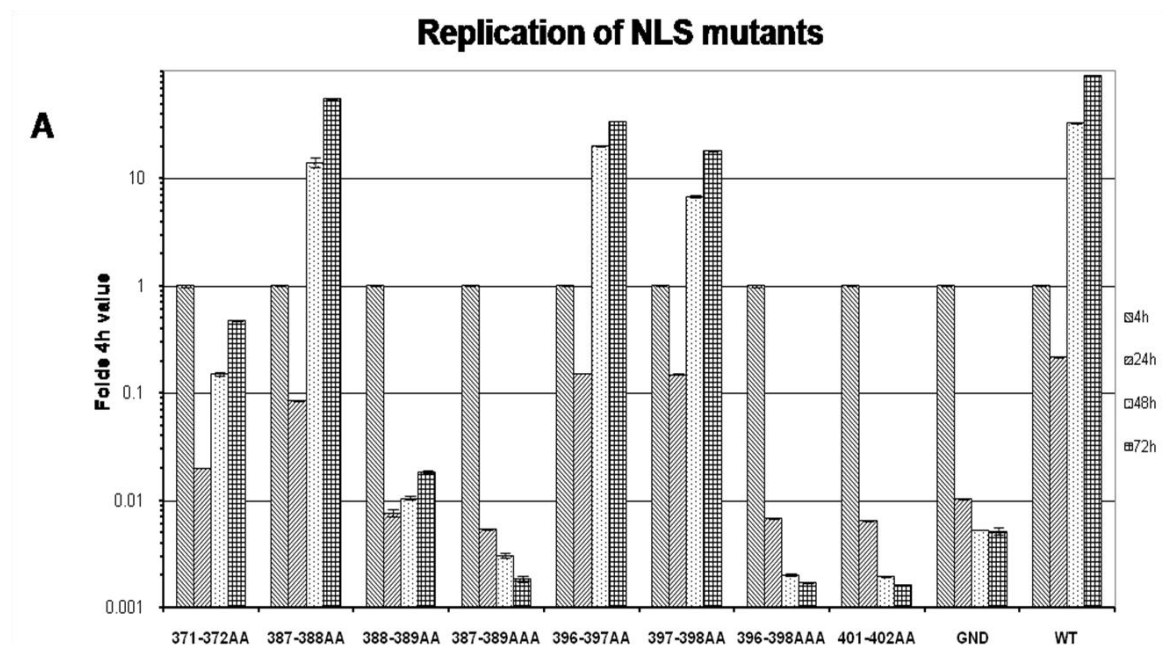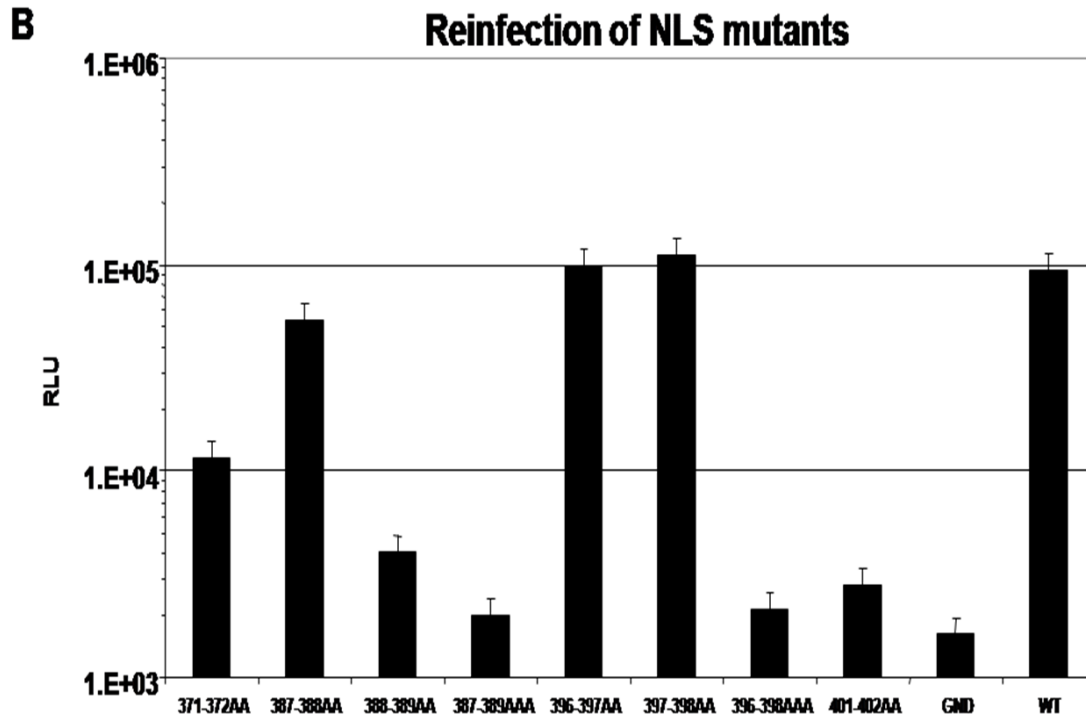
Fig.III.11 Replication competence of NLS mutants in Huh-7 cells. (A) Capped RNA generated by in vitro transcription was transfected by electroporation into Huh-7 cells. Lysates of cells prepared at time points specified in the bottom were used to determine luciferase activity. Values were normalized to the 4h luciferase activity reflecting transfection efficiency. (B) Culture supernatants of transfected cells from panel A were harvested 72h post electroporation and used to infected naive BHK-21 cells. Seventy two hours after infection DENV replication was determined by luciferase reporter assay reflecting infectivity titers released from transfected cells.

III.1.3.2 Transcomplementation of replication deficient NLS mutants

Most of the NLS mutants showing reduced replication also exhibited a reduced accumulation of NS5 in the nucleus. To study the effect of reduced nuclear accumulation of NS5 on replication impairment of NLS mutants, we tested the ability of wild type NS5 provided *in trans* to rescue the replication of NLS mutants. Reporter viruses carrying NLS mutations were transfected into a cell line stably expressing a selectable DENV sub-genomic replicon (Fig.III.12). A reporter virus carrying a partial deletion of NS1 was used as a positive control. The reporter assay of NLS mutants indicated that there was no rescue of their replication in replicon cell lines (Fig. 4A) while the NS1partial deletion construct could be rescued in replication. This experiment indicated that the NLS mutants could not be

complemented *in trans* and reduced replication of NLS mutants was probably not due to the reduced amounts of NS5 accumulated in the nucleus. The lack of rescue of NLS mutants also indicates that inability to counteract antiviral defense or recruit cellular proteins may not be the main reason for their reduced replication.
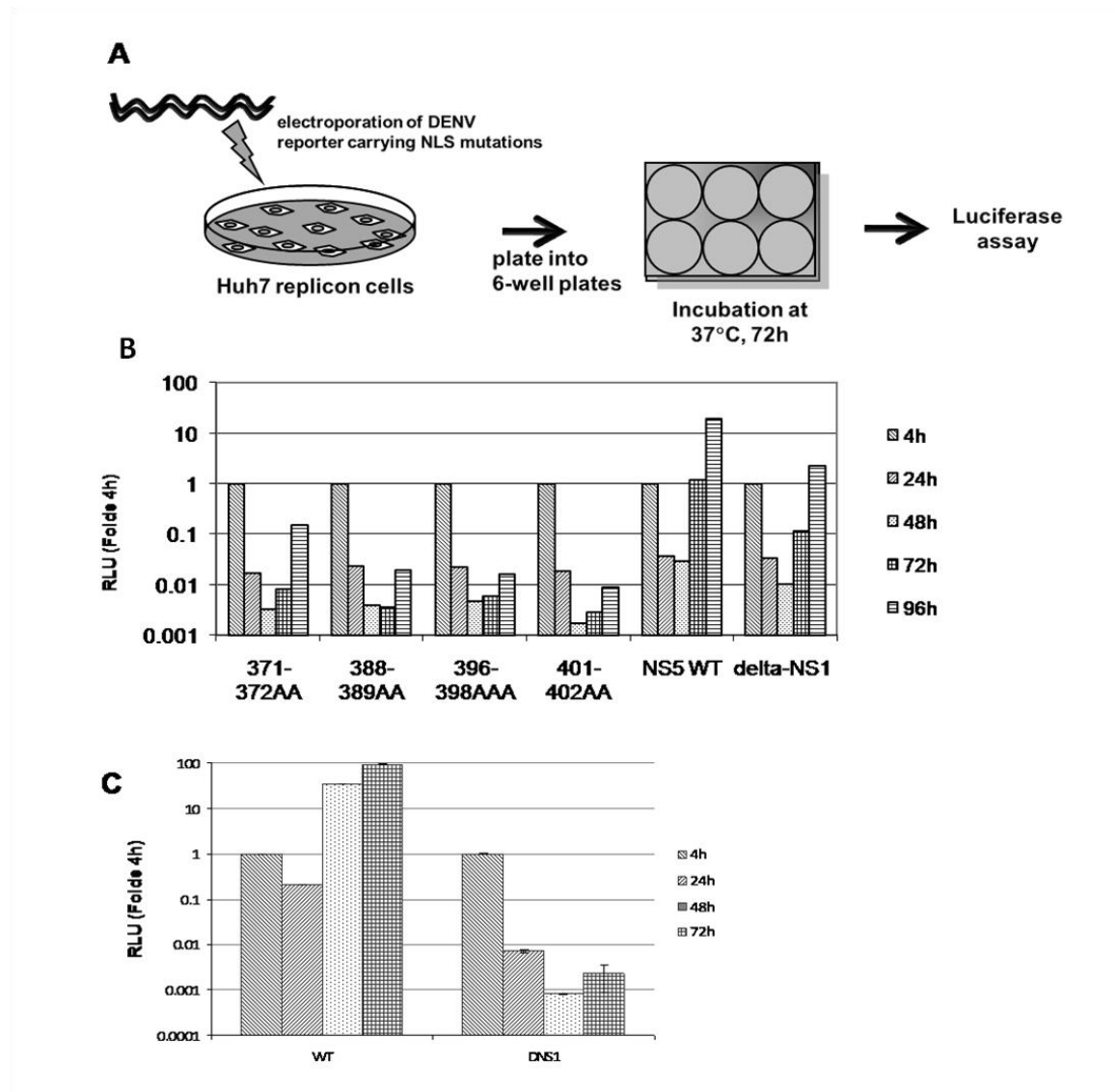
Fig.III.12 Transcomplementation of αβ-NLS mutants. (A) Schematic representation of transcomplementation experiment. (B) NLS mutants were transfected into Huh-7 cells containing a selectable subgenomic DENV-2 replicon. Replication of the NLS mutants was scored by luciferase assay using cell lysates prepared at given time point. The NS1 deletion mutant was used as a positive control. (C) Replication of NS1 deletion mutant in naïve Huh-7 cells

III.1.3.3 Effect of addition of NLS and NES to NS5

The transcomplementation experiments indicated that NLS mutants cannot be rescued in replication by providing NS5 *in trans*. To modulate the nuclear accumulation of NS5 the $\alpha\beta$-NLS of DENV was exchanged with corresponding regions from Kunjin virus(WNV$_{KUN}$). WNV$_{KUN}$ NS5 is reported as exclusively cytoplasmic contrary to DENV NS5. However DENV genomic constructs expressing WNV$_{KUN}$ NS5 $\alpha\beta$-NLS failed to replicate indicating that the exchange of $\alpha\beta$-NLS was not tolerated. Another strategy adopted to modulate NS5 localization was the addition of NLS or NES to NS5 C-terminus. To enhance the localization of the protein in the nucleus a supplementary SV40 NLS or DENV $\alpha\beta$-NLS was added whereas HIV Rev NES or PKI NES were used to enhance nuclear export. As a negative control a mutated SV40 NLS incapable of nuclear targeting was used. The NLS and NES were inserted into DENV luciferase reporter constructs and the replication was measured after electroporation into Huh-7 cells. All the constructs bearing supplementary NLS or NES failed to replicate (Fig.III.13). The failure in replication of constructs carrying mutant SV40 NLS indicates that addition of amino acid residues to the NS5 C-terminus is not tolerated.
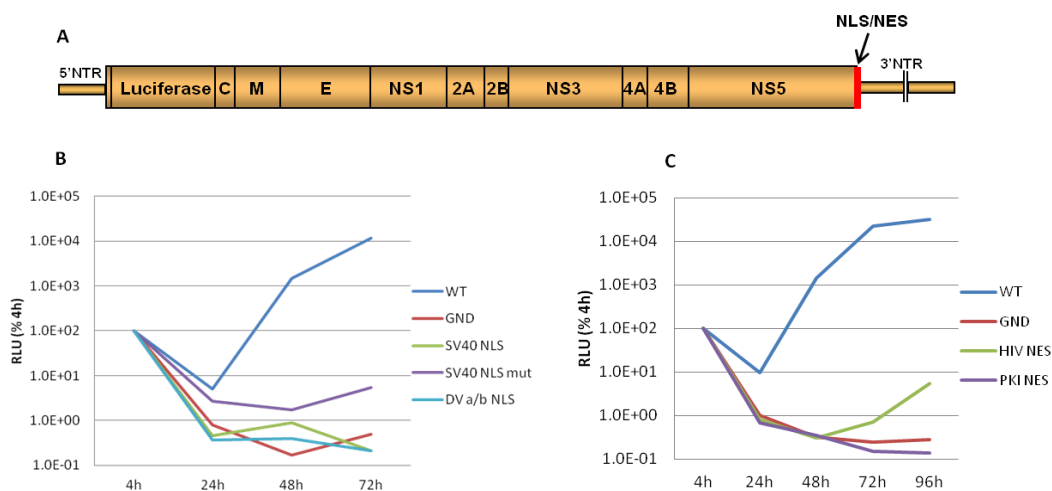
Fig.III.13 Replication of DENV reporter virus carrying a NLS or NES at NS5 C-terminal. A. Schematic representation of NLS or NES insertion at C-terminus of NS5 in DENV luciferase reporter virus. Huh-7 cells were transfected with DENV luciferase reporter viruses carrying NLS or NES and replication measured after different timepoints by luciferase assay. B. Replication of NLS bearing constructs. The NLS screened were DENV $\alpha\beta$-NLS, SV40 Large T-antigen NLS C. Replication of

NES bearing constructs. The NES screened include HIV Rev NES and Protein Kinase Inhibitor (PKI) NES.

III.1.4 Effect of NLS mutations on enzymatic activity of NS5

III.1.4.1 Bacterial expression and purification of NS5

Wild type NS5 could not complement the NLS mutants *in trans* for replication indicating that loss of replication of NLS mutants was probably not due to loss of nuclear accumulation rather from failure of certain *cis*-functions necessary for viral replication. The structural studies on the NS5 RNA dependent RNA polymerase (RdRP) domain had indicated that NLS forms an integral part of the polymerase domain (116) and subsequent genetic studies have revealed that there is significant cross talk between the polymerase domain and methyl transferase domain of NS5(64). The location of NLS mutations within the polymerase domain and the inability to complement their function *in trans* indicated possible disruption in *cis*-acting functions of NS5. To analyze the effect of NLS mutations on NS5 polymerase and methyl transferase activity, we bacterially expressed and purified histidine tagged full length NS5 containing NLS mutations. We first verified the influence of histidine (His) tag addition to the C-terminus of NS5 on viral replication by inserting the His-tag at C-terminus of NS5 in DENV reporter virus and assayed the viral replication. The His-tagged virus showed only a slight reduction (three fold) in viral replication (Fig.III.14) compared to wild type virus indicating that the tagged NS5 is enzymatically functional.
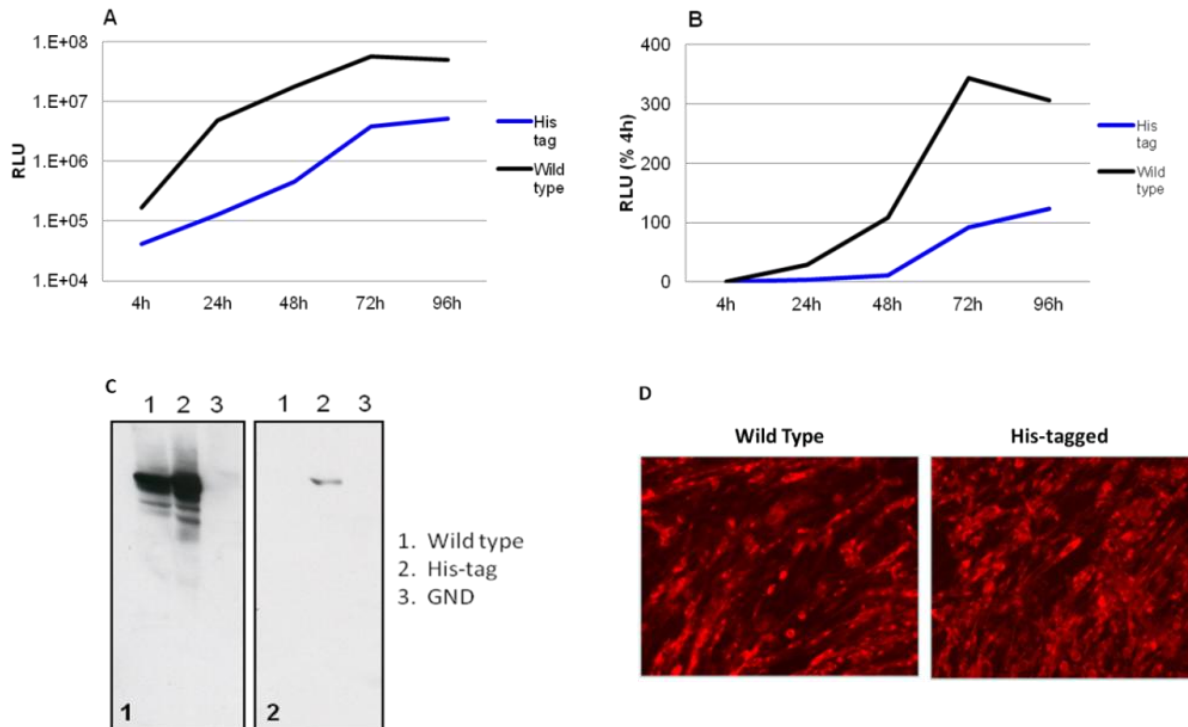
Fig. III.14 Replication of DENV reporter virus carrying C-terminal histidine tagged NS5. A. Replication of tagged virus compared to wild type (without normalization for transfection). B. Replication normalized for transfection efficiency. C. Western blot analysis of tagged virus. $2x10^6$ electroporated BHK-21 cells were plated in 10 cm dish, harvested 72h post transfection in SDS sample buffer and one tenth is loaded per lane. Panel1. probed with anti-NS5 antibody, Panel2. probed with anti-penta histidine antibody. D. Supernatant infectivity of tagged virus. BHK-21 cells were infected with equal volume of supernatant harvested 72h post transfection and infectivity determined by immunofluorescence staining against envelope protein.

Based on these results we cloned the C-terminal His-tagged NS5 into a bacterial protein expression vector under T7 promoter control (pET21b) and expressed it in bacteria. The protein recovered after purification was mostly of lower molecular mass as determined from Coomassie staining and western blot analysis indicating possible proteolytic cleavage within the bacteria (Fig.III.15). To recover full length NS5 after purification an extra hemagglutinin tag (HA) was inserted in N-terminal resulting in a double tagged NS5 protein (HA-NS5-His). Fortunately this construct was resistant to protease cleavage in bacteria enabling recovery of most of the protein in full length form (Fig.III.15C,D). Since the protein was stable and yielded highly pure full length form after His-tag purification, purification via a HA affinity column was not used in subsequent experiments.
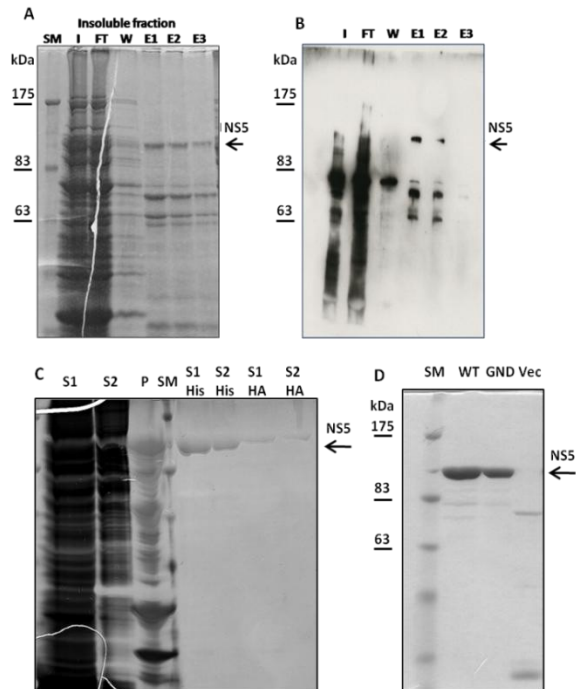
Fig.III.15 Bacterial expression and purification of NS5. A. Purification of NS5 carrying C-terminal histidine tag. I-input, FT-flowthrough, W-wash and E-elution. Purification from 100ml bacterial culture. 200μl bacterial culture worth input and flowthrough and 1/5th of elution fractions were loaded on 8% SDS-PAGE and Coomassie stained. B. Similar protein amounts were used for western blot using anti-NS5 antibody. C. Purification of NS5 carrying a N-terminal HA tag and C-terminal His-tag. Purification from 100ml bacterial culture. 1ml bacterial culture worth input and flowthrough and 1/10th of elution fractions were loaded on 8% SDS-PAGE and Silver stained. D. 5μg purified NS5 wild type and GND mutant loaded on a 8% SDS-PAGE and Coomassie stained. Empty vector is used as a control.

III.1.4.2 Characterization of RdRP activity and MTase activity of NS5

An RdRP assay and MTase assay were established to test the enzymatic activity of the purified NS5. NS5 protein carrying mutations in the polymerase catalytic active site (GND→GDD) and S-adenosyl methionine binding site (S56→A) were used as control for RdRP and MTase assays respectively. *In vitro* transcribed capped DENV genomic RNA was used as template for RdRP assay and the enzymatic activity was assayed by measuring the incorporation of $\alpha[^{32}P]GTP$ into newly synthesized RNA. As compared to GND mutant the wild type protein showed a specific and dose dependent enzymatic activity (Fig.III.16). We further studied the preference of NS5 polymerase different RNA templates in polymerase assay. NS5 was equally efficient in primer extension using polyC tem-

plate primed with OligoG and *de novo* RNA synthesis using capped DENV genomic RNA templates. The single stranded polyC was used as a template albeit with lower efficiency indicating absence of template specificity of purified enzyme. The MTase activity was assayed by measuring the incorporation of [³H] CH$_3$-group from S-adenosyl methionine (SAM) into DENV genomic RNA template containing type 0 cap. A NS5 SAM binding mutant (S56→A) was used as a control for capping reaction. NS5 efficiently incorporated [³H] label into RNA indicating a robust MTase activity compared to the control mutant. Interestingly we observed that non-capped DENV genomic RNA templates also specifically methylated with a lower efficiency indicating either GTase activity is not essential for MTase activity or presence of guanyl transferase activity in NS5 even in absence of NS3. RdRP assay and MTase activity assays indicated that bacterially purified NS5 retained both enzymatic activities.
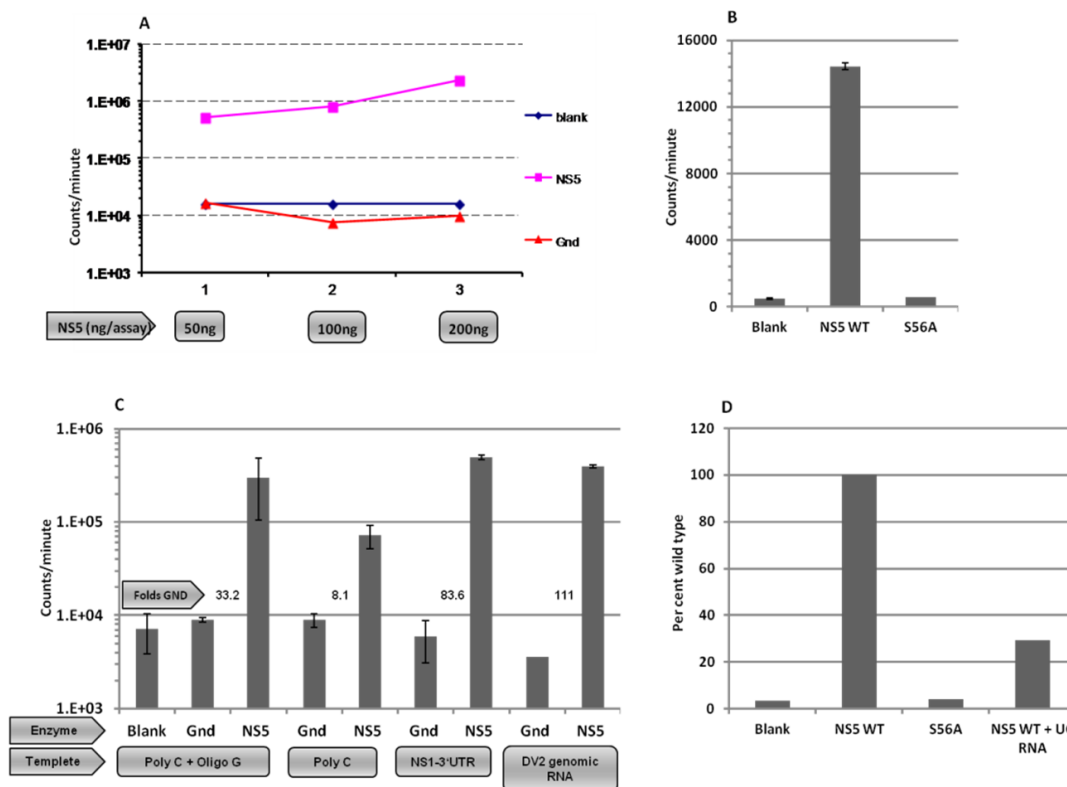
Fig.III.16 Enzymatic activity of bacterially expressed and purified NS5. A. RdRP activity of NS5 assayed on PolyC:Oligo G template. The inactive GND mutant was used as control. B. MTase activ-

ity of NS5. A Type 0 capped DENV 1-172 nucleotide RNA was used as template and SAM binding mutant S56→A was used as control. C. Polymerase activity of NS5 on different RNA templates. 100ng purified NS5 and 400ng RNA template were used for assay at room temperature for 2h. D. MTase activity of NS5 on uncapped RNA and Type 0 capped RNA.

III.1.4.3 RdRp and MTase activity of NS5 NLS mutants

The NS5 protein carrying NLS mutations were also expressed and purified using the bacterial expression system mentioned earlier. The Coomassie staining indicated that the purified proteins were highly pure without detectable contaminating bacterial proteins or degradation products. The RdRP and MTase activities of the mutants were measured using assays standardized earlier. The RdRP assay indicated that the polymerase activity of all NLS mutants was unaffected except mutant 401-402 (Fig. 5B). Interestingly the polymerase activity of mutants 397-398 and 396-398 were slightly higher than the wild type. The RdRP assay of the NLS mutants indicated that the mutations inside $\alpha\beta$-NLS are well tolerated with respect to polymerase activity except in the very C-terminal region. The effect of NLS mutations on 2'O-methyl transferase activity of the protein was analyzed by measuring the incorporation of H^3 methyl group to DENV RNA (1-172 nucleotides). The SAM binding site mutant (S56A) (64) was included as a negative control. The MTase activity of all NLS mutants were comparable to wild type indicating that reduction in replication of NLS mutants could not be attributed to impairment in MTase activity and mutations in $\alpha\beta$-NLS did not have significant effect on MTase activity of NS5. Taken together the *in vitro* assays demonstrated that replication reduction of most NLS mutants were not due to impaired enzymatic activity of NS5 as most mutations in $\alpha\beta$-NLS had no significant effect on enzymatic activity of NS5.
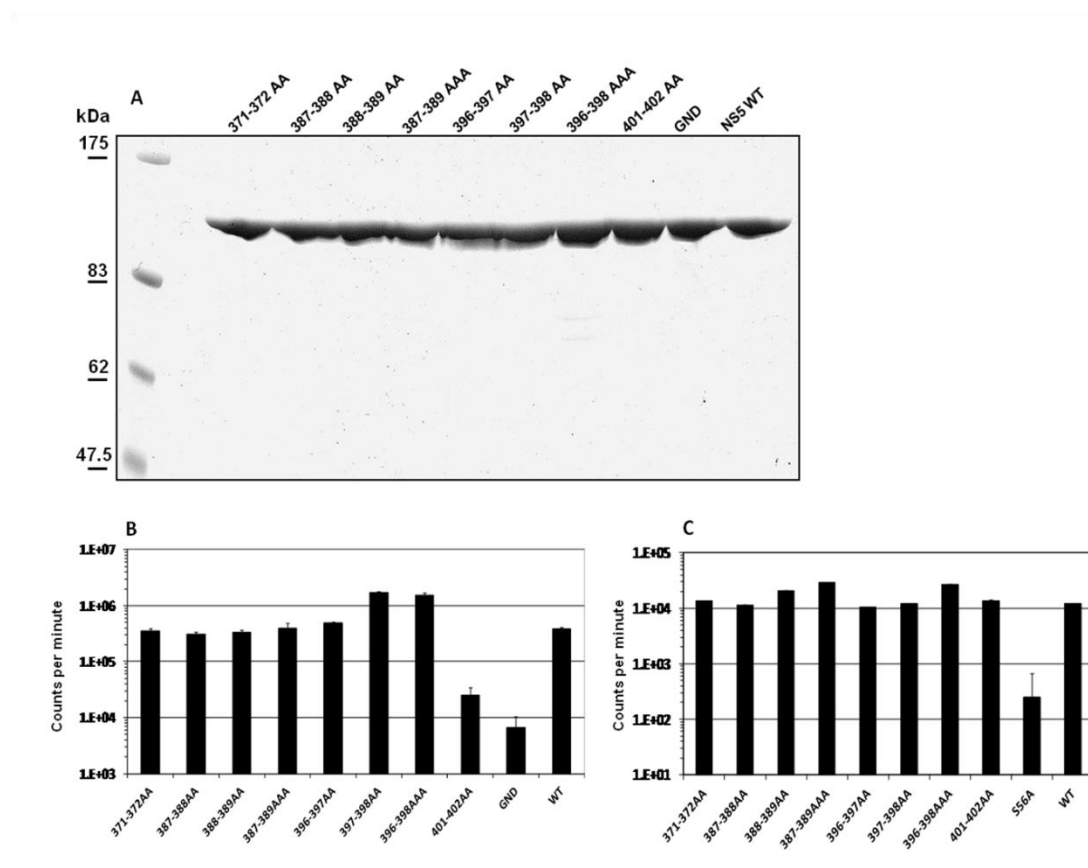
Fig.III.17 MTase and RdRp activity of NS5 carrying NLS mutations (A) Full length NS5 proteins containing a N-terminal HA tag and a C-terminal histidine tag were expressed in *E. coli* strain Rosetta(DE3) and extracted from the cell lysate by Ni-NTI affinity chromatography. Eluted proteins were analyzed for purity and integrity by SDS-PAGE and Coomassie staining. (B) RdRP assay of NLS mutants using in vitro transcribed DENV genomic RNA as template and 100ng purified NS5. Amount of incorporated [^{32}P] radio-labelled GTP was measured by liquid scintillation counting. (C) 2'O-MTase assay of NLS mutants was carried out using DENV genomic RNA template, 100ng purified NS5 and 2 µCi of [^{3}H] labelled S-adenosyl methionine. Tritium incorporation was determined by liquid scintillation counting.

III.1.5 NS5 NLS mutants and cellular innate immune response

III.1.5.1 IFN sensitivity of NLS mutants

Interferon-mediated signaling plays an important role in mounting an effective antiviral defense hence preventing the spread of DENV during an infection. However once replication is established DENV subverts the interferon signaling by degrading STAT2 and hence blocking transcription of interferon-induced genes. NS5 plays an important role in blocking interferon induced signaling by binding to STAT2 and blocking its phopshorylation and nuclear transport (7). We inves-

tigated the effect of NLS mutations on the ability of DENV to counteract interfe-ron mediated antiviral defense. The sensitivity of DENV NLS mutants to IFN-α or IFN-γ were studied to analyze the effect of reduced nuclear accumulation of NS5 on viral replication under interferon treatment. HCV (strain JFH-1) luciferase re-porter virus was used as a control. The addition of interferon-α 24h post electro-poration had a dose-dependent effect on DENV replication in Huh-7 cells with the highest concentration of 10000u/ml resulting in approximately 10 fold re-duction in reporter activity (Fig.III.18). Although the level of replication of un-treated wild type and NLS mutants was different they showed similar sensitivity to IFN-α treatment as observed from the same extent of reduction in replication at different doses. HCV also showed very high sensitivity to interferon-α treat-ment. The interferon-γ treatment had a stronger effect on DENV replication with 1000u/ml reducing viral replication by 100 folds. The NLS mutants showed a similar dose-dependent reduction in replication as compared to wild type indicat-ing that NLS mutations do not confer additional sensitivity to interferon. The re-duction in STAT2 levels in infected cells was also similar between wild type and NLS mutant virus (Fig.III.18C).
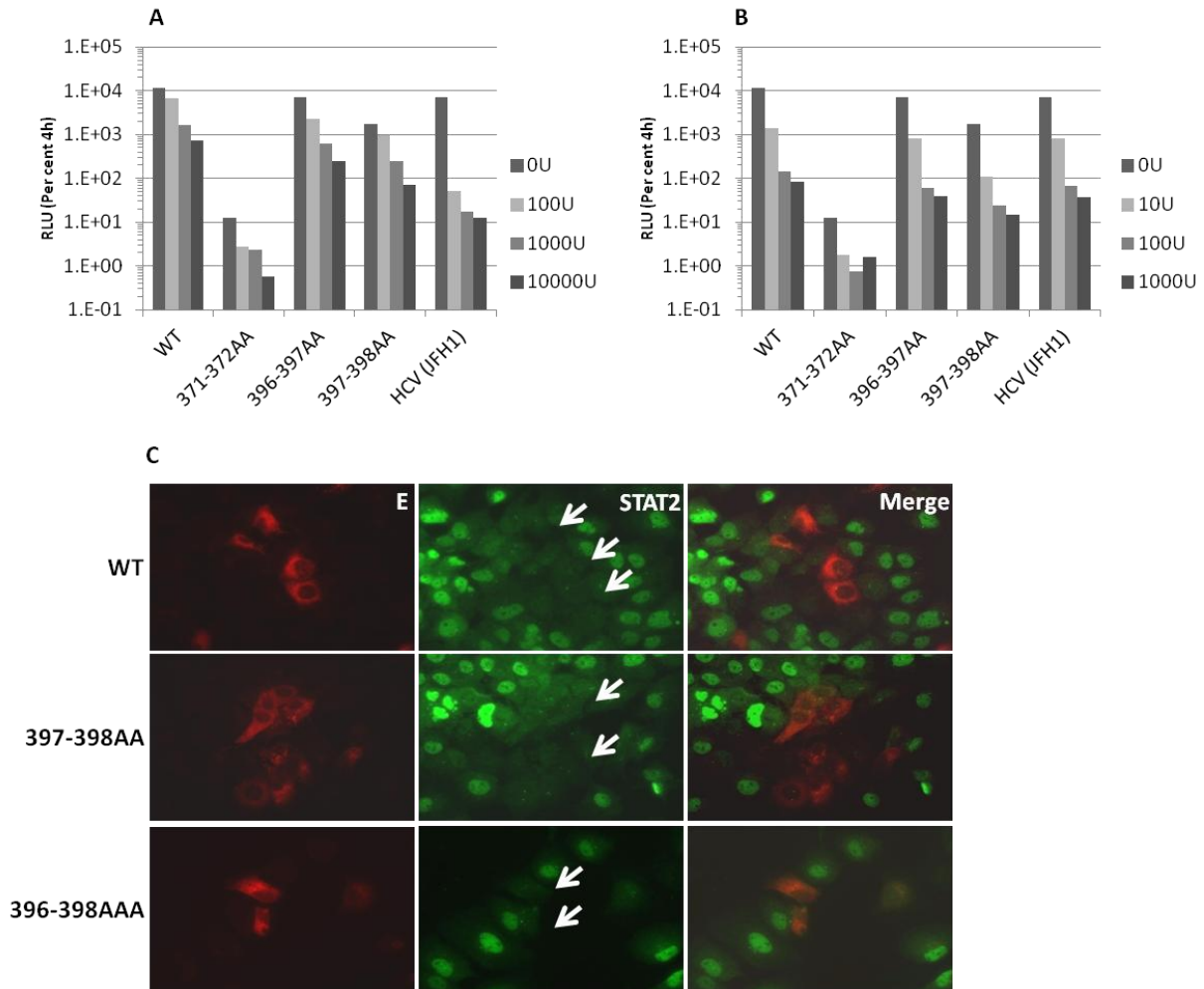
Fig.III.18 IFN sensitivity and STAT2 degradation by NLS mutants. A. Huh-7 cells were electropo-rated with DENV reporter virus containing NS5 NLS mutations and 24h post transfection were treated with varying amounts of interferon-α. The cells were harvested 48h later and viral replica-tion measured by luciferase assay. B. replication of NLS mutants treated with interferon-γ. C. Huh-7 cells electroporated with NLS mutants were treated 72h post electroporation with 100u/ml of interferon-α for two hours and viral infection and STAT2 estimated later by indirect immunofluo-rescence using anti-E and anti-STAT2 antibody.

III.1.5.2 Effect of IL-8 on DENV replication and Induction of IL-8 by NLS mutants

The earlier studies (93) on NS5 nuclear accumulation observed a higher induc-tion of IL-8 during replication of NLS mutants compared to wild type. They sug-gested that reduction in replication of NLS mutants could be due to their ability to induce higher amount of IL-8 compared to wild type. To analyze the effect of IL-8 on DENV replication, we measured replication of reporter viruses grown in

presence of IL-8 which was added either 4h prior to or after infection. The time of addition of IL-8 had a marked effect on its activity with the addition prior to infection significantly reducing viral replication whereas addition post infection had a stimulatory effect on replication (Fig.III.19). This implies that IL-8 does not have an inhibitory effect on an ongoing replication. We also measured the IL-8 induction by NLS mutants with qRT-PCR. The IL-8 mRNA induction by two NLS mutants with different level of replication was compared with the wild type. The results indicated that the level of IL-8 corresponded with the replication level of the mutants and not with the extent of nuclear accumulation of NS5 of the mutants. To further verify this point we transiently expressed pcDNA NS5 NLS mutants in 293T cells and their effect on IL-8 promoter activity was measured by co-transfection of IL-8 promoter driven luciferase reporter plasmid. The results indicated that reduction in nuclear accumulation of NS5 did not result in significant up regulation of IL-8 as compared to the wild type (Fig.III.19D). Taken together the above results shows that IL-8 has no major inhibitory effects on ongoing viral replication and replication NLS mutants does not induce significantly more IL-8 compared to wild type virus.
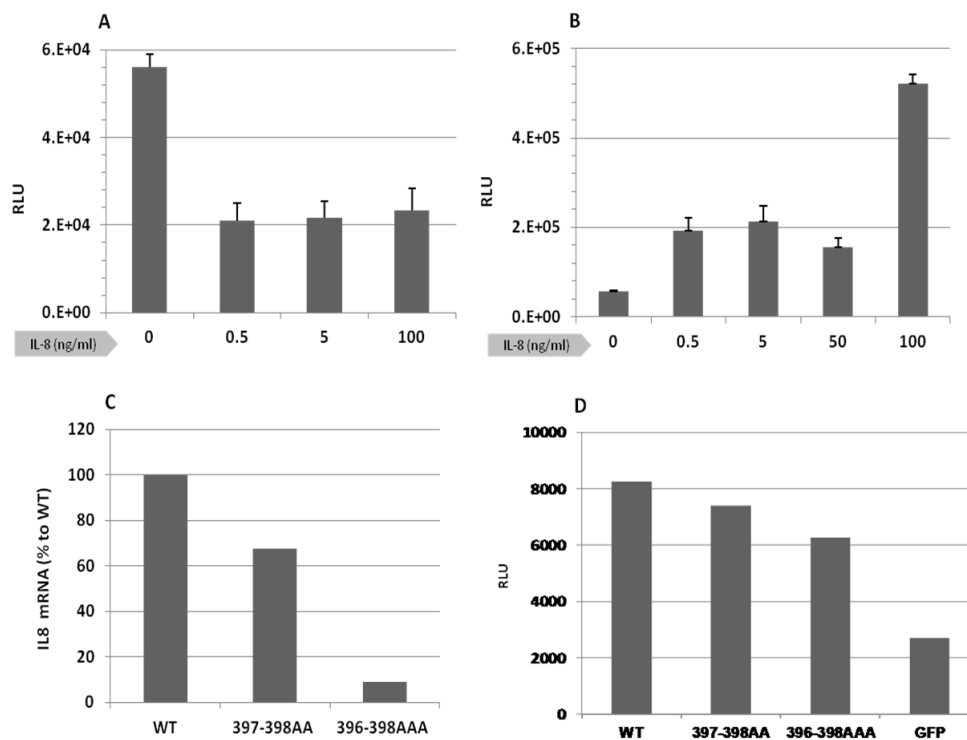
Fig.III.19 IL-8, NLS mutations and DENV replication. A. Effect of pre-treatment of IL-8 on DENV replication. Huh-7 cells were treated with increasing concentration of IL-8 four hours prior to infection with DENV luciferase reporter virus. Replication assayed 72h post infection by luciferase assay. B. Effect of IL-8 treatment 4h post infection. The cells were assayed for viral replication 72h post infection as described earlier. In both A and B the IL-8 was present throughout the period of incubation except during 4h of infection. C. IL-8 mRNA transcript levels 72h post electroporation in Huh-7 cells transfected with either DENV wild type or NLS mutants. Huh-7 cells electroporated with equal amount of in vitro transcribed RNA of full length viruses carrying NLS mutation and harvested 72h later and IL-8 RNA levels determined by quantitative real time PCR. D. IL-8 reporter activity in presence of NS5 NLS mutants measured by co-transfection of pcDNA NS5 NLS mutants and IL-8 firefly luciferase reporter in Huh-7 cells. The cells were harvested after 24h and IL-8 induction measured by luciferase assay. A constitutive renilla luciferase construct was used to normalize transfection efficiencies.

II.1.6 Characterization of NS5 interacting proteins identified by Yeast Two Hybrid Screen

Few cellular proteins like STAT2 and ZO1 are known to interact with NS5. NS5 interaction with STAT2 plays a major role in enabling DENV to counteract cellular antiviral defense. A Yeast Two Hybrid screen was performed to identify potential cellular interaction partners of NS5. This screen was carried out with full

length NS5 as bait and cDNA libraries derived from liver and thymus as prey and it was conducted by our collaborator Dr. Sung-Key Young at 'Panbionet' in Pohang, South Korea. Self-activation was ruled out by control experiments. The screen identified 19 cDNA clones interacting with NS5 which were mapped by sequencing to five cellular proteins. The proteins identified were Remodelling and Spacing Factor 1 (RSF1), Calpain 2(CAPN2), Nephronophthisis 3 (NPHP3), Betaine-homocystein methyl transferase (BHMT) and activating signal cointegrator 1 complex subunit 3-like 1 (ASCC3L1). The functional effects of these proteins on DENV replication was further characterized by siRNA-mediated silencing of these proteins in Huh-7 cells. qRT-PCR was used to measure the efficiency of silencing and the viral replication was assayed using a DENV reporter virus. The silencing of these proteins had minimal effect on DENV entry and replication in Huh-7 cells indicating that higher levels of these proteins were not necessary for efficient DENV replication (Fig.III.20).
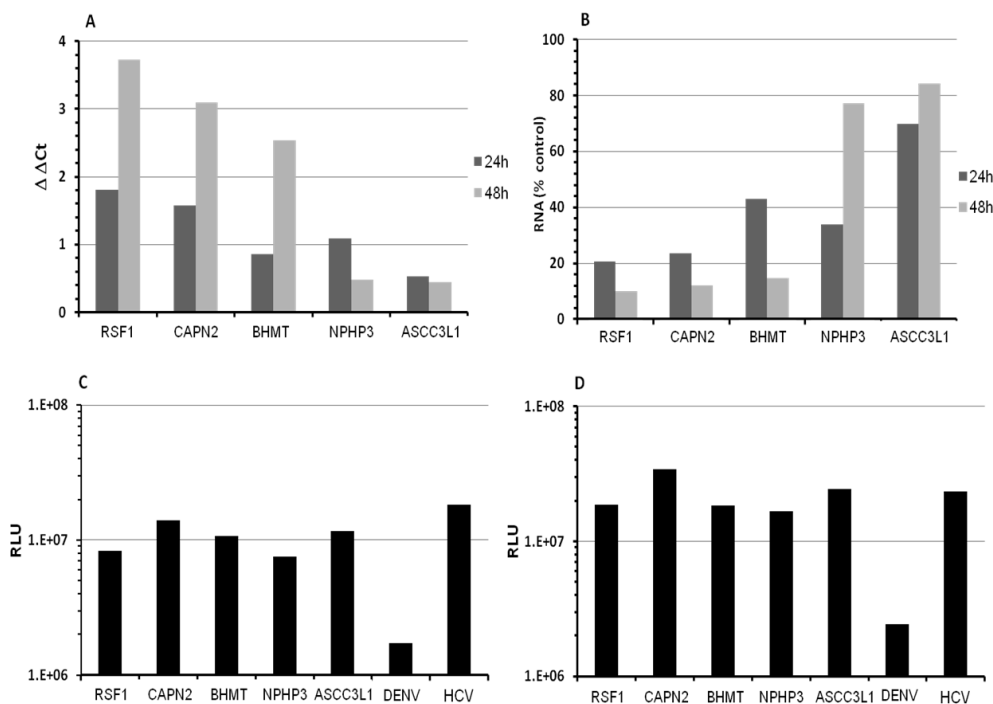
FigIII.20 Effect of siRNA silencing of cellular genes on DENV replication. The Huh-7 cells were transfected with 5nM siRNA of two different siRNAs targeting same gene and 24 or 48h later in-

fected with DENV reporter virus. The cells were lyzed 72h post infection and viral replication assayed by luciferase assay. A. qRT-PCR analysis of silencing of cellular genes measured 72h post infection. B. The residual RNA amounts after silencing. C,D: The viral replication in cells silenced with siRNAs targeting cellular genes. siRNA against DENV and HCV were used as positive and negative controls respectively. C. Infection 24h post silencing D. Infection 48h post silencing.

III.2 Identification of cellular kinases influencing DENV infection through genome-wide kinase RNAi screen

Flaviviruses encodes only a limited set of proteins essential for their infection cycle. They extensively depend on host cell proteins during different steps of life cycle including virion attachment, entry, replication, particle assembly and secretion. Although extensively studies were carried out to understand the functions of viral proteins, there is only limited understanding on the role played by various cellular proteins during DENV infection. Initial studies on cellular factors modulating flaviviral infection were carried out by characterizing cellular proteins that directly interacted with viral proteins or viral RNA. Knocking-in or knocking-out of some of these genes had significant impact on viral life cycle. However due to technical limitations the number of cellular genes identified by these techniques was very few. Few siRNA-based (RNAi) screens and drug-based screens recently published (23, 63, 98, 103) identified an array of cellular genes influencing DENV life cycle. However the RNAi screens done so far did not directly focus on host cell candidates influencing DENV infection in human cell. The first screen primarily investigated the cellular genes affecting WNV infection and genes identified were later screened for their effect on DENV replication as well (63). Mosquitoes being the vector of DENV, the second screen investigated the insect genes crucial for DENV replication and identified 116 host genes among which 42 had human homologues with significant effect on viral replication in Huh-7 cells (103).

In this study we planned to identify cellular kinases having significant influence on DENV entry and replication using a RNAi screen in Huh-7 cells. Another important parallel goal of this study was to establish a RNAi screening platform adapted to flaviviruses, develop the necessary tools and standardize protocols in view to perform larger scale RNAi screens later. Parameters like spotting of siRNA, cell seeding and handling, infection with DENV, immunostaining, image acquisition and analysis and statistical tools for data analysis had to be optimized for this study.

III.2.1 Establishment of high-throughput siRNA screening platform DENV

The establishment of RNAi screening platform for DENV involved developing an optimal screening pipeline for efficient siRNA delivery, viral infection, scoring viral infection and appropriate statistical tools for data analysis. The technology required for siRNA spotting, image analysis and statistical and bioinformatical analysis of the data were developed by external research groups having expertise in relevant fields in collaboration with us and were later optimized for DENV screen. However the procedures for cell seeding, viral infection and immunostaining and image acquisition were standardized by us during the course of this study.

III.2.1.1 Optimization of transfection conditions

The efficiency of siRNAs delivery into cells is one of the most critical parameters for a successful siRNA-mediated gene silencing experiment. This depends on the combination of cell type, transfection reagent used and duration of silencing. It is known that cell lines respond differently to various transfection reagents. We screened various commercially available transfection reagents to identify the optimal reagent which gives the best silencing efficiency without apparent cytotoxicity. A validated siRNA directed against the cellular protein p53 was transfected with various transfection reagents and 48h later the silencing efficiency, cytostatic and cytotoxic effects were monitored by immunofluorescence. Among the transfection reagent screened Lipofectamine 2000® was found to be most efficient with a silencing efficiency of more than 90% in Huh-7 cells (Fig.III.21). No cytotoxic or cytostatic effects were observed during this time period. Based on these observations all further experiments were carried out using this transfection reagent.
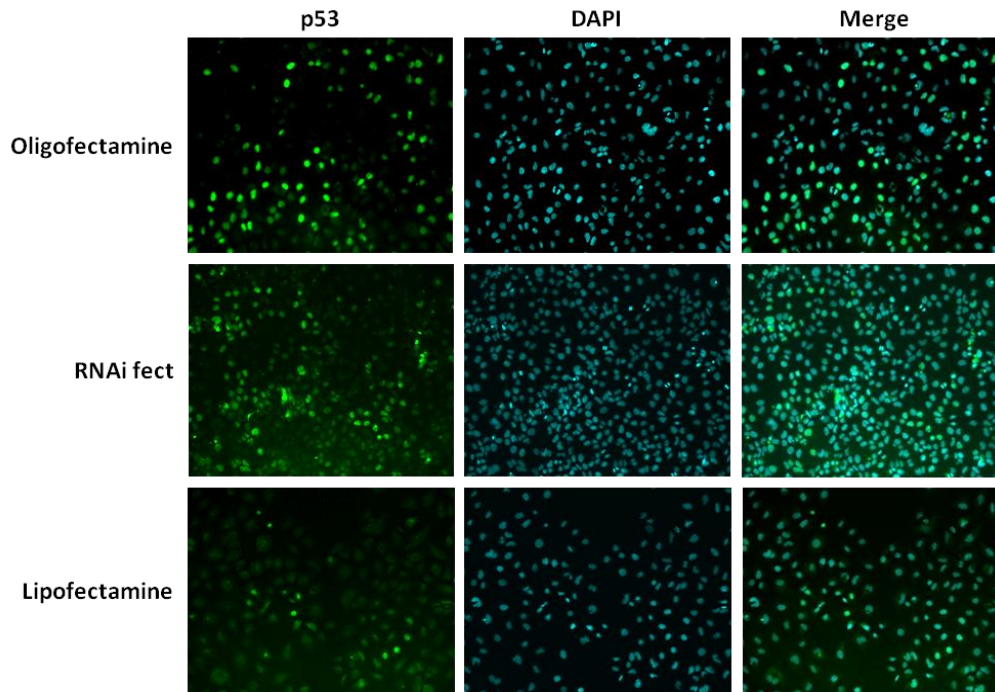
Fig.III.21 Screening of transfection reagents for silencing efficiency. Huh-7 cells seeded on cover slips in 24-well plates and 24h later transfected with 5nM siRNA against p53 protein using different transfection reagents according to manufacturer's protocol and the silencing efficiency was analyzed 48h later by immunofluorescence assay using anti-p53 antibody.

III.2.1.2 Validation of siRNAs targeting the DENV genome

During the establishment phase of the screen no cellular or viral siRNAs that can efficiently down regulate DENV replication was yet described. A siRNA with clear effect on viral replication was important in the screening procedure to validate the efficiency of gene silencing and to serve as a positive control against which the test candidates could be compared. To identify a siRNA which can efficiently reduce DENV replication a panel of siRNAs targeting various regions of DENV2 genome was generated and their effect on viral replication was studied. The Huh-7 cells transfected with viral siRNAs were infected with DENV2 at an MOI of 2-5 and 48h later viral replication was estimated by either immunofluorescence assay or western blot analysis. A siRNA against HCV was used as control. The siRNAs targeting the NS1 region was found most efficient in reducing viral replication followed by siRNA targeting NS3 region (Fig.III.22). The other siRNAs

tested had only minor effects on viral replication. The NS1 and NS3 siRNAs were selected as positive control in all subsequent experiments.
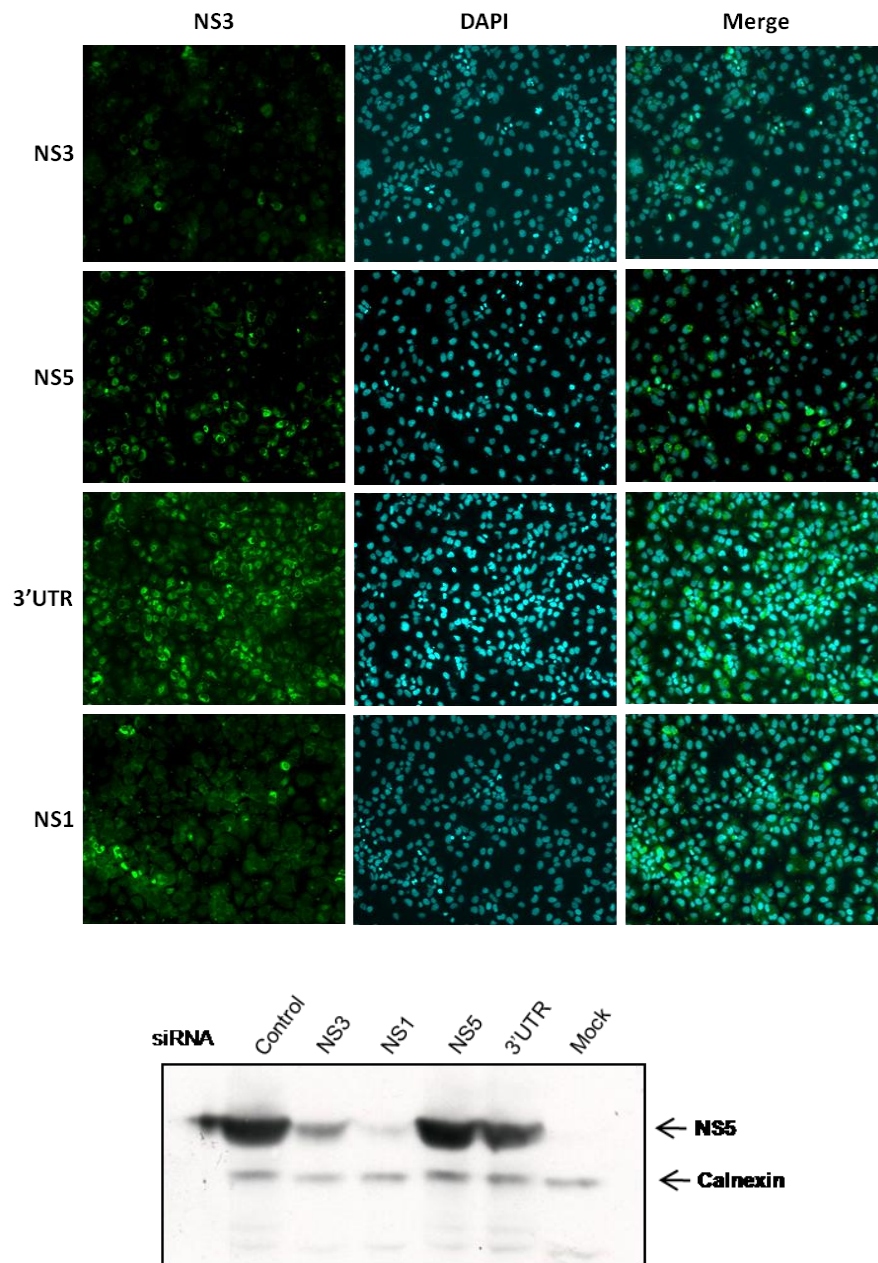
Fig.III.22 Effect of various siRNAs on DENV replication. A. Huh-7 cells seeded in 6-well plates containing cover slips were transfected with 5nM siRNAs at 50-60% confluency and infected 24h later with DENV at MOI of 2-5. 48h later the coverslips were processed for immunofluorescence using anti-NS3 antibody whereas the rest of the cells were harvested in SDS sample buffer and western blot was carried using anti-DENV NS5 and anti-Calnexin antibody.

To test whether the selected siRNAs were as efficient in reverse-transfection format, the siRNAs were spotted on to chambered slides, Huh-7 cells were seeded on these plates, infected with DENV and viral replication was assayed by indirect immunofluorescence. The viral infection was reduced more than 80% in spots containing NS1 siRNA compared to control siRNA spots (Fig.III.23), proving that NS1 siRNA was highly efficient in suppressing viral replication in reverse-transfection experiments.
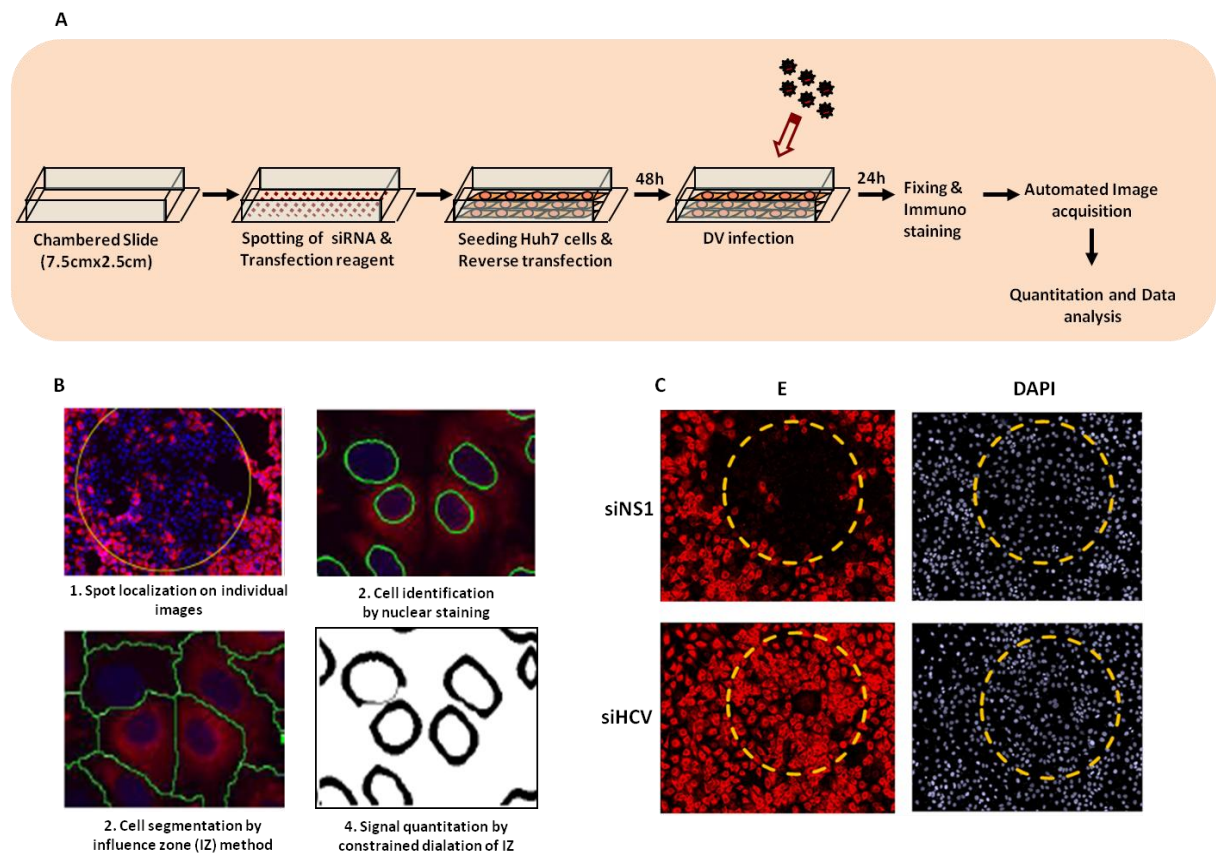
 Fig.III.23 Reverse transfection based RNAi screen. A. Schematic representation of siRNA silencing by reverse-transfection. Chambered slides were spotted with siRNA/transfection reagent mix. The spots were dried and cells were seeded on siRNA spotted chambered slides. The siRNA is taken up by cells growing on top of spots by reverse transfection. The cells were later infected with DENV and 24hr later infection is measured by immunostaining with DENV-E antibody and the nucleus visualized by DAPI staining. B. Steps involved in image processing and signal quantitation C.The viral replication in spots transfected with NS1 siRNA or control HCV siRNA visualized by immunostaining against DENV envelope protein.

III.2.1.3 Enhancement of Immunofluorescence signal

When images generated by conventional immunofluorescence staining protocol were quantified, the signal to noise ratio of images for non-silencing control siR-NA spots was found less than two folds (signal intensity of ~ 550 units and a background noise of 220 units for a 10 bit image) resulting in a very limited observation window. To improve the signal to noise ration two different modifications of the immunofluorescence techniques were tested. In the first approach a fluorescently labeled tertiary antibody against the fluorescently labeled secondary antibody to double the number of fluorescently labeled antibodies binding to each primary antibody. In the second approach the standard staining procedure involving primary and secondary antibody was repeated twice to form antibody trees containing multiple antibodies binding to the original primary antibody. We observed that the second method (Fig.III.24) resulted in higher signal to noise ration compared to the first method which was better than the standard staining procedure. This modified staining protocol was adopted for all further siRNA screens. Similarly optimizations were also done for defining the dilution of primary and secondary antibodies and the duration of staining (data not shown) to develop a highly sensitive staining procedure for the screening assay.
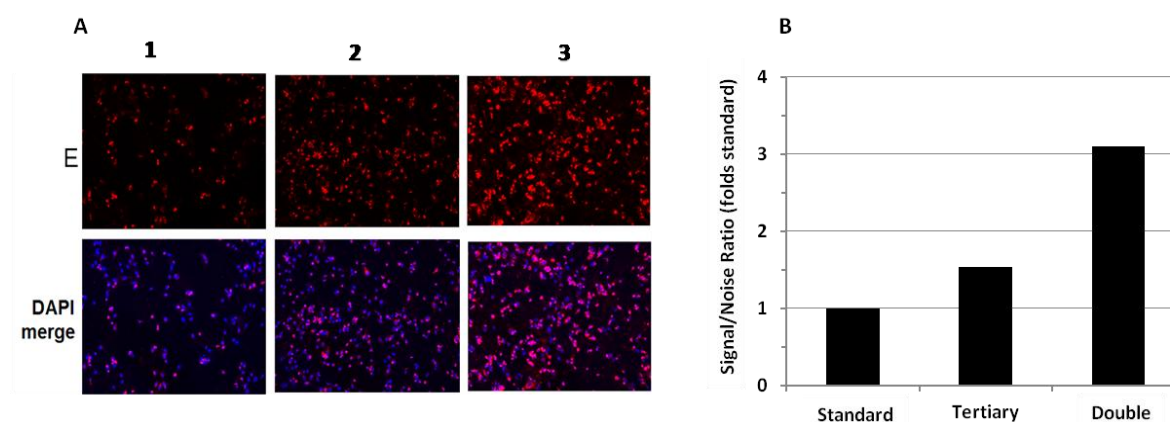
Fig.III.24 Immunofluorescence staining modifications to improve specific signal. A. Immunofluorescence staining. Huh-7 cells seeded on cover slips in 24-well plates were transfected with 5nM non-silencing control siRNAs at 30-40% confluency, infected with DENV2 at 2-5 m.o.i. 24hr later, cells were fixed and immunostained. 1. Standard staining (primary and secondary antibody staining) 2. Stained with primary, secondary and tertiary antibodies, 3. Double staining (primary and secondary staining followed again with primary and secondary staining). B. Quantitation of aver-

age signal intensity: The mean signal intensity of images was quantified using software ImageJ and the values were normalized to cell number.

III.2.1.4 Pilot siRNA screen

A pilot siRNA screen was carried out with limited number of genes to study the performance of control siRNAs and to validate the assay setup based on reverse transfection. Huh-7 cells were seeded on chambered slides spotted with selected cellular siRNAs, infected with DENV and viral replication was measured by im-munostaining and image quantitation. The candidate genes were selected based on their reporter interaction with DENV or other flaviviral proteins. The first and last spots contained fluorescently labeled siRNAs to properly orient the plates during image acquisition and to check the directional accuracy of the micro-scope. siRNA targeting HCV and scrambled siRNA were used as negative control while siRNAs targeting NS1 and NS3 regions of DENV genome were used as pos-itive control. Though none of the cellular genes checked showed a phenotype for DENV replication the positive control siRNAs efficiently reduced viral replication to 20% of nonsilencing control.

siRNAs
1. DENV 3'UTR-TRITC
2. PTB
3. VapA
4. DENV NS3
5. DENV NS1
6. HCV 321
7. CypB
8. CD81
9. Importin-β
10. p53
11. CD81
12. La
13. HSP70
14. TSG101
15. SR-B1
16. Scrambled
17. HCV 321
18. DENV 3'UTR-TRITC
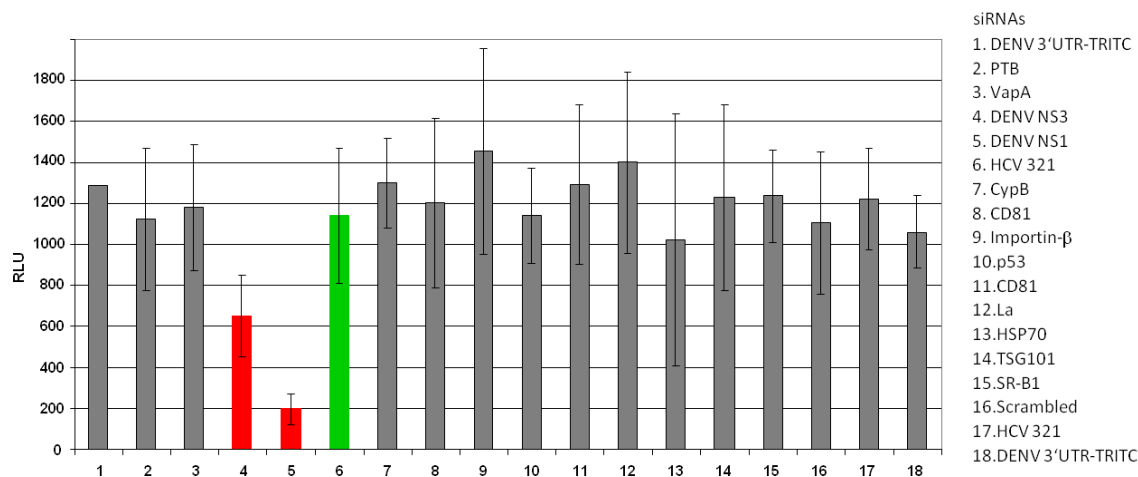
Fig.III.25 Pilot imaging based RNAi screen. Chambered slides spotted with siRNAs against 11 cel-lular genes and positive and negative controls were seeded with Huh-7 cells and 48h later infected with DENV at a MOI of 2. The viral replication was measured 24hr later by immunostaining with DENV-E antibody and the nucleus visualized by DAPI staining. The images acquired by Olympus Scan^R microscope were quantitated with ImageJ software.

III.2.2 siRNA-based primary screen of the human kinome

The primary screen was performed with a genome-wide kinase siRNA library containing siRNAs targeting 719 cellular kinases with three independent siRNAs against each gene. The library was spotted onto seven chambered slides with 4 positive controls (DENV NS1 and NS3 siRNAs in duplicate) and 13 negative control siRNAs spotted in each slide and each slide carried 384 siRNA spots. The image-based screen was carried out in duplicates and was repeated six times. The experiments were subjected to quality checks to eliminate images with staining artifacts, out of focus images etc. Nine experiments were finally utilized for statistical analysis and selection of the candidate genes. The statistical analyses included normalization of cell number between plates of the same experiment, normalization of signal within plates based on cell count using Lowess to remove systematic effect of cell number on signal and finally normalization between plates based on signal by B-Score computation (for details refer methods section). The Z-score was calculated from the mean signal over replicates and the p-values were calculated for each siRNA using Student's T-test. The candidate genes for validation screen were selected with low stringency criteria of a Z-score ≥ ±1 and a p-value of 0.05 with at least one siRNA against each gene. By these criteria 60 host susceptibility kinase candidates and 50 host resistance candidates were selected for further evaluation. We observed that for most of the selected candidates only one among the three siRNAs targeting them showed a phenotype. This could possibly be due to the nature of the screening library where most of the siRNAs used were bioinformatically derived and their silencing efficiency was not validated in actual experiments. The image based primary screen showed high variation between mean image intensities between some experiments primarily due to the immunostaining variations between the experiments and the variations introduced by the prototype scanning microscopes used to acquire images from the initial set of experiments. The variations in siRNA spotting can account for some of the variance of the controls within and among experiments.

III.2.3 Validation of candidates from primary screen

The candidates selected from the primary screen were further verified for their role in DENV entry or replication in a secondary screen where each selected gene was targeted with three new siRNAs. The image-based screen was replaced with a luciferase reporter virus based screen in 96-well format which enabled a more robust assay due to more number of cells and showed higher sensitivity and skipped the steps involving immunostaining, image acquisition and analysis. To establish the method a pilot screen was carried out using few candidates selected from the primary screen and control siRNAs. The 96-well plates were coated with siRNAs along with transfection reagents and Huh-7 cells seeded on them were infected with DENV renilla luciferase reporter virus and replication was measured by luciferase assay 48h post infection. The positive control NS1 siRNA reduced the viral replication by 80% compared to non-silencing control siRNA. The siRNAs against host susceptibility factors LEDGF and CKI-α identified from primary screen slightly reduced viral replication and siRNA against host resistance factor CD2 increased viral replication by two fold (Fig.III.26).
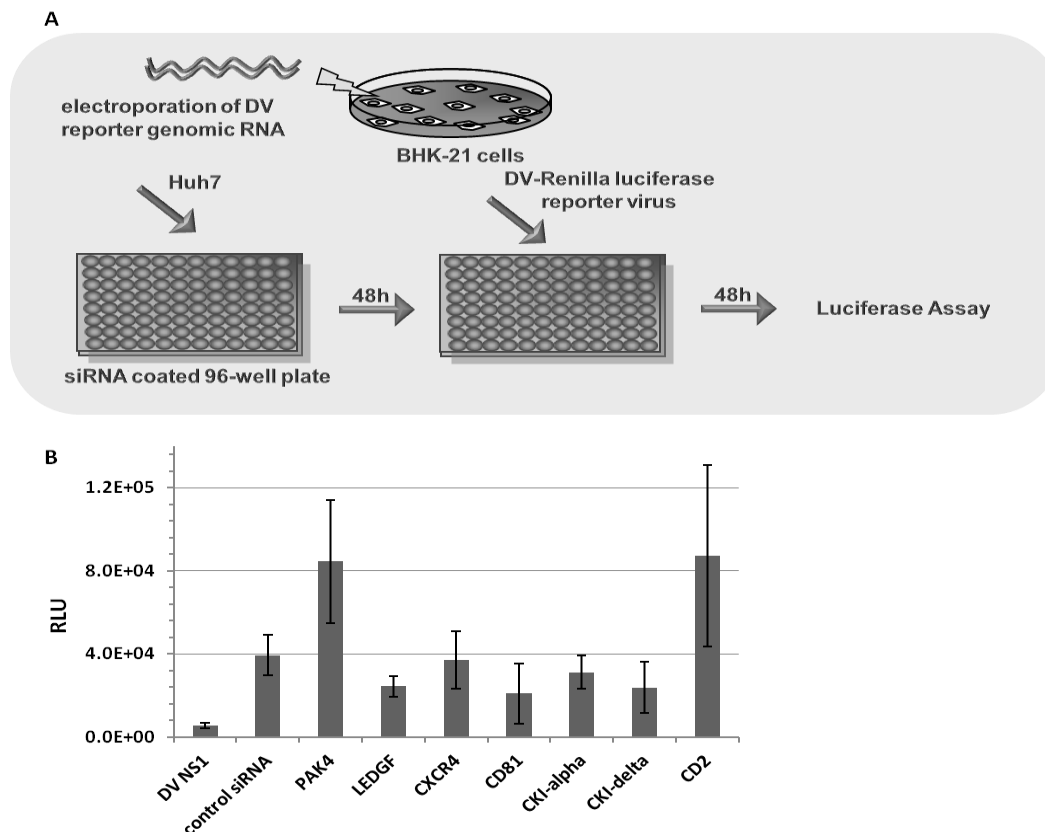
Fig.III.26 Pilot luciferase based RNAi screen. A. Schematic representation of the screen. 96-well plates with siRNAs against 7 cellular genes and positive and negative controls were seeded with 1.5×10^5 Huh-7 cells/well and 48h later infected with DENV (generated by electroporation of capped DENV reporter construct in BHK-21 cells) at MOI of 0.5. The viral replication was measured 48hr later by luciferase assay. B. Replication of DENV reporter virus in cells silenced with siRNAs against various genes as measured by luciferase reporter assay. The values are expressed as relative luminescence units ± SD

III.2.3.1 Validation by infection based RNAi screen

110 kinases selected from the primary screen were screened in the second round with a new set of three siRNAs targeting each gene. The validation screen for selected kinases was performed twice in duplicate. The statistical analysis showed that the replicates had a very high correlation and all positive controls significantly reduced viral replication; however the nonsilencing controls showed a high variability.
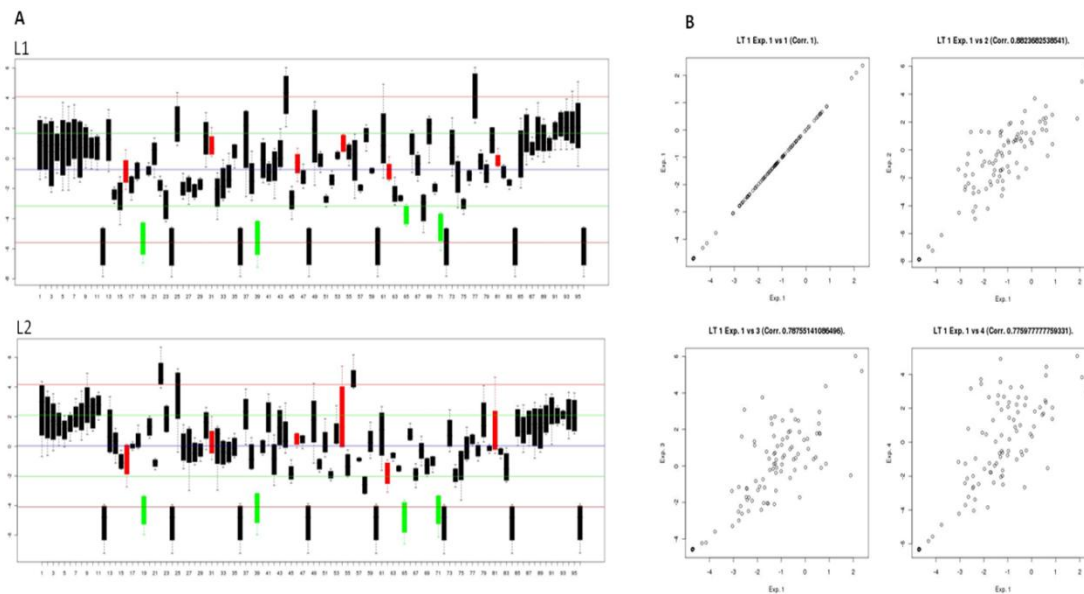
Fig.III.27 Statistical analysis of validation screen. A. The box plot representation of normalized luciferase signal from four experiments. The L1 and L2 and the plates 1 and 2 out of the total seven plates used. The red bars represent negative control wells whereas green bars represent positive control wells. To minimize variations due to medium evaporation, the outer row of wells of the 96-well plate were not spotted with siRNAs and hence not used. B. Pearson correlation of individual wells between experiments. The correlation of wells in plate 1 between four repetitions is given as an example.

Following statistical analysis the kinases having significant impact on entry or replication of DENV were selected by the hit criteria of Z-score greater than ±2 for at least one siRNA targeting each gene. Based on these criteria 18 host susceptibility kinases and 14 host resistance kinases were identified to have significant effect on entry/replication of DENV. One kinase (MAP3K7) showed significant up and down regulation of viral replication with different siRNAs indicating off-target effect with at least one siRNA.

Table III.1 List of genes identified by infection based validation screen

A. Host dependency kinases

	Gene Name	Z-Score
1	FGFR4	-3.29
2	FES	-3.26
3	NEK5	-3.07
4	C19orf35	-3.03
5	MAP3K7	-2.75
6	CDK4	-2.72
7	CALM2	-2.64
8	DGKQ	-2.61
9	PRKCM	-2.61
10	ANKK1	-2.52
11	ACVR1	-2.40
12	BTK	-2.36
13	MPP1	-2.34
14	ERBB3	-2.29
15	BLK	-2.29
16	FLT3	-2.27
17	ANKK1	-2.22
18	CSNK1D	-2.20
19	CDK5	-2.16
20	CD2	-2.03
21	ALS2CR2	-2.01

B. Host resistance kinases

	Gene Name	Z-Score
1	PRKY	2.14
2	DAPK1	2.18
3	MKNK2	2.39
4	FGFRL1	2.39
5	PRKCQ	2.72
6	ERBB4	2.82
7	ROCK1	3.13
8	ERBB2	3.33
9	MAP3K7	3.69
10	CSNK1A1	3.74
11	UMP-CMPK	3.95
12	CIB4	4.14
13	IHPK3	4.21
14	C9orf96	4.56
15	CDKL3	4.90

III.2.3.2 Validation by DENV reporter replicon based RNAi screen

The kinase candidates identified by DENV infection based validation screen could be essential for either viral entry or replication. To delineate the role of candidate kinases on either entry or replication of DENV, a RNAi screen was carried out on Huh-7 cells stably bearing a DENV subgenomic renilla luciferase reporter replicon. As there is no virion entry step involved and viral replication is already established in this cell line the observed effects of silencing different kinase will solely be due to their effect on ongoing DENV replication. The candidates were selected after 48h silencing of Huh-7 cells carrying DENV subgenomic replicon bearing renilla luciferase reporter. The screen identified 4 kinases essential for maintaining viral replication and 11 kinases reducing viral replication. Only very few candidates from the infection based screen were identified (2/18 dependency kinases and 2/15 resistance kinases) and with several new genes were newly identified which were not present among those identified by infection based screen. The kinases which were not identified as host dependency factors

in this screen might have role in either viral entry or establishment of replication. The host dependency kinases which were newly identified might have role in maintenance of replication but not in the early stages like formation of replication complexes. Similarly the newly identified host resistance factors might be crucial in reducing ongoing viral replication but might not have major role in preventing the formation of replication complexes.

Table III.2 List of genes identified by replicon based validation screen

A. Host dependency kinases

	Gene Name	Z-score	p-Value
1	PIP5K2C	-2.96	0.04
2	C19orf35	-2.68	0.02
3	AURKB	-1.66	0.02
4	CD2	-1.63	0.01

B. Host resistance kinases

	Gene Name	Z-score	p-Value
1	PRPS1L1	4.75	0.02
2	ERN2	3.43	0.04
3	PRPS1L1	2.87	0.04
4	MKNK2	2.38	0.03
5	STK32A	2.38	0.04
6	ACVR1	2.16	0.04
7	C9orf96	2.14	0.04
8	CDK3	2.12	0.02
9	DTYMK	2.08	0.03
10	TK2	2.05	0.03
11	PRPSAP1	2.02	0.03

III.2.4 Validation of selected candidates with chemical inhibitors

The effect of three selected candidates Fibroblast growth factor receptor 4 (FGFR4), Mitogen activated kinase kinase kinase 7 (MAP3K7) and Diacylglycerol kinase θ (DAGQ) on DENV entry and replication was validated by using chemical inhibitors targeting these genes. Huh-7 cells were treated with FGFR4 inhibitor PD173074, MAP3K7 inhibitor 5Z-7-Oxozeaenol or DAGQ inhibitors R59-022 and Dioctanoylglycol with varying concentration and their effect on DENV replication was measured by infection with DENV luciferase reporter virus. The FGFR4 inhibitor PD173074 and DAGQ inhibitor R59-022 showed dose dependent inhibition of DENV replication (Fig. III.28). The cytotoxic effects measured with Cyto-Tox 96 kit (Promega) indicated no detectable cytotoxic or cytostatic effects for

PD173074 whereas R59-022 showed cytotoxicity at higher concentrations (100µM). DENV replicon cells bearing luciferase reporter was treated with chemical inhibitors to differentiate their effect on viral entry and replication. The DAGQ inhibitor R59-022 showed a dose dependent decrease in viral replication whereas FGFR4 inhibitor PD173074 had only mild effect indicating FGFR4 might be involved in viral entry and DAGQ in viral replication.
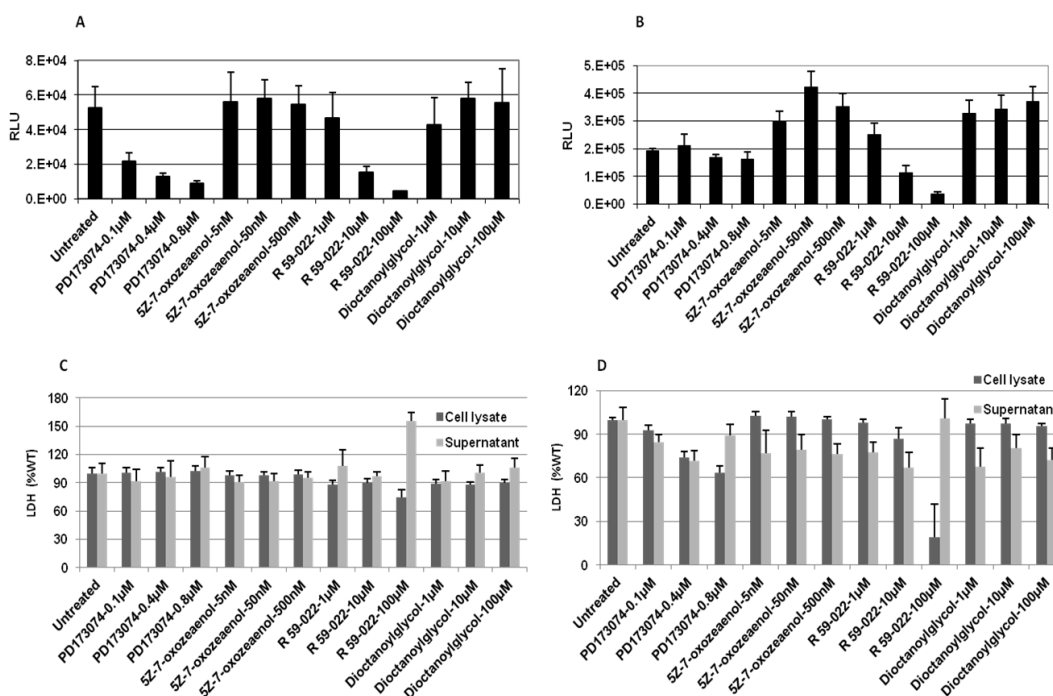
Fig.III.28 Effect of kinase inhibitors on DENV replication. A. Huh-7 cells treated with kinase inhibitors at different concentrations for 16h and infected with DENV luciferase reporter virus at MOI of 0.5 and replication measured after 48h by luciferase assay B. Huh-7 DENV replicon cells treated with kinase inhibitors at different concentrations and replication measured after 48h by luciferase assay C. Cytotoxicity of kinase inhibitors on Huh-7 cells measured with CytoTox96® (Promega) kit. Higher Lactate dehydrogenase (LDH) activity in medium indicates apoptosis while lower LDH activity in cell lysate indicates cytostatic effects D. Cytotoxicity of kinase inhibitors on Huh-7 cells measured with CytoTox96® (Promega) kit.

IV Discussion

IV.1.1 DENV NS5 nuclear localization upon infection

Flaviviral polymerases are multifunctional enzymes playing important role in viral replication and subverting the cellular innate immune response. Despite all their currently known activities taking place in the cytoplasm substantial amount of NS5 accumulate in nucleus of DENV and YFV infected cells. However NS5 nuclear localization is not reported for other flaviviruses like WNV and WNV$_{KUN}$ indicating that its functional role is virus specific. It is also interesting to note that both DENV and YFV are lymphotrophic (replicating mainly in the human circulatory system) whereas WNV is neurotrophic. The nuclear accumulation of NS5 in DENV infected cells was reported by several earlier studies as reviewed here (29) however the functional role of this phenomenon is not clear yet.

We started the study by examining whether NS5 nuclear accumulation is a common theme in all DENV replication supporting cell lines. We observed NS5 nuclear accumulation in a wide range of mammalian cell lines and insect cell line (C6/36) indicating that this phenomenon is highly conserved among insect and mammalian hosts of DENV. This also implies that the mechanisms regulating the partitioning of the protein between the cytoplasmic and nuclear compartments is conserved among both host species and nuclear accumulation of NS5 may have important functional roles in both human and arthropod host.

The nuclear localization of NS5 when expressed alone was similar to an infection event indicating that NS5 does not dependent on other viral proteins for its nuclear transport, though this does not rule out probable modulation of this process by its interaction with other viral proteins. An intriguing observation made during this study was that NS5 nuclear transport was much less efficient when expressed under a T7 polymerase transcription system as compared to cellular transcription machinery or DENV replication. Further analysis on this observation revealed that NS5 expressed from a T7 driven system could not be mobilized into nucleus by co-expression of other DENV non-structural proteins or by wild

type infection. The role of mRNA capping was ruled out by treatment of pcDNA NS5 expressing cells with RNA cap methylation inhibitor Sinefungin. Western blot analysis showed same apparent size for NS5 produced during DENV infection and by transient expression under T7 promoter. These observations indicate that the nuclear transport of NS5 can be modulated by external factors like expression system however more experiments are required to elucidate the exact reason for this observation.

The polymerase protein of several flaviviruses is known to be phosphorylated (10, 11, 79, 95). The phosphorylation of DENV polymerase was reported block its interaction with NS3 and results in its nuclear accumulation (59). *In vitro* phosphorylation studies have identified a CKII phosphorylation site within NS5 (36) while a mass spectrometric analysis discovered a Protein kinase G (PKG) phosphorylation site (12). To examine whether NS5 phosphorylation occur in Huh-7 cells we did orthophosphate labeling of DENV replicon cells followed by immunoprecipitation. However the assay failed to detect any phosphorylated bands of NS5 despite successful immunoprecipitation and radiolabeling of control protein. The initial studies on DENV NS5 phosphorylation carried out on CV-1 cells observed that the hyperphosphorylated form of NS5 was only found during low serum conditions indicating phosphorylation could be regulated by physiological conditions. The reasons for our failure to detect the phosphorylated form of the protein may be a lower sensitivity of the assay, preferential binding of the antibody used to nonphosphorylated form of the protein or low proportion of phosphorylated protein in the total pool of NS5 in Huh-7 cells. Recent mass spectrometric studies indicate amino acid 449 within NS5 polymerase domain is phosphorylated by PKG and mutation of this residue severely affects viral titers. Further investigations are required to know whether NS5 phosphorylation is cell line dependent and it regulates the nuclear accumulation of NS5.

A recent study identified a NES within β-NLS indicating that NS5 is exported from the nucleus (94) implying NS5 is highly mobile protein shuttling between cytoplasm and nucleus. We used NS5 N-terminally fused with GFP to study the rate of mobility of the protein between and within cytoplasm and nucleus. The

protein showed free diffusion within the nucleus indicating that major portion of the protein within the nucleus is not bound to cellular structures. However within the cytoplasm the diffusion was much restricted indicating possible interaction with membrane bound cellular proteins. The approximately tenfold difference observed between the import rate and export rate of the protein into the nucleus indicates an efficient import mechanism resulting in eventual nuclear accumulation of NS5 with very little nuclear export. Though this approach is limited by possible difference in mobility between GFP-NS5 and NS5 during an infection, it gives the closest possible approximation on NS5 shuttling between the compartments. The role of NS5 shuttling between two compartments on viral life cycle is not clearly understood presently. The earlier studies indicated that blocking nuclear export of NS5 by leptomycin results in a moderate phenotype of twofold increase in viral titer and a twofold reduction in IL-8 production. However since leptomycin induced block of CRM1-mediated nuclear export may have pleiotropic effects on several cellular processes it is difficult to delineate the effects due to block in NS5 export from general effects on the cellular metabolism.

Taken together earlier studies and our data indicate that nuclear accumulation of NS5 is cell type independent and occurs in both human and insect cells. Current models suggest that phosphorylation may act as a switch between NS5 cytoplasmic retention by its interaction with NS3 and its nuclear transport. However our experiments to detect phosphorylated form of NS5 in Huh-7 cells were not successful. So additional experiments are required to verify this model for NS5 nuclear transport.

IV.1.2 Contribution of NLS on NS5 nuclear transport

A systematic deletion mapping of NS5 NLSs was carried out to identify the residues which are most critical for nuclear accumulation. The deletion mapping of NS5 NLSs revealed that deletion of β-NLS increased the cytoplasmic retention of the protein however did not completely block the transport of the protein in to the nucleus. The deletion of $\alpha\beta$-NLS completely retained the protein in cytoplasm indicating its essential role in NS5 nuclear transport. These observations being

clearly in line with the earlier study (93) indicates that though $\alpha\beta$-NLS is critical for nuclear import, several other regions may influence nuclear transport probably due to their role in formation of proper topology or regulating factors influencing importin binding. The $\alpha\beta$-NLS carrying a classical bipartite NLS motif ($RRX_{14}RRR$) was systematically mutated to narrow down the most essential residues within this region required for NS5 nuclear transport. Unlike the previous studies which concentrated on the putative bipartite NLS motif within this region, a systematic mutational analysis of all charged residues within the $\alpha\beta$-NLS was undertaken in the present work for mapping the relative contribution of these residues in NS5 nuclear transport.

Though the mutations of bipartite NLS reduced nuclear transport, the mutations of a charge cluster ($_{396}REE_{398}$) downstream of bipartite NLS fully abrogated NS5 nuclear transport. This observation was interesting since this mutation could successfully block the activity of both NLS motifs without altering them directly. This could probably due to its influence on the protein topology or direct weakening of NS5-importins interaction. Further binding studies between the mutants and importins might reveal the precise mechanism involved. Apart from mapping the critical amino acid motifs essential for NS5 nuclear transport, the mutational analyses also generated several NLS mutants with varying degree of nuclear accumulation which were used in further functional investigations.

IV.1.3 Replication of NLS mutants

The next question we addressed was the effect of NLS mutations on DENV replication. In order to address this question we inserted the mutations into DENV luciferase reporter virus and their replication efficiency assayed by electroporating them into permissive cells. The NLS mutants replicated with varying efficiencies and most of them showed a positive correlation between their NS5 nuclear accumulation and replication. However one mutant having significant cytoplasmic retention of NS5 replicated like wild type in BHK-21 cells and about 3-5fold lower than wild type in Huh-7 cells indicating partial reduction in nuclear transport of the protein does not adversely affect viral replication. The mutant with

no detectable NS5 in the nucleus replicated to 2-5% of wild type levels indicating detectable amount of nuclear NS5 accumulation may not be essential for minimal viral replication.

The reduction in replication of mutants was higher in Huh-7 compared to BHK-21 cells indicating cell type specific effects. Alternatively this could be due to the lower permissibility of Huh-7 cells for DENV which amplifies the small difference in replication efficiencies between mutants due to its ability to mount a stronger antiviral defense. In addition attempts to adapt the NLS mutants resulted in reversion back to higher replicating forms having a higher nuclear NS5 accumulation indicating nuclear accumulation of NS5 is linked with increased replication efficiency.

Since we observed a link between higher replication and higher nuclear accumulation in case of most mutants, the next question addressed was whether the replication of NLS mutants can be rescued by providing wild type NS5 enabling to restore possible functions of nuclear NS5. A transcomplementation experiment was carried out in Huh-7 cells where replication of NLS mutants was analyzed in presence wild type NS5 supplied by either stably replicating DENV subgenomic replicon or wild type infectious virus. Interestingly none of the mutants could be rescued in replication by the presence of nuclear localizing wild type NS5 indicating the observed replication defects could not be due to absence of NS5 capable of nuclear transport.

This result indicates that reduced replication of NLS mutants is probably not entirely due to its inability to move into nucleus and perform some vital functions necessary for replication but rather be due to its effects on enzymatic activities of the protein or its ability to interact with other viral or cellular proteins. Though the previous studies (93) directly correlated the reduced replication of NLS mutants with reduction in nuclear accumulation to establish a direct link between the two phenotypes, the effects of NLS mutations on viral replication seems more complex and is governed by the multiple effects these mutations might have on various structural and functional aspects of this protein. The above experiments indicate that it is likely that the same residues essential for

nuclear accumulation could also be involved in certain functions directly related to replication. If both the phenotypes are linked to same residues, the defects in replication of NLS mutants will be coincidental rather than caused by reduced nuclear accumulation. However more experiments employing larger number of mutants may be needed to resolve this problem.

IV.1.4 Bacterial expression and purification of NS5

The structural studies of NS5 revealed that NLS forms an integral part of polymerase domain and any mutations in NLS may have multiple effects on the enzymatic activities of the protein (117). To investigate the effects of NLS mutations on enzymatic activities of NS5 we set out to bacterially express and purify NS5 protein carrying the mutations. The protein was cloned with a C-terminal histidine tag and expressed in bacteria. The initial efforts to purify the protein were unsuccessful since most of the protein obtained after purification was truncated products. As an alternate strategy a dual tagged NS5 construct carrying a HA-tag on the N-terminal and Histidine tag on the C-terminal was created to carry out a two step purification using both tags to obtain the full length protein. However surprisingly the dual tagged NS5 was resistant to protease cleavage and full length protein with high purity could be obtained by one step His-tag purification. The exact reason for the increased stability of dual tagged NS5 protein is unclear.

The bacterially purified NS5 protein showed both RdRP and MTase activities on *in vitro* transcribed DENV genomic RNA template. Interestingly the protein could also utilize viral RNA templates lacking 5'UTR and even non viral RNA templates (polyC) indicating an apparent lack of template specificity. This observation was contrary to earlier studies suggesting a very high preference for authentic DENV RNA template containing cyclization sequence and both 5'UTR and 3'UTR (1). The discrepancy between our present observations with earlier findings could be due to either the subtle differences like different tags used for protein purification in both studies or the difference in assay buffer composition. However it is noteworthy that some flaviviral polymerases like DENV and WNV when ex-

pressed alone are reported to show template specificity (1, 87) while others like TBE and KUNV are not (48). More studies using purified NS5 from different strains of DENV is required to resolve these contradicting observations. The MTase activity was observed on both capped and uncapped DENV RNA templates indicating either GTase activity is not a prerequisite for MTase activity or NS5 in initially performing GTase activity followed by MTase activity even in absence of extraneously supplied GTP. Further investigations are ongoing to unveil the complex regulation between various enzymatic activities residing in NS5 protein.

IV.1.5 Effect of NLS mutations on RdRP and MTase activity of NS5

The inability of transcomplement replication of NLS mutants with wild type NS5 strongly indicated loss of certain *cis-acting* functions of the protein required for replication which includes its enzymatic activity or interaction with other proteins in the replication complex. The polymerase and MTase activity of NLS mutants were studied using bacterially expressed and purified NS5 protein. Despite high level of variation in replication ability all mutants except one showed RdRP activity similar to wild type and none of the mutants showed any reduction in MTase activity. These results indicate that the reduction in replication of NLS mutants could be due to factors other than RdRP and MTase activities of the protein such as the interaction with other proteins in the replication complex or the regulation between various enzymatic activities of NS5. The GTase activity of the mutants also needs to be investigated. Recent studies indicate that a close coordination between NS3 and NS5 proteins are required for GTase activity of NS5 (54) Owing to its proximity to NS3 interaction site and importin binding sites, NLS mutations could probably alter the protein topology and hence interaction of NS5 with other proteins. A comprehensive analysis of all known interactions of NS5 may be required to elucidate the exact reason for replication defect of certain NLS mutants.

IV.1.6 Influence of IL-8 in DENV replication

Several cytokines and chemokines are induced in patients infected with DENV (16, 21) and their levels are closely linked to various disease manifestations. Studies on DENV infection in primary human monocytes identified IL-8 as one of the major chemokines released. Higher amount of IL-8 secretion was also observed when 293T and ECV304 cells lines were infected with DENV (14). Later studies identified NS5 as the major determinant for IL-8 release (73) which is mediated mainly through activation of CAAT/enhancer binding protein. Recent studies investigated the relationship between NS5 nuclear accumulation and IL-8 induction and reported that increased cytoplasmic retention of the protein resulted in increased IL-8 secretion (93). This study also suggested that the strong antiviral response elicited by NLS mutants by their ability to induce higher amounts of IL-8 during replication could be a major determinant in their impaired replication. To investigate more into this observation, we studied the direct effect of IL-8 on dengue replication. Huh-7 cells infected with DENV reporter virus were treated with IL-8 either prior or after virus infection. The results clearly demonstrated that cells pretreated with IL-8 supported less viral replication but IL-8 treatment just 4h post infection rather had a positive effect on viral replication. This suggests that a higher induction of IL-8 might not adversely affect an ongoing infection implying higher IL-8 induction during replication of NLS mutants alone cannot be the major determinant for their impaired replication.

Further investigations on induction of IL-8 by different NLS mutants revealed that their level of replication rather than NS5 nuclear localization was the main determinant of IL-8 induction. The amount of IL-8 RNA transcripts induced by wild type was ≥10 fold over the lower replicating nuclear localization deficient mutants. To normalize for the difference in NS5 protein expression due to varying levels of replication of NLS mutants, pcDNA NS5 wild type and NLS mutant constructs were compared for their IL-8 induction ability by co-transfection with IL-8 promoter driven luciferase reporter construct. The results suggested similar ability of wild type and NLS mutant constructs to induce IL-8 reporter activity

further indicating NLS mutations does not significantly increase the IL-8 induction ability of NS5.

As a summary we did not find significant effect of IL-8 on ongoing DENV replication and observed that viral replication rather than NS5 nuclear accumulation had a stronger effect on IL-8 release during DENV replication. In our studies NLS mutants also did not show higher ability of induce IL-8 compared to wild type NS5. Taken together these results suggest that IL-8 induction during virus replication cannot explain the drastic drop in replication observed for certain NLS mutants.

IV.1.7 Cellular proteins interacting with NS5

Only limited number of cellular proteins is known to interact with NS5. The NS5 interaction with Importins is shown by yeast two hybrid and immunoprecipitation studies and is required for the nuclear transport of the protein. NS5 also bind to STAT2, prevents its phosphorylation and facilitates its proteasome mediated degradation, blocking IFN mediated gene expression (7, 72). Zonula occuledens-1 (ZO-1) is reported to interact with NS5 in the nucleus, however the functional aspects of this interaction are not known.

We carried out a yeast two hybrid screen using human thymus and liver cDNA libraries to identify potential cellular interaction partners of NS5. The screen identified five cellular proteins interacting with NS5. Three proteins viz. CAPN2, BHMT and NPHP3 were cytoplasmic whereas the other two RSF1 and ASCC3L1 had nuclear functions. CAPN2 is a cysteine protease associated with ER, Golgi or lipid rafts and is implicated in signal transduction (78) while BHMT is involved in homocysteine homeostasis (89). The NPHP3 may be involved in renal tubular development and its mutant alleles are implicated in heritable genetic disorder, adolescent nephronophthisis (88). The nuclear protein RSF1 is essential for formation of regular nucleosome arrays and also suppresses TNF-alpha induced transcription by NF-κB (52) whereas ASCC3L1 is a small nuclear ribonucleoprotein having probable role in cellular RNA splicing.

We addressed the functional significance of NS5 interaction with these cellular proteins on viral replication by gene silencing by RNAi. siRNA mediated silencing of these five proteins however had very minor effect on viral replication indicating that either the residual level of proteins following silencing was sufficient to maintain their function or these proteins are unlikely to play important roles in DENV replication. It could also be possible that these interactions are nonspecific or might have some functional significance in human infection which is not apparent in cell culture based systems.

IV.2.1 Identification of cellular kinases influencing DENV replication

Most RNA viruses codes for only a limited repertoire of proteins and depend extensively on host cell proteins for successful completion of their life cycle. Extensive studies have been carried out on functional aspects of viral proteins leading to a deeper understanding about their role in viral life cycle. However the functional studies of the role of cellular proteins were hampered in the past due to lack of high throughput tools required for their easier manipulation. The siRNA based silencing technique develop in the last decade enabled specific down regulate individual genes enabling rapid screening for their functions in viral life cycle. The genome-wide siRNA screen for WNV (63) revealed the importance of several cellular pathways important in WNV life cycle. Interestingly many of those genes also had significant impact on DENV suggesting conserved pathways exploited by both viruses. The siRNA screen which identified more than hundred insect genes essential for propagation of DENV in insect cells (103) have observed that mammalian counterpart of about 40% of those genes altered the viral replication in mammalian cells as well indicating DENV may be exploiting similar cellular pathways in both insect and human host for its survival.

Protein kinases are a group of proteins involved in protein phosphorylation (transfer of phosphate groups from high energy donors like ATP into proteins). An estimated 30% of cellular proteins are phosphorylated and this post transla-

tional modification modulates their activity, interaction and stability and plays an important role in many important cellular process including cell division, signal transduction, cell death, innate immune response etc. Several steps in cellular innate antiviral defense pathways involved in production of IFN and activation of IFN-induced genes depends on phosphorylation by cellular kinases for proper function. Owing to their crucial role in many important cellular processes we selected this subset of genes to establish a siRNA screening platform and investigate their role in entry and replication of DENV.

IV.2.2 Establishment of siRNA screening platform for DENV

The optimizations were carried out for cell seeding, duration of silencing prior to infection, multiplicity of infection, duration of infection, and protocols required for fixation, permeabilization and immunostaining and image acquisition were developed during this study. The Huh-7 cells were selected for screening due to its human origin and growth properties which were optimal for microscopy including superior adhesion to chambered slides, formation of uniform monolayer, and larger cytoplasm. To ensure proper quality control for silencing experiments development of a siRNA that can consistently down regulate viral replication was important. Since no cellular genes that could down regulate DENV entry or replication was know during the initial phase of the project, we screened siRNAs targeting various regions of DENV genome to identify an efficient siRNA that can downregulate DENV replication. The siRNAs targeting NS1 region of the genome was found most efficient followed by one targeting NS3 region. The siRNAs performed equally well in both liquid transfection and reverse transcription formats.

Another obstacle we faced during establishment of an imaging based RNAi screen was the weak specific signal (with the signal to noise ratio of two folds) obtained after standard immunostaining protocol which greatly reduced the measuring window. Among the modification of the immunostaining protocol checked, repeating the antibody staining twice resulted in a signal to noise ratio of fivefold, improving the detection window. As the experiment envisioned only a single round of infection, a higher MOI of 2-5 was used to ensure infection of

more than 90% cells. Similarly optimizations were also done for duration of silencing and the concentration of primary and secondary antibodies to enable a higher detection window. In summary every individual step in the experimental protocol was optimized to maximize the measurement window and to minimize the variability introduced during various steps of the experiment.

To test the screening pipe line developed, a pilot RNAi screen was carried out with siRNAs targeting a few cellular proteins reported to interact with flaviviruses and positive and negative controls. Though none of the cellular genes screened had significant effect on viral replication, the positive control siRNA reduced viral replication more than 80% delivering a clear measuring window to score the candidates and the overall performance of various steps of the screen was as expected.

IV.2.3 Primary screen and validation screen

The primary screen being imaging based faced numerous technical difficulties during screening phase. Three out of 12 experimental repetitions done were discarded due to poor performance of control siRNAs and suboptimal image acquisition. About 15% of the images acquired within the selected experiments were also discarded due to staining artifacts and out of focus images. Despite various quality control measures implemented the primary screen still showed a high variation (Pearson correlation coefficient between 0.1 and 0.7) between the repetitions and this was also strongly related to quality variations between different batches of siRNA spotted chambered slides. Due to high data variability a less stringent selection criteria (Z ≥1, p ≤0.05) was employed to select candidates for further validation. However even with these criteria, for more than 95% of the candidate genes selected, only one among the three siRNAs showed significant effect on viral replication. A higher chance of off-target effects exist when candidates are selected based on performance of single siRNAs. However since it was not practical to verify the silencing efficiency of all genes selected from primary screen, we selected three siRNAs different from primary screen for

the validation screen. By this strategy we could verify each gene with at least two independent siRNAs when both screens are taken together.

To develop a more statistically robust and faster screening system for validation experiments a 96-well plate based DENV luciferase reporter assay was developed. The luciferase read out enabled to skip the immunostaining, image acquisition and image analysis steps which were majorly contributing to assay variability. In 96-well plate based assay, each measurement was made from 10 fold more cells compared to image based screen further increasing the assay robustness. The validation screen was carried out with a set of 3 siRNAs against each gene and was 96-well plate based using DENV reporter virus and was repeated twice in duplicate resulting in four independent experiments. The analysis of the data indicated a robust performance of control siRNAs and a higher correlation (Pearson correlation coefficient ≥0.8) between the replicates. A stringent candidate selection criterion ($Z \geq \pm 2$, $p \leq 0.05$) resulted in identification of 19 HSFs and 15 HRFs. Similar to primary screen all the hits identified showed effect with one among the three siRNAs used. A DENV luciferase reporter replicon based validation screen was used to differentiate between kinases essential for entry and establishment of replication and for ongoing replication. With a moderately stringent hit criteria of ($-1.5 \geq Z \geq 2$, $p \leq 0.05$), this screen identified 4 HSFs and 11 HRFs with only 4 genes in common with the infection based validation screen. The newly identified HSFs might only be essential for maintenance of viral replication whereas the HRFs could be essential to reduce ongoing viral replication.

More experiments need to be done to verify the silencing of target genes and to remove the candidates showing off-target effects. In summary the statistical robustness of reporter virus based validation screen could be attributed to the higher sensitivity of luciferase reporter system, elimination of image acquisition and analysis steps and use of 96-well plates containing approximately 0.3-0.5million cells per well compared to few hundred cells per siRNA spot on chambered slides.

Further validation of selected candidates was done using specific chemical inhibitors on either and infection based or DENV replicon based assay. These studies indicated that FGFR4 might be involved in viral entry whereas DAGQ might be involved in viral replication. The mechanism behind these observations need further investigation. Chemical inhibitors and gene knock-in studies has to be carried out to further verify the gene candidates and rule out siRNA off-target effects.

The gene ontology analysis of the confirmed kinases did not show enrichment of any specific pathway, and most were associated with more global networks. This could be due to the very limited number of candidates derived from the screen and kinases constitute only a small part of most cellular pathways. However once gene candidates are validated with high confidence, the effect of the pathways where these genes form a part can be analyzed further.

IV.2.4 Comparison of Kinase siRNA screen with other published screens

The first flavivirus siRNA screen identified 15 cellular kinases essential for WNV replication and among which 8 were identified essential for DENV infection. Our experiments identified 24 HSFs and 16 HRFs having significant effect of DENV entry or replication. There was no overlap between the candidates identified by both screens. This could probably be due to the different screen setups used in both studies including different cells lines (HeLa in WNV screen and Huh-7 in our screen), duration of silencing (72h in WNV screen compared to 48h in present screen) and different sources of siRNA libraries. The screen which investigated the insect genes essential for viral replication and identified 116 drosophila genes essential for DENV replication among which 42 had human homologues showing significant effects in Huh-7 cells. Since none of the Huh-7 homologues identified were kinases, the candidates from this screen could not be compared to our screen. The variations in siRNA libraries and screening procedures followed could be the reason behind the very less overlap between the candidates identified by different screens. It is also notable that only sec16 and vATPase

were the only two common candidates between the WNV and DENV drosophila screen (22). The limited overlap between candidates identified by various screens are also noted for other viruses like HIV indicating the experimental procedures like selection of RNAi library, cell lines used and silencing duration etc. can have big influence on the candidates identified. Validation the candidates with different assays are hence an important step to improve the quality of RNAi screens.

V. Bibliography

1.   **Ackermann, M., and R. Padmanabhan.** 2001. De novo synthesis of RNA by the dengue virus RNA-dependent RNA polymerase exhibits temperature dependence at the initiation but not elongation phase. J Biol Chem **276:**39926-37.

2.   **Alvarez, D. E., A. L. De Lella Ezcurra, S. Fucito, and A. V. Gamarnik.** 2005. Role of RNA structures present at the 3'UTR of dengue virus on translation, RNA synthesis, and viral replication. Virology **339:**200-12.

3.   **Alvarez, D. E., C. V. Filomatori, and A. V. Gamarnik.** 2008. Functional analysis of dengue virus cyclization sequences located at the 5' and 3'UTRs. Virology **375:**223-35.

4.   **Alvarez, D. E., M. F. Lodeiro, S. J. Luduena, L. I. Pietrasanta, and A. V. Gamarnik.** 2005. Long-range RNA-RNA interactions circularize the dengue virus genome. J Virol **79:**6631-43.

5.   **Alvisi, G., S. M. Rawlinson, R. Ghildyal, A. Ripalti, and D. A. Jans.** 2008. Regulated nucleocytoplasmic trafficking of viral gene products: a therapeutic target? Biochim Biophys Acta **1784:**213-27.

6.   **Anderson, R.** 2003. Manipulation of cell surface macromolecules by flaviviruses. Adv Virus Res **59:**229-74.

7.   **Ashour, J., M. Laurent-Rolle, P. Y. Shi, and A. Garcia-Sastre.** 2009. NS5 of dengue virus mediates STAT2 binding and degradation. J Virol **83:**5408-18.

8.   **Ausubel, F. M.** 1988. (ed) Current Protocols: Molecular Biology. John Wiley & Sons Inc, Hoboken, NJ.

9.   **Bartenschlager, R., and S. Miller.** 2008. Molecular aspects of Dengue virus replication. Future Microbiol **3:**155-65.

10.   **Bhattacharya, D., I. H. Ansari, and R. Striker.** 2009. The flaviviral methyltransferase is a substrate of Casein Kinase 1. Virus Res **141:**101-4.

11.   **Bhattacharya, D., S. Hoover, S. P. Falk, B. Weisblum, M. Vestling, and R. Striker.** 2008. Phosphorylation of yellow fever virus NS5 alters methyltransferase activity. Virology **380:**276-84.

12.   **Bhattacharya, D., Mayuri, S. M. Best, R. Perera, R. J. Kuhn, and R. Striker.** 2009. Protein kinase G phosphorylates mosquito-borne flavivirus NS5. J Virol **83:**9195-205.

13.   **Bhuvanakantham, R., J. Li, T. T. Tan, and M. L. Ng.** 2009. Human Sec3 protein is a novel transcriptional and translational repressor of flavivirus. Cell Microbiol.

14.   **Bosch, I., K. Xhaja, L. Estevez, G. Raines, H. Melichar, R. V. Warke, M. V. Fournier, F. A. Ennis, and A. L. Rothman.** 2002. Increased production of interleukin-8 in primary human monocytes and in human epithelial and endothelial cell lines after dengue virus challenge. J Virol **76:**5588-97.

15.   **Boutros, M., L. P. Bras, and W. Huber.** 2006. Analysis of cell-based RNAi screens. Genome Biol **7:**R66.

16.   **Bozza, F. A., O. G. Cruz, S. M. Zagne, E. L. Azeredo, R. M. Nogueira, E. F. Assis, P. T. Bozza, and C. F. Kubelka.** 2008. Multiplex cytokine profile from dengue patients: MIP-1beta and IFN-gamma as predictive factors for severity. BMC Infect Dis **8:**86.

17.   **Brass, A. L., D. M. Dykxhoorn, Y. Benita, N. Yan, A. Engelman, R. J. Xavier, J. Lieberman, and S. J. Elledge.** 2008. Identification of host proteins required for HIV infection through a functional genomic screen. Science **319:**921-6.

18.   **Brideau, C., B. Gunter, B. Pikounis, and A. Liaw.** 2003. Improved statistical methods for hit selection in high-throughput screening. J Biomol Screen **8:**634-47.

19.   **Brooks, A. J., M. Johansson, A. V. John, Y. Xu, D. A. Jans, and S. G. Vasudevan.** 2002. The interdomain region of dengue NS5 protein that binds to the viral helicase NS3 contains independently functional importin beta 1 and importin alpha/beta-recognized nuclear localization signals. J Biol Chem **277:**36399-407.

20.   **Buckley, A., S. Gaidamovich, A. Turchinskaya, and E. A. Gould.** 1992. Monoclonal antibodies identify the NS5 yellow fever virus non-structural protein in the nuclei of infected cells. J Gen Virol **73 (Pt 5):**1125-30.

21.   **Chaturvedi, U. C., R. Agarwal, E. A. Elbishbishi, and A. S. Mustafa.** 2000. Cytokine cascade in dengue hemorrhagic fever: implications for pathogenesis. FEMS Immunol Med Microbiol **28:**183-8.

22.   **Cherry, S.** 2009. What have RNAi screens taught us about viral-host interactions? Current Opinion in Microbiology **12:**446-452.

23.   **Chu, J. J., and P. L. Yang.** 2007. c-Src protein kinase inhibitors block assembly and maturation of dengue virus. Proc Natl Acad Sci U S A **104:**3520-5.

24.   **Chua, J. J., R. Bhuvanakantham, V. T. Chow, and M. L. Ng.** 2005. Recombinant non-structural 1 (NS1) protein of dengue-2 virus interacts with human STAT3beta protein. Virus Res **112:**85-94.

25.   **Chua, J. J., M. M. Ng, and V. T. Chow.** 2004. The non-structural 3 (NS3) protein of dengue virus type 2 interacts with human nuclear receptor binding protein and is associated with alterations in membrane structure. Virus Res **102:**151-63.

26.   **Cleveland, W. S.** 1979. Robust locally weighted regression and smoothing scatterplots. Journal of the American Statistical Association **74:**829-836.

27.   **Clyde, K., J. L. Kyle, and E. Harris.** 2006. Recent advances in deciphering viral and host determinants of dengue virus replication and pathogenesis. J Virol **80:**11418-31.

28.   **Cui, T., R. J. Sugrue, Q. Xu, A. K. Lee, Y. C. Chan, and J. Fu.** 1998. Recombinant dengue virus type 1 NS3 protein exhibits specific viral RNA binding and NTPase activity regulated by the NS5 protein. Virology **246:**409-17.

29.   **Davidson, A. D.** 2009. Chapter 2. New insights into flavivirus nonstructural protein 5. Adv Virus Res **74:**41-101.

30.   **De Nova-Ocampo, M., N. Villegas-Sepulveda, and R. M. del Angel.** 2002. Translation elongation factor-1alpha, La, and PTB interact with the 3' untranslated region of dengue 4 virus RNA. Virology **295:**337-47.

31.   **Duan, X., X. Lu, J. Li, and Y. Liu.** 2008. Novel binding between pre-membrane protein and vacuolar ATPase is required for efficient dengue virus secretion. Biochem Biophys Res Commun **373:**319-24.

32.   **Egloff, M. P., D. Benarroch, B. Selisko, J. L. Romette, and B. Canard.** 2002. An RNA cap (nucleoside-2'-O-)-methyltransferase in the flavivirus RNA polymerase NS5: crystal structure and functional characterization. EMBO J **21:**2757-68.

33.   **Ellencrona, K., A. Syed, and M. Johansson.** 2009. Flavivirus NS5 associates with host-cell proteins zonula occludens-1 (ZO-1) and regulating synaptic membrane exocytosis-2 (RIMS2) via an internal PDZ binding mechanism. Biol Chem **390:**319-23.

34. **Erfle, H., B. Neumann, P. Rogers, J. Bulkescher, J. Ellenberg, and R. Pepperkok.** 2008. Work flow for multiplexing siRNA assays by solid-phase reverse transfection in multiwell plates. J Biomol Screen **13:**575-80.

35. **Fire, A., S. Xu, M. K. Montgomery, S. A. Kostas, S. E. Driver, and C. C. Mello.** 1998. Potent and specific genetic interference by double-stranded RNA in Caenorhabditis elegans. Nature **391:**806-11.

36. **Forwood, J. K., A. Brooks, L. J. Briggs, C. Y. Xiao, D. A. Jans, and S. G. Vasudevan.** 1999. The 37-amino-acid interdomain of dengue virus NS5 protein contains a functional NLS and inhibitory CK2 site. Biochem Biophys Res Commun **257:**731-7.

37. **Fraser, K. B., and M. Gharpure.** 1962. Immunofluorescent tracing of polyoma virus in transformation experiments with BHK 21 cells. Virology **18:**505-7.

38. **Gao, F., X. Duan, X. Lu, Y. Liu, L. Zheng, Z. Ding, and J. Li.** 2009. Novel binding between pre-membrane protein and claudin-1 is required for efficient dengue virus entry. Biochem Biophys Res Commun.

39. **Garcia-Montalvo, B. M., F. Medina, and R. M. del Angel.** 2004. La protein binds to NS5 and NS3 and to the 5' and 3' ends of Dengue 4 virus RNA. Virus Res **102:**141-50.

40. **Giard, D. J., S. A. Aaronson, G. J. Todaro, P. Arnstein, J. H. Kersey, H. Dosik, and W. P. Parks.** 1973. In vitro cultivation of human tumors: establishment of cell lines derived from a series of solid tumors. J Natl Cancer Inst **51:**1417-23.

41. **Graham, F. L., J. Smiley, W. C. Russell, and R. Nairn.** 1977. Characteristics of a human cell line transformed by DNA from human adenovirus type 5. J Gen Virol **36:**59-74.

42. **Gubler, D. J.** 1998. Dengue and dengue hemorrhagic fever. Clin Microbiol Rev **11:**480-96.

43. **Gubler, D. J.** 1997. Dengue and dengue hemorrhagic fever: its history and resurgence as a global public health problem. . In: Gubler, D.J., Kuno, G. (Eds.), Dengue and Dengue Hemorrhagic Fever. CAB International, New York**:**1-22.

44. **Gunther, J., J. P. Martinez-Munoz, D. G. Perez-Ishiwara, and J. Salas-Benito.** 2007. Evidence of vertical transmission of dengue virus in two endemic localities in the state of Oaxaca, Mexico. Intervirology **50:**347-52.

45. **Guo, Y., T. C. Walther, M. Rao, N. Stuurman, G. Goshima, K. Terayama, J. S. Wong, R. D. Vale, P. Walter, and R. V. Farese.** 2008. Functional genomic screen reveals genes involved in lipid-droplet formation and utilization. Nature **453:**657-61.

46. **Guy, B., and J. W. Almond.** 2008. Towards a dengue vaccine: progress to date and remaining challenges. Comp Immunol Microbiol Infect Dis **31:**239-52.

47. **Guy, B., F. Guirakhoo, V. Barban, S. Higgs, T. P. Monath, and J. Lang.** 2009. Preclinical and clinical development of YFV 17D-based chimeric vaccines against dengue, West Nile and Japanese encephalitis viruses. Vaccine.

48. **Guyatt, K. J., E. G. Westaway, and A. A. Khromykh.** 2001. Expression and purification of enzymatically active recombinant RNA-dependent RNA polymerase (NS5) of the flavivirus Kunjin. J Virol Methods **92:**37-44.

49. **Halstead, S. B.** 2007. Dengue. Lancet **370:**1644-52.

50. **Heinz, F. X., MS, C., Purcell, R. H., Gould, E. A., Howard, C. R., Houghton, M.,, and R. J. M. Moormann, Rice, C. M., and Thiel, H. J.** 2000. Family *Flaviviridae*. In ''Virus Taxonomy: 7th International Committee for the Taxonomy of Viruses'', (M. H. V. Regenmortel, C. M. Fauquet, D. H. L. Bishop, E. Carstens, M. K. Estes, S. Lemon, J. Maniloff, M. A. Mayo, D. McGeogh, C. R. Pringle, and R. B. Wickner, Eds.). Academic Press, San Diego.

51. **Hershkovitz, O., B. Rosental, L. A. Rosenberg, M. E. Navarro-Sanchez, S. Jivov, A. Zilka, O. Gershoni-Yahalom, E. Brient-Litzler, H. Bedouelle, J. W. Ho, K. S. Campbell, B. Rager-Zisman, P. Despres, and A. Porgador.** 2009. NKp44 receptor mediates interaction of the

envelope glycoproteins from the West Nile and dengue viruses with NK cells. J Immunol **183:**2610-21.

52. **Huang, J. Y., B. J. Shen, W. H. Tsai, and S. C. Lee.** 2004. Functional interaction between nuclear matrix-associated HBXAP and NF-kappaB. Exp Cell Res **298:**133-43.

53. **Igarashi, A.** 1978. Isolation of a Singh's Aedes albopictus cell clone sensitive to Dengue and Chikungunya viruses. J Gen Virol **40:**531-44.

54. **Issur, M., B. J. Geiss, I. Bougie, F. Picard-Jean, S. Despins, J. Mayette, S. E. Hobdey, and M. Bisaillon.** 2009. The flavivirus NS5 protein is a true RNA guanylyltransferase that catalyzes a two-step reaction to form the RNA cap structure. RNA.

55. **Jacobs, M. G., P. J. Robinson, C. Bletchly, J. M. Mackenzie, and P. R. Young.** 2000. Dengue virus nonstructural protein 1 is expressed in a glycosyl-phosphatidylinositol-linked form that is capable of signal transduction. FASEB J **14:**1603-10.

56. **Johansson, M., A. J. Brooks, D. A. Jans, and S. G. Vasudevan.** 2001. A small region of the dengue virus-encoded RNA-dependent RNA polymerase, NS5, confers interaction with both the nuclear transport receptor importin-beta and the viral helicase, NS3. J Gen Virol **82:**735-45.

57. **Jones, M., A. Davidson, L. Hibbert, P. Gruenwald, J. Schlaak, S. Ball, G. R. Foster, and M. Jacobs.** 2005. Dengue virus inhibits alpha interferon signaling by reducing STAT2 expression. J Virol **79:**5414-20.

58. **Kapoor, M., L. Zhang, P. M. Mohan, and R. Padmanabhan.** 1995. Synthesis and characterization of an infectious dengue virus type-2 RNA genome (New Guinea C strain). Gene **162:**175-80.

59. **Kapoor, M., L. Zhang, M. Ramachandra, J. Kusukawa, K. E. Ebner, and R. Padmanabhan.** 1995. Association between NS3 and NS5 proteins of dengue virus type 2 in the putative RNA replicase is linked to differential phosphorylation of NS5. J Biol Chem **270:**19100-6.

60. **Kittler, R., L. Pelletier, A. K. Heninger, M. Slabicki, M. Theis, L. Miroslaw, I. Poser, S. Lawo, H. Grabner, K. Kozak, J. Wagner, V. Surendranath, C. Richter, W. Bowen, A. L. Jackson, B. Habermann, A. A. Hyman, and F. Buchholz.** 2007. Genome-scale RNAi profiling of cell division in human tissue culture cells. Nat Cell Biol **9:**1401-12.

61. **Konig, R., S. Stertz, Y. Zhou, A. Inoue, H. Heinrich Hoffmann, S. Bhattacharyya, J. G. Alamares, D. M. Tscherne, M. B. Ortigoza, Y. Liang, Q. Gao, S. E. Andrews, S. Bandyopadhyay, P. De Jesus, B. P. Tu, L. Pache, C. Shih, A. Orth, G. Bonamy, L. Miraglia, T. Ideker, A. Garcia-Sastre, J. A. Young, P. Palese, M. L. Shaw, and S. K. Chanda.** 2009. Human host factors required for influenza virus replication. Nature.

62. **Konig, R., Y. Zhou, D. Elleder, T. L. Diamond, G. M. Bonamy, J. T. Irelan, C. Y. Chiang, B. P. Tu, P. D. De Jesus, C. E. Lilley, S. Seidel, A. M. Opaluch, J. S. Caldwell, M. D. Weitzman, K. L. Kuhen, S. Bandyopadhyay, T. Ideker, A. P. Orth, L. J. Miraglia, F. D. Bushman, J. A. Young, and S. K. Chanda.** 2008. Global analysis of host-pathogen interactions that regulate early-stage HIV-1 replication. Cell **135:**49-60.

63. **Krishnan, M. N., A. Ng, B. Sukumaran, F. D. Gilfoy, P. D. Uchil, H. Sultana, A. L. Brass, R. Adametz, M. Tsui, F. Qian, R. R. Montgomery, S. Lev, P. W. Mason, R. A. Koski, S. J. Elledge, R. J. Xavier, H. Agaisse, and E. Fikrig.** 2008. RNA interference screen for human genes associated with West Nile virus infection. Nature **455:**242-5.

64. **Kroschewski, H., S. P. Lim, R. E. Butcher, T. L. Yap, J. Lescar, P. J. Wright, S. G. Vasudevan, and A. D. Davidson.** 2008. Mutagenesis of the dengue virus type 2 NS5 methyltransferase domain. J Biol Chem **283:**19410-21.

65. **Kuhn, R. J., W. Zhang, M. G. Rossmann, S. V. Pletnev, J. Corver, E. Lenches, C. T. Jones, S. Mukhopadhyay, P. R. Chipman, E. G. Strauss, T. S. Baker, and J. H. Strauss.** 2002. Structure

of dengue virus: implications for flavivirus organization, maturation, and fusion. Cell **108:**717-25.

66. **Kurosu, T., P. Chaichana, M. Yamate, S. Anantapreecha, and K. Ikuta.** 2007. Secreted complement regulatory protein clusterin interacts with dengue virus nonstructural protein 1. Biochem Biophys Res Commun **362:**1051-6.

67. **Kyle, J. L., and E. Harris.** 2008. Global spread and persistence of dengue. Annu Rev Microbiol **62:**71-92.

68. **Li, L., S. M. Lok, I. M. Yu, Y. Zhang, R. J. Kuhn, J. Chen, and M. G. Rossmann.** 2008. The flavivirus precursor membrane-envelope protein complex: structure and maturation. Science **319:**1830-4.

69. **Limjindaporn, T., W. Wongwiwat, S. Noisakran, C. Srisawat, J. Netsawang, C. Puttikhunt, W. Kasinrerk, P. Avirutnan, S. Thiemmeca, R. Sriburi, N. Sittisombut, P. Malasit, and P. T. Yenchitsomanus.** 2009. Interaction of dengue virus envelope protein with endoplasmic reticulum-resident chaperones facilitates dengue virus production. Biochem Biophys Res Commun **379:**196-200.

70. **Lindenbach, B. D., and C. M. Rice.** 1999. Genetic interaction of flavivirus nonstructural proteins NS1 and NS4A as a determinant of replicase function. J Virol **73:**4611-21.

71. **Matula, P., A. Kumar, I. Worz, H. Erfle, R. Bartenschlager, R. Eils, and K. Rohr.** 2009. Single-cell-based image analysis of high-throughput cell array screens for quantification of viral infection. Cytometry A **75:**309-18.

72. **Mazzon, M., M. Jones, A. Davidson, B. Chain, and M. Jacobs.** 2009. Dengue virus NS5 inhibits interferon-alpha signaling by blocking signal transducer and activator of transcription 2 phosphorylation. J Infect Dis **200:**1261-70.

73. **Medin, C. L., K. A. Fitzgerald, and A. L. Rothman.** 2005. Dengue virus nonstructural protein NS5 induces interleukin-8 transcription and secretion. J Virol **79:**11053-61.

74. **Men, R., M. Bray, D. Clark, R. M. Chanock, and C. J. Lai.** 1996. Dengue type 4 virus mutants containing deletions in the 3' noncoding region of the RNA genome: analysis of growth restriction in cell culture and altered viremia pattern and immunogenicity in rhesus monkeys. J Virol **70:**3930-7.

75. **Miller, S.** 2007. *Untersuchungen zur Topologie, Funktion und Lokalisation der Proteine NS4A und NS4B des Dengue Virus*. Ph. D. Thesis. University of Heidelberg: Germany.

76. **Miller, S., S. Sparacio, and R. Bartenschlager.** 2006. Subcellular localization and membrane topology of the Dengue virus type 2 Non-structural protein 4B. J Biol Chem **281:**8854-63.

77. **Mongkolsapaya, J., W. Dejnirattisai, X. N. Xu, S. Vasanawathana, N. Tangthawornchaikul, A. Chairunsri, S. Sawasdivorn, T. Duangchinda, T. Dong, S. Rowland-Jones, P. T. Yenchitsomanus, A. McMichael, P. Malasit, and G. Screaton.** 2003. Original antigenic sin and apoptosis in the pathogenesis of dengue hemorrhagic fever. Nat Med **9:**921-7.

78. **Morford, L. A., K. Forrest, B. Logan, L. K. Overstreet, J. Goebel, W. H. Brooks, and T. L. Roszman.** 2002. Calpain II colocalizes with detergent-insoluble rafts on human and Jurkat T-cells. Biochem Biophys Res Commun **295:**540-6.

79. **Morozova, O. V., N. A. Tsekhanovskaya, T. G. Maksimova, V. N. Bachvalova, V. A. Matveeva, and Y. Kit.** 1997. Phosphorylation of tick-borne encephalitis virus NS5 protein. Virus Res **49:**9-15.

80. **Mosca, J. D., and P. M. Pitha.** 1986. Transcriptional and posttranscriptional regulation of exogenous human beta interferon gene in simian cells defective in interferon synthesis. Mol Cell Biol **6:**2279-83.

81. **Munoz-Jordan, J. L., M. Laurent-Rolle, J. Ashour, L. Martinez-Sobrido, M. Ashok, W. I. Lipkin, and A. Garcia-Sastre.** 2005. Inhibition of alpha/beta interferon signaling by the NS4B protein of flaviviruses. J Virol **79:**8004-13.

82. **Munoz-Jordan, J. L., G. G. Sanchez-Burgos, M. Laurent-Rolle, and A. Garcia-Sastre.** 2003. Inhibition of interferon signaling by dengue virus. Proc Natl Acad Sci U S A **100:**14333-8.

83. **Nakabayashi, H., K. Taketa, K. Miyano, T. Yamane, and J. Sato.** 1982. Growth of human hepatoma cells lines with differentiated functions in chemically defined medium. Cancer Res **42:**3858-63.

84. **Netsawang, J., S. Noisakran, C. Puttikhunt, W. Kasinrerk, W. Wongwiwat, P. Malasit, P. T. Yenchitsomanus, and T. Limjindaporn.** 2009. Nuclear localization of dengue virus capsid protein is required for DAXX interaction and apoptosis. Virus Res.

85. **Ng, T. I., H. Mo, T. Pilot-Matias, Y. He, G. Koev, P. Krishnan, R. Mondal, R. Pithawalla, W. He, T. Dekhtyar, J. Packer, M. Schurdak, and A. Molla.** 2007. Identification of host genes involved in hepatitis C virus replication by small interfering RNA technology. Hepatology **45:**1413-21.

86. **Noisakran, S., S. Sengsai, V. Thongboonkerd, R. Kanlaya, S. Sinchaikul, S. T. Chen, C. Puttikhunt, W. Kasinrerk, T. Limjindaporn, W. Wongwiwat, P. Malasit, and P. T. Yenchitsomanus.** 2008. Identification of human hnRNP C1/C2 as a dengue virus NS1-interacting protein. Biochem Biophys Res Commun **372:**67-72.

87. **Nomaguchi, M., T. Teramoto, L. Yu, L. Markoff, and R. Padmanabhan.** 2004. Requirements for West Nile virus (-)- and (+)-strand subgenomic RNA synthesis in vitro by the viral RNA-dependent RNA polymerase expressed in Escherichia coli. J Biol Chem **279:**12141-51.

88. **Omran, H., C. Fernandez, M. Jung, K. Haffner, B. Fargier, A. Villaquiran, R. Waldherr, N. Gretz, M. Brandis, F. Ruschendorf, A. Reis, and F. Hildebrandt.** 2000. Identification of a new gene locus for adolescent nephronophthisis, on chromosome 3q22 in a large Venezuelan pedigree. Am J Hum Genet **66:**118-27.

89. **Ou, X., H. Yang, K. Ramani, A. I. Ara, H. Chen, J. M. Mato, and S. C. Lu.** 2007. Inhibition of human betaine-homocysteine methyltransferase expression by S-adenosylmethionine and methylthioadenosine. Biochem J **401:**87-96.

90. **Pelkmans, L., E. Fava, H. Grabner, M. Hannus, B. Habermann, E. Krausz, and M. Zerial.** 2005. Genome-wide analysis of human kinases in clathrin- and caveolae/raft-mediated endocytosis. Nature **436:**78-86.

91. **Polacek, C., P. Friebe, and E. Harris.** 2009. Poly(A)-binding protein binds to the non-polyadenylated 3' untranslated region of dengue virus and modulates translation efficiency. J Gen Virol **90:**687-92.

92. **Pryor, M. J., J. M. Carr, H. Hocking, A. D. Davidson, P. Li, and P. J. Wright.** 2001. Replication of dengue virus type 2 in human monocyte-derived macrophages: comparisons of isolates and recombinant viruses with substitutions at amino acid 390 in the envelope glycoprotein. Am J Trop Med Hyg **65:**427-34.

93. **Pryor, M. J., S. M. Rawlinson, R. E. Butcher, C. L. Barton, T. A. Waterhouse, S. G. Vasudevan, P. G. Bardin, P. J. Wright, D. A. Jans, and A. D. Davidson.** 2007. Nuclear localization of dengue virus nonstructural protein 5 through its importin alpha/beta-recognized nuclear localization sequences is integral to viral infection. Traffic **8:**795-807.

94. **Rawlinson, S. M., M. J. Pryor, P. J. Wright, and D. A. Jans.** 2009. CRM1-mediated nuclear export of dengue virus RNA polymerase NS5 modulates interleukin-8 induction and virus production. J Biol Chem **284:**15589-97.

95. **Reed, K. E., A. E. Gorbalenya, and C. M. Rice.** 1998. The NS5A/NS5 proteins of viruses from three genera of the family flaviviridae are phosphorylated by associated serine/threonine kinases. J Virol **72:**6199-206.

96. **Rico-Hesse, R.** 1990. Molecular evolution and distribution of dengue viruses type 1 and 2 in nature. Virology **174:**479-93.

97. **Rieber, N., B. Knapp, R. Eils, and L. Kaderali.** 2009. RNAither, an automated pipeline for the statistical analysis of high-throughput RNAi screens. Bioinformatics **25:**678-9.

98. **Rothwell, C., A. Lebreton, C. Young Ng, J. Y. Lim, W. Liu, S. Vasudevan, M. Labow, F. Gu, and L. A. Gaither.** 2009. Cholesterol biosynthesis modulation regulates dengue viral replication. Virology **389:**8-19.

99. **Salazar, M. I., J. H. Richardson, I. Sanchez-Vargas, K. E. Olson, and B. J. Beaty.** 2007. Dengue virus type 2: replication and tropisms in orally infected Aedes aegypti mosquitoes. BMC Microbiol **7:**9.

100. **Sambrook, J., Russell, D.** 2001. Molecular Cloning: A Laboratory Manual. Cold Spring Harbor Laboratory Press, Cold Spring Harbor, NY.

101. **Sampath, A., and R. Padmanabhan.** 2009. Molecular targets for flavivirus drug discovery. Antiviral Res **81:**6-15.

102. **Seidman, C. E., K. Struhl, J. Sheen, and T. Jessen.** 2001. Introduction of plasmid DNA into cells. Curr Protoc Mol Biol **Chapter 1:**Unit1 8.

103. **Sessions, O. M., N. J. Barrows, J. A. Souza-Neto, T. J. Robinson, C. L. Hershey, M. A. Rodgers, J. L. Ramirez, G. Dimopoulos, P. L. Yang, J. L. Pearson, and M. A. Garcia-Blanco.** 2009. Discovery of insect and human dengue virus host factors. Nature **458:**1047-50.

104. **Singh, K. R. P.** 1967. Cell cultures derived from larvae of Aedes albopictus (Skuse) and Aedes aegypti (L.). Current Science **36:**506-508.

105. **Stoker, M.** 1962. Characteristics of normal and transformed clones arising from BHK21 cells exposed to polyoma virus. Virology **18:**649-51.

106. **Supekova, L., F. Supek, J. Lee, S. Chen, N. Gray, J. P. Pezacki, A. Schlapbach, and P. G. Schultz.** 2008. Identification of human kinases involved in hepatitis C virus replication by small interference RNA library screening. J Biol Chem **283:**29-36.

107. **Tai, A. W., Y. Benita, L. F. Peng, S. S. Kim, N. Sakamoto, R. J. Xavier, and R. T. Chung.** 2009. A functional genomic screen identifies cellular cofactors of hepatitis C virus replication. Cell Host Microbe **5:**298-307.

108. **Tan, B. H., J. Fu, R. J. Sugrue, E. H. Yap, Y. C. Chan, and Y. H. Tan.** 1996. Recombinant dengue type 1 virus NS5 protein expressed in Escherichia coli exhibits RNA-dependent RNA polymerase activity. Virology **216:**317-25.

109. **Twiddy, S. S., E. C. Holmes, and A. Rambaut.** 2003. Inferring the rate and time-scale of dengue virus evolution. Mol Biol Evol **20:**122-9.

110. **Umareddy, I., A. Chao, A. Sampath, F. Gu, and S. G. Vasudevan.** 2006. Dengue virus NS4B interacts with NS3 and dissociates it from single-stranded RNA. J Gen Virol **87:**2605-14.

111. **van den Hoff, M. J., V. M. Christoffels, W. T. Labruyere, A. F. Moorman, and W. H. Lamers.** 1995. Electrotransfection with "intracellular" buffer. Methods Mol Biol **48:**185-97.

112. **Vasilakis, N., and S. C. Weaver.** 2008. The history and evolution of human dengue emergence. Adv Virus Res **72:**1-76.

113. **Weaver, S. C., and N. Vasilakis.** 2009. Molecular evolution of dengue viruses: contributions of phylogenetics to understanding the history and epidemiology of the preeminent arboviral disease. Infect Genet Evol **9:**523-40.

114. **Webster, D. P., J. Farrar, and S. Rowland-Jones.** 2009. Progress towards a dengue vaccine. Lancet Infect Dis **9:**678-87.

115. **Welsch, S., S. Miller, I. Romero-Brey, A. Merz, C. K. Bleck, P. Walther, S. D. Fuller, C. Antony, J. Krijnse-Locker, and R. Bartenschlager.** 2009. Composition and three-dimensional architecture of the dengue virus replication and assembly sites. Cell Host Microbe **5:**365-75.
116. **Yap, T. L., Y. L. Chen, T. Xu, D. Wen, S. G. Vasudevan, and J. Lescar.** 2007. A multi-step strategy to obtain crystals of the dengue virus RNA-dependent RNA polymerase that diffract to high resolution. Acta Crystallogr Sect F Struct Biol Cryst Commun **63:**78-83.
117. **Yap, T. L., T. Xu, Y. L. Chen, H. Malet, M. P. Egloff, B. Canard, S. G. Vasudevan, and J. Lescar.** 2007. Crystal structure of the dengue virus RNA-dependent RNA polymerase catalytic domain at 1.85-angstrom resolution. J Virol **81:**4753-65.
118. **Yocupicio-Monroy, R. M., F. Medina, J. Reyes-del Valle, and R. M. del Angel.** 2003. Cellular proteins from human monocytes bind to dengue 4 virus minus-strand 3' untranslated region RNA. J Virol **77:**3067-76.
119. **Zhou, H., M. Xu, Q. Huang, A. T. Gates, X. D. Zhang, J. C. Castle, E. Stec, M. Ferrer, B. Strulovici, D. J. Hazuda, and A. S. Espeseth.** 2008. Genome-scale RNAi screen for host factors required for HIV replication. Cell Host Microbe **4:**495-504.

VI Appendix

siRNA screens: Supplementary Data

Table VI.1 List of siRNAs used in the primary siRNA screen (*Silencer*® Human Kinase siRNA Library V3, AM80010V3). Each gene was silenced with three separate siRNA. The gene IDs, siRNA IDs and plate layout of the siRNAs in the screen are given in this table. The table is attached as an electronic appendix.

Table VI.2 Statistical analysis of the primary RNAi screen. The index.html file allows navigation through the results which include the list of candidates, the data normalization process and intra and inter-experiment correlation. The table is attached as an electronic appendix.

Table VI.3 List of siRNAs used in validation screen. Each gene was silenced with three separate siRNA. The gene IDs, siRNA IDs and plate layout of the siRNAs in the screen are given in this table. The table is attached as an electronic appendix.

Table VI.4 Statistical analysis of the infection based validation screen. The index.html file allows navigation through the results which include the list of candidates, the data normalization process and intra and inter-experiment correlation. The table is attached as an electronic appendix.

Table VI.5 Statistical analysis of the DENV replicon based validation screen. The index.html file allows navigation through the results which include the list of candidates, the data normalization process and intra and inter-experiment correlation. The table is attached as an electronic appendix.

Table VI.6 List of host susceptibility genes selected after primary screen.

No:	Gene Symbol	Full Gene Name	RefSeq Acc No:	Gene ID	Sense siRNA Sequence	Exon(s) Targeted	Validated	Z-score	pValue
1	COPB	coatomer protein complex, subunit beta	NM_016451	1315	GGAUCUUCAA-CAUCCUAAUtt	3,4		-1.89	0.017
2	CDK7	cyclin-dependent kinase 7 (MO15 homolog, Xenopus laevis, cdk-activating kinase)	NM_001799	1022	GGCCAGAGAUAA-GAAUACCtt	2	Yes	-1.83	0.001
3	LEDGF /p75	Lens epidermal growth factor			AGACAGCAUGAG-GAAGCGAtt	ND		-1.80	0.003
4	MAP3K7IP2	mitogen-activated protein kinase kinase kinase 7 interacting protein 2	NM_145342	23118	GCAAAGGAACAU-CUAGCCUtt	3		-1.79	0.036
5	FES	feline sarcoma oncogene	NM_002005	2242	GGACAUUGAGAAG-CUGAAGtt	4		-1.79	0.026
6	CKI-delta				CCUGCUGCUUGCU-GACCAAtt	ND		-1.78	0.021
7	IRAK1	interleukin-1 receptor-associated kinase 1	NM_001025242	3654	GGUUUCGUCACC-CAAACAUtt	6,7	Yes	-1.69	0.005
8	PRPS1	phosphoribosyl pyrophosphate synthetase 1	NM_002764	5631	CGCAUGCUUU-GAGGCAGUAtt	6		-1.69	0.005
9	LOC390975	-	XM_372749	390975	UUUUGC-CUUCGCCCAGGAGtt	4		-1.66	0.015
10	ERBB4	v-erb-a erythroblastic leukemia viral oncogene homolog 4 (avian)	NM_005235	2066	GGAUCGAUAUGC-CUUGGCAtt	3	Yes	-1.65	0.008
11	RPS6K	ribosomal protein S6 kinase, 70kDa,	NM_003	6198	GGACAUGGCAGGA-	2	Yes	-1.64	0.045

APPENDIX

#	Gene	Description	NM	GeneID	Sequence	Exon	Validated	Ratio	p
	B1	polypeptide 1	161		GUGUUUtt				
12	LEDGF /p75				AGACAGCAUGAG-GAAGCGAtt	ND		-1.64	0.015
13	CDKL3	cyclin-dependent kinase-like 3	NM_016 508	51265	GGAGAUAUCUCA-GAACCAAtt	8	Yes	-1.60	0.027
14	COPB	coatomer protein complex, subunit beta	NM_016 451	1315	GGAUCUUCAA-CAUCCUAAUtt	3,4		-1.53	0.025
15	PRKY	protein kinase, Y-linked	NM_002 760	5616	GGAGCAGCACGUG-CACAAUtt	2	Yes	-1.53	0.006
16	RYK	RYK receptor-like tyrosine kinase	NM_002 958	6259	GGAUUGAACUG-GAUGACAGtt	8,9	Yes	-1.50	0.010
17	CXCR4				GCAUGACGGACAA-GUACAGtt	ND		-1.48	0.035
18	PLXNA 2	plexin A2	NM_025 179	5362	GGACAUGAAUGC-CUACCUCtt	31		-1.47	0.015
19	PAPSS 1	3-phosphoadenosine 5-phosphosulfate synthase 1	NM_005 443	9061	GGUGGCUUUCGUG-GUUGCAtt	2	Yes	-1.47	0.004
20	AKAP8 L	A kinase (PRKA) anchor protein 8-like	NM_014 371	26993	GGAUCCAGUUUGU-GUGUUCtt	10		-1.44	0.010
21	RPS6K A5	ribosomal protein S6 kinase, 90kDa, polypeptide 5	NM_004 755	9252	GGCAACAAUCGUU-CAAAAGtt	3	Yes	-1.43	0.016
22	MAP3 K7	mitogen-activated protein kinase kinase kinase 7	NM_003 188	6885	GGAGAUCGAGGUG-GAAGAGtt	1	Yes	-1.41	0.033
23	NTRK1	neurotrophic tyrosine kinase, receptor, type 1	NM_001 012331	4914	GAAACAAGUUUGG-GAUCAAtt	12		-1.41	0.009
24	LOC34 0371	nuclear receptor binding protein 2	NM_178 564	34037 1	GGUACAAAAUCGU-GAAUCUtt	17		-1.40	0.014
25	FLT3	fms-related tyrosine kinase 3	NM_004 119	2322	GGGAACAUUUCCU-GUCUCUtt	3		-1.39	0.027
26	CDK5	cyclin-dependent kinase 5	NM_004 935	1020	GGAGCUGAAGCA-CAAGAACtt	3	Yes	-1.34	0.013
27	NTRK3	neurotrophic tyrosine kinase, receptor, type 3	NM_002 530	4916	GGAUUCAGGGAA-CAGCAAUtt	2		-1.34	0.020
28	PKN3	protein kinase N3	NM_013 355	29941	GGAGCUACAG-CAUCGACUGtt	5	Yes	-1.32	0.006
29	HCK	hemopoietic cell kinase	NM_002 110	3055	GGGAGAUACCGU-GAAACAUtt	7		-1.32	0.006
30	C9orf9 6	chromosome 9 open reading frame 96	NM_153 710	16943 6	CGACCAUGGAGCU-ACAUGAtt	ND		-1.32	0.018
31	ANKK1	ankyrin repeat and kinase domain containing 1	NM_178 510	25523 9	GGGUUCAACAU-GAUGAUGAtt	4,5		-1.31	0.034
32	MPP1	membrane protein, palmitoylated 1, 55kDa	NM_002 436	4354	GCCGUCUUCCUG-CACUACAtt	5		-1.31	0.003
33	DKFZP 434C1 31	unc-51-like kinase 3 (C. elegans)	NM_015 518	25989	CGGAAUAUCUCU-CACCUGGtt	4		-1.31	0.007
34	MARK 1	MAP/microtubule affinity-regulating kinase 1	NM_018 650	4139	GGCUGAAAACCUU-CUCCUUtt	6,7		-1.28	0.018
35	CDK4	cyclin-dependent kinase 4	NM_000 075	1019	GGCUUUUGAG-CAUCCCAAUtt	2	Yes	-1.27	0.007
36	ACVR1	activin A receptor, type I	NM_001 105	90	GGCUGCUUCCAG-GUUUAUGtt	4	Yes	-1.24	0.039
37	LEDGF /p75				AGACAGCAUGAG-GAAGCGAtt	ND		-1.20	0.015
38	ALS2C R2	amyotrophic lateral sclerosis 2 (juvenile) chromosome region, candidate 2	NM_018 571	55437	GGAUUUGACAA-CUUGACUUtt	5	Yes	-1.20	0.009
39	EGFR	epidermal growth factor receptor (erythroblastic leukemia viral (v-erb-b) oncogene homolog, avian)	NM_201 284	1956	GGUGGUCCUUGG-GAAUUUGtt	2		-1.20	0.005
40	DAPK1	death-associated protein kinase 1	NM_004 938	1612	GGACGGACA-CAUUGCCCUUtt	17	Yes	-1.19	0.031
41	STK22 C	serine/threonine kinase 22C (spermiogenesis associated)	NM_052 841	81629	GGGCCAGAAGA-GUUUAUCCtt	2		-1.18	0.008
42	NEK8	NIMA (never in mitosis gene a)-related kinase 8	NM_178 170	28408 6	CCACUUUGUUCUC-CUACCAtt	15		-1.18	0.039
43	DGKQ	diacylglycerol kinase, theta 110kDa	NM_001 347	1609	GGCUGCACAA-CAAGGGUGtt	19,20		-1.18	0.004
44	NEK5	NIMA (never in mitosis gene a)-related kinase 5	NM_199 289	34167 6	CCGACCAUC-CAUAAAUUCCtt	ND		-1.18	0.017
45	LOC91 807	LOC91807	NM_182 493	91807	GGUUAAG-GAAAUUUCCAACtt	13		-1.17	0.003
46	RIPK3	receptor-interacting serine-threonine kinase 3	NM_006 871	11035	GGCCACAGGGUUG-GUAUAAtt	10		-1.17	0.048
47	TK2	thymidine kinase 2, mitochondrial	NM_004 614	7084	GGCAUACUCGUC-CUCAGGUtt	5,6	Yes	-1.17	0.015
48	LY6G5 B	lymphocyte antigen 6 complex, locus G5B	NM_021 221	58496	GAUUCAGUGGUU-CUACCAGtt	1		-1.16	0.009
49	MAP2	mitogen-activated protein kinase	NM_030	5605	GGUGGAAGAAGUG-	11	Yes	-1.16	0.004

117

	K2	kinase 2	662		GAUUUUtt				
50	EPHA8	EPH receptor A8	NM_020 526	2046	GCCAGUUCCU-CAAAAUCGAtt	3		-1.15	0.032
51	AMHR 2	anti-Mullerian hormone receptor, type II	NM_020 547	269	GGCGAACCUGUGU-GUUCUUtt	2		-1.14	0.011
52	PRKCI	protein kinase C, iota	NM_002 740	5584	GGUUCGAGACAU-GUGUUCUtt	2	Yes	-1.12	0.045
53	PRPSA P1	phosphoribosyl pyrophosphate synthetase-associated protein 1	NM_002 766	5635	GGCACAUAAAGU-CUUAACUtt	11		-1.12	0.024
54	COPB	coatomer protein complex, subunit beta	NM_016 451	1315	GGAUCUUCAA-CAUCCUAAUtt	3,4		-1.12	0.049
55	LEDGF /p75				AGACAGCAUGAG-GAAGCGAtt	ND		-1.11	0.017
56	FLJ250 06	FLJ25006	NM_144 610	12492 3	CCAGGAAUCC-CUAAAGCCAtt	2		-1.11	0.029
57	IHPK3	inositol hexaphosphate kinase 3	NM_054 111	11728 3	GGUUGAGAGGAA-GAGCUUCtt	4		-1.11	0.026
58	PRKCQ	protein kinase C, theta	NM_006 257	5588	GGAUUUUAUCUUG-CACAAAtt	11		-1.09	0.017
59	ULK1	unc-51-like kinase 1 (C. elegans)	NM_003 565	8408	CGCCACAUAACAGA-CAAAAtt	28		-1.09	0.011
60	NEK6	NIMA (never in mitosis gene a)-related kinase 6	NM_014 397	10783	GGAUUGCUGACA-GACAGAAtt	10		-1.07	0.008
61	CDK3	cyclin-dependent kinase 3	NM_001 258	1018	CGAGAGGAAGCU-CUAUCUGtt	3		-1.06	0.013
62	MVK	mevalonate kinase (mevalonic aciduria)	NM_000 431	4598	GGUAGCACUGGCU-GUAUCCtt	2,3	Yes	-1.04	0.025
63	EEF2K	eukaryotic elongation factor-2 kinase	NM_013 302	29904	GGUUAAUAAGUA-CUACAGCtt	3	Yes	-1.04	0.049
64	SCAP1	src family associated phosphoprotein 1	NM_003 726	8631	GCCAGGUA-CUAUUGGGAUUtt	2,3		-1.04	0.036
65	DKFZp 434C1 418	EPH receptor A6	NM_173 655	28522 0	CCAGUAAUGAUU-GUGGUGGtt	10		-1.03	0.017
66	MELK	maternal embryonic leucine zipper kinase	NM_014 791	9833	GGCCUUGAAGAAC-CUGAGAtt	4	Yes	-1.03	0.034
67	ERBB2	v-erb-b2 erythroblastic leukemia viral oncogene homolog 2, neu-ro/glioblastoma derived oncogene homolog (avian)	NM_004 448	2064	GGACACGAUUUU-GUGGAAGtt	5,6		-1.03	0.025
68	CKI-alpha				GAAACAUGGU-GUCCGGUUUtt	ND		-1.03	0.034
69	PLXNA 3	plexin A3	NM_017 514	55558	GGAUGAGUUUGU-GUCCUCCtt	3		-1.02	0.009
70	PTK2B	PTK2B protein tyrosine kinase 2 beta	NM_173 176	2185	GGCUGAAGCACAU-GAAGUCtt	7		-1.01	0.014
71	KIAA09 99	KIAA0999	NM_025 164	23387	GGAACUGUUCAGG-CACAUGtt	20	Yes	-1.01	0.004
72	LOC39 1295	-	XM_497 791	39129 5	CCUCAAGUGUUA-GAACCUUtt	2		-1.01	0.016
73	FGFRL 1	fibroblast growth factor receptor-like 1	NM_021 923	53834	GGAAGAAGAAGUG-GACACUtt	4		-1.01	0.010
74	INSR	insulin receptor	NM_000 208	3643	GGAACUCGGCCU-CUACAACtt	2	Yes	-1.00	0.012

Table VI.7 List of host resistance genes selected after primary screen.

No:	Gene Sym-bol	Full Gene Name	RefSeq Acc No:	Gene ID	Sense siRNA Se-quence	Exon(s) targeted	Vali-dated	Z-score	pVa-lue
1	LIMK1	LIM domain kinase 1	NM_016 735	3984	GGAUCUAU-GAUGGCCAGUAtt	2	Yes	1.96	0.009
2	CD2	CD2 antigen (p50), sheep red blood cell receptor	NM_001 767	914	CCUGUAUCAA-GAUGGGAAAtt	3		1.80	0.004
3	GRK1	G protein-coupled receptor kinase 1	NM_002 929	6011	GCAGGUUCAUCGU-GUCUCUtt	2		1.76	0.001
4	ERBB3	v-erb-b2 erythroblastic leukemia viral oncogene homolog 3 (avian)	NM_001 005915	2065	CCUUGAGAUUGUG-CUCACGtt	2		1.74	0.006
5	PNKP	polynucleotide kinase 3-phosphatase	NM_007 254	11284	GGAUCUUGUA-CCCAGAGAUtt	5,6		1.70	0.021
6	AURKB	aurora kinase B	NM_004 217	9212	GGAGGAUCUACUU-GAUUCUtt	6	Yes	1.66	0.003
7	MAP4 K5	mitogen-activated protein kinase kinase kinase kinase 5	NM_006 575	11183	GGGUCUUGC-CUAUUUGCAUtt	6,7	Yes	1.58	0.017
8	ERN2	endoplasmic reticulum to nucleus signalling 2	NM_033 266	10595	GGAUGAAACUGG-CUUCUAUtt	ND		1.54	0.001

9	FN3KRP	FN3KRP	NM_024619	79672	GGACGAGUGUUC-GUGAAAGtt	1	Yes	1.45	0.002
10	PRKWNK1	WNK lysine deficient protein kinase 1	NM_018979	65125	GGAUGAUAUCGAA-GAGCUGtt	1	Yes	1.45	0.007
11	CSNK1D	casein kinase 1, delta	NM_139062	1453	GGAUUAGCGAGAA-GAAAAUtt	5		1.43	0.008
12	MKNK2	MAP kinase interacting serine/threonine kinase 2	NM_017572	2872	GGAGUACGCCGU-CAAGAUCtt	5,6	Yes	1.41	0.031
13	KIS	U2AF homology motif (UHM) kinase 1	NM_144624	127933	GGCAAUCAGGAU-GUAAAGUtt	2,3	Yes	1.38	0.014
14	CAMK1G	calcium/calmodulin-dependent protein kinase IG	NM_020439	57172	GGUCUUGUCGGCA-GUGAAAtt	5		1.35	0.016
15	PIK3C2G	phosphoinositide-3-kinase, class 2, gamma polypeptide	NM_004570	5288	GGAAAGCUAUCUC-GAAAGCtt	6		1.32	0.004
16	CIB4	-	NM_001029881	130106	UGACAUGUCUGAG-GACCUCtt	ND		1.31	0.011
17	UMP-CMPK	cytidylate kinase	NM_016308	51727	GGAAGAACCCA-GAUUCACAtt	2	Yes	1.31	0.039
18	CSK	c-src tyrosine kinase	NM_004383	1445	GGAGAAAGAAAGU-ACCCAGtt	13	Yes	1.30	0.042
19	CIB1	calcium and integrin binding 1 (calmyrin)	NM_006384	10519	GGGAUGGAACCAU-CAACCUtt	6		1.25	0.023
20	SCGB2A1	secretoglobin, family 2A, member 1	NM_002407	4246	CCAUCAAUUCCGA-CAUAUCtt	2		1.23	0.009
21	PIP5K2C	phosphatidylinositol-4-phosphate 5-kinase, type II, gamma	NM_024779	79837	GGCCAGCUCCAA-GAUCAGtt	2		1.21	0.009
22	MAPK4	mitogen-activated protein kinase 4	NM_002747	5596	GGGUGAGCUGUU-CAAGUUCtt	1	Yes	1.20	0.031
23	OSRF	OSRF	NM_012382	23548	GCACUACAGUUAA-CUCCAAtt	3	Yes	1.19	0.032
24	C19orf35	chromosome 19 open reading frame 35	NM_198532	374872	GCAUUUGUGUA-GGCUGUUCtt	4		1.16	0.017
25	BLK	B lymphoid tyrosine kinase	NM_001715	640	GGAAGAGAAGG-CUAUGUGCtt	5		1.16	0.029
26	LTK	leukocyte tyrosine kinase	NM_206961	4058	CCCGGAUGUGCU-GAAUUCAtt	19		1.16	0.039
27	LOC340371	nuclear receptor binding protein 2	NM_178564	340371	GCCACCUCUUU-GACCCUUUtt	17		1.16	0.003
28	PANK2	pantothenate kinase 2 (Hallervorden-Spatz syndrome)	NM_153640	80025	GCAUUCGGAA-GUACCUGACtt	2	Yes	1.15	0.008
29	JAK2	Janus kinase 2 (a protein tyrosine kinase)	NM_004972	3717	GGUGUAUCUUUA-CCAUUCCtt	3	Yes	1.14	0.007
30	MAP3K4	mitogen-activated protein kinase kinase kinase 4	NM_006724	4216	GCCAGUCGGU-CUAAUUUGAtt	2		1.14	0.037
31	LOC442141	-	XM_498022	442141	GGCACCUUCAUG-GUGAAAUtt	1,2		1.13	0.029
32	SPHK1	sphingosine kinase 1	NM_021972	8877	GGCUGAAAUCUC-CUUCACGtt	3	Yes	1.13	0.004
33	DGKB	diacylglycerol kinase, beta 90kDa	NM_145695	1607	GCUCGGAGCUA-GAAAAUAUtt	6,7		1.12	0.036
34	HK1	hexokinase 1	NM_033496	3098	GGAAGGAGAUGAA-GAAUGGtt	2	Yes	1.10	0.014
35	TRIB2	tribbles homolog 2 (Drosophila)	NM_021643	28951	GGAUUUCGAAGA-GUUGUCGtt	1	Yes	1.10	0.036
36	LOC388221	-	XM_370939	388221	GCUGUGAUUAGCA-CUAAGUtt	7,8		1.10	0.031
37	FGFR4	fibroblast growth factor receptor 4	NM_002011	2264	GAGCAGGAGCUGA-CAGUAGtt	2		1.07	0.025
38	LATS1	LATS, large tumor suppressor, homolog 1 (Drosophila)	NM_004690	9113	GGUUCUGAGA-GUAAAAUUAtt	8		1.07	0.005
39	ROCK1	Rho-associated, coiled-coil containing protein kinase 1	NM_005406	6093	GGCAGA-CAAUUUAAAAGGUtt	20		1.06	0.005
40	BTK	Bruton agammaglobulinemia tyrosine kinase	NM_000061	695	GGUAAUAUACCAU-CAUGUACtt	18		1.06	0.013
41	PRKCM	protein kinase D1	NM_002742	5587	GGAAGAGAUGUAG-CUAUUAtt	13	Yes	1.05	0.005
42	DTYMK	deoxythymidylate kinase (thymidylate kinase)	NM_012145	1841	GGAAAAGUUGAGC-CAGGGCtt	3	Yes	1.04	0.016
43	CALM2	calmodulin 2 (phosphorylase kinase, delta)	NM_001743	805	GGAAUUGGGAACU-GUAAUGtt	3		1.02	0.021
44	GCKR	glucokinase (hexokinase 4) regulator	NM_001486	2646	CGGAAAUCGAUA-CUGUGGUtt	14		1.01	0.047
45	STK32A	serine/threonine kinase 32A	NM_145001	202374	GUGCGUG-GAGCGCAAUGAAtt	4		1.01	0.013
46	MAP3K4	mitogen-activated protein kinase kinase kinase 4	NM_005922	4216	CCUCGACAGAU-GAAACGCAtt	2		1.00	0.046

Table VI.8 Infection based Validation screen: The list of host susceptibility factors with significant effect on DENV infection.

No:	Gene Symbol	Full Gene Name	RefSeq Acc No:	Gene ID	Sense siRNA Sequence	Exon(s) Targeted	Validated	Z-score
1	FGFR4	fibroblast growth factor receptor 4	NM_002011	2264	UCAAGAUGCU-CAAAGACAAtt	11,9,11	No	-3.3
2	FES	feline sarcoma oncogene	NM_002005	2242	AGUGGGUGCU-GAACCAUGAtt	13	No	-3.3
3	NEK5	NIMA (never in mitosis gene a)-related kinase 5	NM_199289	341676	CUACAA-CAAUAAAACGGAUtt	8	No	-3.1
4	C19orf35	chromosome 19 open reading frame 35	NM_198532	374872	CGCUGAUCAAUGU-CUCUCUtt	4	No	-3.0
5	MAP3K7	mitogen-activated protein kinase kinase kinase 7	NM_003188	6885	CGUGUGAACCAUC-CUAAUAtt	3,3,3,3	Yes	-2.8
6	CDK4	cyclin-dependent kinase 4	NM_000075	1019	UGCUGA-CUUUUAACCCACAtt	8	Yes	-2.7
7	CALM2	calmodulin 2 (phosphorylase kinase, delta)	NM_001743	805	AAAGGAAUUGG-GAACUGUAtt	3	Yes	-2.6
8	DGKQ	diacylglycerol kinase, theta 110kDa	NM_001347	1609	GGAAGCUACU-GAACCCUCAtt	16	No	-2.6
9	PRKD1	protein kinase D1	NM_002742	5587	CAUCAUCUAU-GUAAGCCUAtt	16	No	-2.6
10	ANKK1	ankyrin repeat and kinase domain containing 1	NM_178510	255239	AGCACAUCGUGU-CUAUCUAtt	2	No	-2.5
11	ACVR1	activin A receptor, type I	NM_001105	90	GAGGCAU-GAAAAUAUCUUAtt	7	Yes	-2.4
12	BTK	Bruton agammaglobulinemia tyrosine kinase	NM_000061	695	GAAACUGUUUG-GUAAACGAtt	16	No	-2.4
13	MPP1	membrane protein, palmitoylated 1, 55kDa	NM_002436	4354	CAGUGCACCAGAUC-CAUAAtt	10	No	-2.3
14	ERBB3	v-erb-b2 erythroblastic leukemia viral oncogene homolog 3 (avian)	NM_001005915	2065	UCGUCAUGUUGAA-CUAUAAtt	3,3	No	-2.3
15	BLK	B lymphoid tyrosine kinase	NM_001715	640	UGAUGGAAGUUGU-CACUUAtt	12	No	-2.3
16	FLT3	fms-related tyrosine kinase 3	NM_004119	2322	CAACUAUCUAA-GAAGUAAAtt	17	No	-2.3
17	ANKK1	ankyrin repeat and kinase domain containing 1	NM_178510	255239	GGUUCCGCAU-CAUCCAUGAtt	2	No	-2.2
18	CSNK1D	casein kinase 1, delta	NM_001893	1453	CACGCACCUUG-GAAUUGAAtt	4,4	No	-2.2
19	CDK5	cyclin-dependent kinase 5	NM_004935	1020	GCAAUGAUGUC-GAUGACCAtt	9	Yes	-2.2
20	CD2	CD2 molecule	NM_001767	914	GGACAUCUAUCU-CAUCAUUtt	4	No	-2.0
21	ALS2CR2	amyotrophic lateral sclerosis 2 (juvenile) chromosome region, candidate 2	NM_018571	55437	GCUUUACA-GAAAGCCGUGAtt	5	Yes	-2.0
22	GCKR	glucokinase (hexokinase 4) regulator	NM_001486	2646	CCCUGUUAUUA-GCAGCCCAtt	10	No	-2.0
23	HK1	hexokinase 1	NM_000188	3098	CAUCCACACUUCUC-CAGAAtt	17,17,20,20,21	Yes	-2.0
24	MAP3K4	mitogen-activated protein kinase kinase kinase 4	NM_005922	4216	CUAACGAACUGAU-CUGGUUtt	3,3	No	-2.0
25	PTK2B	PTK2B protein tyrosine kinase 2 beta	NM_004103	2185	CAGGAGAA-CUUAAAGCCCAtt	11,12,7,7	No	-1.9
26	CDK4	cyclin-dependent kinase 4	NM_000075	1019	CACCCGUGGUU-GUUACACUtt	4	Yes	-1.9
27	ALS2CR2	amyotrophic lateral sclerosis 2 (juvenile) chromosome region, candidate 2	NM_018571	55437	CCUCAAUCAGAAUC-CAGAAtt	10	Yes	-1.9
28	DGKB	diacylglycerol kinase, beta 90kDa	NM_004080	1607	GGUUUUGGAUUG-CAUAGAAtt	17,17	No	-1.9
29	TK2	thymidine kinase 2, mitochondrial	NM_004614	7084	GCUCUGUGAUA-CCCAAUAAtt	10		-1.9
30	LY6G5B	lymphocyte antigen 6 complex, locus G5B	NM_021221	58496	CCUUCUGUAG-GAUGCAUUUtt	2	No	-1.8
31	MAP3K7IP2	mitogen-activated protein kinase kinase kinase 7 interacting protein 2	NM_015093	23118	GAAUAAGUGAAA-CACGGAAtt	3	Yes	-1.8
32	CDK7	cyclin-dependent kinase 7	NM_001799	1022	CCUUAAAGGAG-CAAUCAAAtt	11	Yes	-1.8
33	FGFR4	fibroblast growth factor receptor 4	NM_002011	2264	ACACCUGCCUGGU-AGAGAAtt	6,5,6	No	-1.8
34	PIK3C2G	phosphoinositide-3-kinase, class 2, gamma polypeptide	NM_004570	5288	GUAGCAUUCCUC-CAACAAAtt	2	No	-1.8
35	DAPK1	death-associated protein kinase 1	NM_004938	1612	GAUCAAGCCUAAA-GAUACAtt	9	No	-1.8
36	C9orf96	chromosome 9 open reading frame 96	NM_153710	169436	CGACCAUGGAGCU-ACAUGAtt	12	No	-1.7

37	DGKQ	diacylglycerol kinase, theta 110kDa	NM_001 347	1609	GGAUUGCCCAGG-GUUCCUAtt	22	No	-1.7
38	FN3KRP	fructosamine-3-kinase-related protein	NM_024 619	79672	ACAAGAAGCUUG-GAGAGAUtt	3	Yes	-1.7
39	MAPK4	mitogen-activated protein kinase 4	NM_002 747	5596	CAGAAGGGUUG-GUAACAAAtt	3	No	-1.7
40	LY6G5B	lymphocyte antigen 6 complex, locus G5B	NM_021 221	58496	GCUCAUCCCUGUG-CAUGGUtt	2	No	-1.6
41	CSK	c-src tyrosine kinase	NM_004 383	1445	CGAUUACCGAGG-GAACAAAtt	8	No	-1.6
42	LOC2311 7	KIAA0220-like protein	XM_933 834	23117	GCGUUUCCGACAA-GUUAUAtt	ND	No	-1.6
43	KIAA099 9	KIAA0999 protein	NM_025 164	23387	CAGUAAGAGUU-CAAGUACAtt	20	No	-1.6
44	PLXNA3	plexin A3	NM_017 514	55558	GCAGUGAACCGA-GUCUUUAtt	2	No	-1.5
45	MKNK2	MAP kinase interacting se-rine/threonine kinase 2	NM_017 572	2872	GGAAUUUUGUAUU-CUGUUUtt	14,14	Yes	-1.5

Table VI.9 Infection based validation screen: The list of host resistance ki-nases with significant effect on DENV infection.

No:	Gene Symbol	Full Gene Name	RefSeq Acc No:	Gene ID	Sense siRNA Se-quence	Exon(s) Targeted	Vali-dated	Z-score
1	CDKL3	cyclin-dependent kinase-like 3	NM_016 508	51265	GGAUAUCAUCUA-GUGAUCUtt	7	No	**4.9**
2	C9orf96	chromosome 9 open reading frame 96	NM_153 710	169436	AGAAAAUCAUUGA-CUCUGAtt	5	No	**4.6**
3	IHPK3	inositol hexaphosphate kinase 3	NM_054 111	117283	UGACUUUGCUCAU-ACCACAtt	6	No	**4.2**
4	CIB4	calcium and integrin binding family member 4	NM_001 029881	130106	GAAGAUUGA-GUAUGCCUUtt	4	No	**4.1**
5	CMPK1	cytidine monophosphate (UMP-CMP) kinase 1, cytosolic	NM_016 308	51727	GAUUGAUGG-GUUUCCAAGAtt	3	Yes	**3.9**
6	CSNK1A1	casein kinase 1, alpha 1	NM_001 025105	1452	GAAUUUGCGAUGU-ACUUAAtt	9,8	Yes	**3.7**
7	MAP3K7	mitogen-activated protein kinase kinase kinase 7	NM_003 188	6885	AGAUACCAAUG-GAUCAGAUtt	13,14,14, 13	Yes	**3.7**
8	ERBB2	v-erb-b2 erythroblastic leukemia viral oncogene homolog 2, neu-ro/glioblastoma derived oncogene homolog (avian)	NM_001 005862	2064	GUUGGAUGAUUGA-CUCUGAtt	26,23	Yes	**3.3**
9	ROCK1	Rho-associated, coiled-coil containing protein kinase 1	NM_005 406	6093	GUAUGAAGAU-GAAUAAGGAtt	6	No	**3.1**
10	ERBB4	v-erb-a erythroblastic leukemia viral oncogene homolog 4 (avian)	NM_001 042599	2066	CCCGUAAUGUCUU-AGUGAAtt	21,21	No	**2.8**
11	PRKCQ	protein kinase C, theta	NM_006 257	5588	GCUGCUUAAGA-GAUACUGAtt	10	No	**2.7**
12	FGFRL1	fibroblast growth factor receptor-like 1	NM_001 004356	53834	AAGAAGAAGUGGA-CACUGAtt	5,5,4	Yes	**2.4**
13	MKNK2	MAP kinase interacting se-rine/threonine kinase 2	NM_017 572	2872	GCAGCGGCAUCAAA-CUCAAtt	10,10	Yes	**2.4**
14	DAPK1	death-associated protein kinase 1	NM_004 938	1612	GGGACACCUC-CAUUACUCAtt	13	Yes	**2.2**
15	PRKY	protein kinase, Y-linked	NM_002 760	5616	CAAUGCAUU-GUAUUCAGAAtt	8	No	**2.1**
16	RPS6KB1	ribosomal protein S6 kinase, 70kDa, polypeptide 1	NM_003 161	6198	CAUGGAACAUUGU-GAGAAAtt	3	Yes	**2.0**
17	MAP3K7	mitogen-activated protein kinase kinase kinase 7	NM_003 188	6885	GACUCGUUGUUG-GUCUAAAtt	8,8,8,8	Yes	1.9
18	ULK3	unc-51-like kinase 3 (C. elegans)	XM_001 134013	25989	GCAUGAACG-GAAUAUCUCUtt	ND	No	1.8
19	GRK1	G protein-coupled receptor kinase 1	NM_002 929	6011	GCAAUGUCCGGAU-CUCUGAtt	ND	No	1.8
20	WNK1	WNK lysine deficient protein kinase 1	NM_018 979	65125	CAUCAUCCCUUA-GUCUACAtt	19	Yes	1.8
21	WNK1	WNK lysine deficient protein kinase 1	NM_018 979	65125	CAAUGAGUCA-GAUAUCGAAtt	24	Yes	1.7
22	PRKCI	protein kinase C, iota	NM_002 740	5584	GUAAUUC-CAUAUAAUCCUUtt	7	No	1.7
23	TSSK3	testis-specific serine kinase 3	NM_052 841	81629	GGGACCUACU-CAAAAGUCAtt	1	No	1.7
24	NTRK3	neurotrophic tyrosine kinase, recep-tor, type 3	NM_001 007156	4916	CGGAUAACUUUAU-CUUGUUtt	10,10,10	No	1.6

25	ULK3	unc-51-like kinase 3 (C. elegans)	XM_001 134013	25989	CAGCGGAAGGAGG-CAAUUAtt	Not Deter-mined	No	1.6
26	CIB1	calcium and integrin binding 1 (calmy-rin)	NM_006 384	10519	CGUCAUCUCCC-GUUCUCCAtt	6	No	1.6
27	MVK	mevalonate kinase	NM_000 431	4598	GGCUGCUCAA-GUUCCCAGAtt	8	No	1.5

VII Publications and Presentations

Publications

Matula P, <u>Kumar A</u>, Wörz I, Erfle H, Bartenschlager R, Eils R, Rohr K, 2009: Single-cell-based image analysis of high-throughput cell array screens for quantification of viral infection. Cytometry A. 75 (4):309-18.

Manuscript under preparation

<u>Anil Kumar</u>, Sandra Buehler, Andrew Davidson, Sven Miller, Ralf Bartenschlager: Role of NS5 nuclear localization in dengue replication and IL-8 induction.

Oral Presentations

4th Asian Dengue Research Network Meeting, Singapore, December 9th-11th 2009. Role of NS5 nuclear localization in dengue replication and IL-8 induction. <u>Anil Kumar</u>, Sandra Buehler, Andrew Davidson, Sven Miller, Ralf Bartenschlager

Fourth Joint PhD students Meeting of the Sonderforschungsbereich (SFB) 544, 630 and 766. Bronnbach, Germany, 20th-22nd November 2008. Identification of cellular kinases essential for Dengue virus infection through genome-wide kinase siRNA screen. . <u>Anil Kumar</u>, Holger Erfle, Petr Matula, Lars Kaderali, Sandra Bühler, Karl Rohr, Rainer Pepperkok, Ralf Bartenschlager

Seventh Workshop on Cell Biology of Viral Infections, German Society for Virology, Deidesheim, October 6th-8th 2008. Studies on dengue NS5 nuclear localization. <u>Anil Kumar</u>, Sven Miller, Sandra Bühler, Ralf Bartenschlager.

Poster presentations

German Symposium on Systems Biology. Heidelberg, May 12-15, 2009: Identification of cellular kinases involved in dengue infection. <u>Anil Kumar</u>, Holger Erfle, Petr Matula, Lars Kaderali, Nina Beil, Jürgen Beneke, Karl Rohr, Roland Eils, Sandra Bühler, Rainer Pepperkok, Ralf Bartenschlager

Third European Congress of Virology. Nürnberg, September 1-5, 2007: Role of nuclear localized NS5 in dengue virus infection. <u>Anil Kumar</u>, Sven Miller, Ralf Bartenschlager, Sandra Sparacio.

3rd Asian Regional Dengue Research Network Meeting. Taipei, Taiwan, 21-24th August, 2007: Characterization of nuclear localized NS5 of dengue virus. <u>Anil Kumar</u>, Sven Miller, Ralf Bartenschlager, Sandra Sparacio.